SCK•CEN
STUDIECENTRUM VOOR KERNENERGIE
CENTRE D'ÉTUDE DE L'ÉNERGIE NUCLÉAIRE

NUCLEAR FISSION AND
RADIATION PROTECTION

EURATOM

Severe Accident Facilities for European Safety Targets

SAFEST

Grant Agreement n° 604771

SAFEST-DRR-D2.4

European safety research roadmap for next generation plants

Authors:
F.Belloni (SCK•CEN), C. Journeau (CEA), P. Vacha (ÚJV Řež), S. Bechta (KTH), D. Manara (JRC)

Period covered:		Delivery date:
Start date of SAFEST project: July 1, 2014		Duration: 4 years
WP N°2	WP leader: Dario Manara	His organization name: JRC

Severe Accident Facilities for European Safety Targets

SAFEST

EC project officer: **Dr. Roberto Passalacqua (EU DG RTD G.4)**

Work package N°:	2	**Task N°:**	3
SAFEST Identification:		**Revision:**	

➥Short description of revision:

Summary:

The SAFEST facilities are able to perform unique experiments aimed to investigate severe accident phenomenology of LWR reactors. The objective of the present work is assessing the possibility to extend the application field of the SAFEST facilities to the Gen IV fast reactor technology issues, in particular focusing on the technologies that are part of the European Union's Strategic Energy Technology Plan (SET-Plan). The SAFEST partners have identified the most relevant phenomena influencing severe accident sequences and expressed their assessment on the possibility to investigate them in the SAFEST facilities.
This report has to be intended as a first step towards a detailed roadmap for R&D concerning severe accident for GEN IV reactors.

Report title:	European safety research roadmap for next generation plants
Issued by:	
Internal reference by editing partner:	
Status:	Under review

Project co-funded by the European Commission within the 7th Framework Programme (2007-2013)		
Dissemination Level		
PU	Public	X
RE	Restricted to a group specified by the SAFEST partners	
CO	Confidential, only for SAFEST partners	
CR	Confidential, only for SAFEST partners working on the same subject	

Table of Contents

Acronyms

ALFRED	Advanced Lead Fast Reactor European Demonstrator
ALLEGRO	Gas fast reactor demonstrator
ANL	Argonne National Laboratory
ARDECO	ASTRID R&D European Co-operation
ASTRID	Advanced Sodium Technological Reactor for Industrial Demonstration
CDA	Core Disruptive Accident
CEA	Commissariat à l'énergie atomique et aux énergies
CFV	Cœur à Faible Vidange
CIEMAT	Centro de Investigaciones Energéticas, Medioambientales y Tecnológicas
CRGT	Control Rod Guide Tube
CHF	Critical Heat Flux
CNEN	Comitato Nazionale Energia Nucleare
DEM	Discrete Element Method
DHR	Decay Heat Removal
EBR	Experimental Breeder Reactor
EDF	Électricité de France
EDX	Energy Dispersive X-ray spectrometry
EELS	Electron Energy Loss Spectroscopy
ENEA	Agenzia nazionale per le nuove tecnologie, l'energia e lo sviluppo economico sostenibile
EOS	Equation of State
ESFR	European Sodium Fast Reactor
ESNII	European Sustainable Industrial Initiative
ETPP	European Technology Pilot Plant
Euratom	European Atomic Energy Community
FA	Fuel Assembly
FAIDUS	Fuel Assembly with Inner DUct Structure
FCI	Fuel coolant interaction
FFTF	Fast Flux Test Facility
FZK	Forschungszentrum Karlsruhe
Gen IV	Generation IV
GIF	Generation IV International Forum
GFR	Gas Fast Reactor
HCDA	Hypothetical Core Disruptive Accident
HLM	Heavy-Liquid Metal
HZDR	Helmholtz-Zentrum Dresden-Rossendorf
INL	Idaho National Laboratory
IRSN	Institut de Protection et de Sûreté Nucléaire
JAEA	Japan Atomic Energy Agency
JRC	Joint Research Centre
JSFR	Japan Sodium Fast Reactor
KFK	Kernforschungszentrum Karlsruhe

KIT	Karlsruhe Institute of Technology
KTH	Kungliga Tekniska Högskolan
LBE	Lead-Bismuth Eutectic
LFR	Lead/LBE Fast Reactor
LMFBR	Liquid Metal Fast Breeder Reactor
LOCA	LOss of Coolant Accident
LOF	LOss of Flow
MAXSIMA	Methodology, Analysis, eXperiments, for the safety In-MYRRHA Assessement
MYRTE	MYRRHA Research and Transmutation Endeavour
MOX	Mixed Oxide fuel
MTA-EK	Magyar Tudományos Akadémia Energiatudományi Kutatóközpont
MFTF	Molten Fuel Test Facility
MYRRHA	Multipurpose hYbrid Research Reactor for High-end Applications
MSR	Molten Salt Reactor
NCBJ	Narodowe Centrum Badań Jądrowych
NNC/RK	National Nuclear Research Center of the Republic of Kazakhstan
NNL	National Nuclear Laboratory
PCMI	Pellet Cladding Mechanical Interaction
PDS	Particulate Debris Spreading
PFR	Prototype Fast Reactor
PNC	Power Reactor and Nuclear Fuel Development Corporation
PSI	Paul Scherrer Institut
R&D	Research and Development
R&I	Research and Industrialization
RD&D	Research, Development and Deployment
RIA	Reactivity Insertion Accident
RPV	Reactor Pressure Vessel
RTCS	Reactor Top Cooling System
RVACS	Reactor Vessel Auxiliary Cooling System
SAFEST	Severe Accident Facilities for European Safety Targets
SCK•CEN	Studiecentrum voor Kernenergie/ Centre d'Etude de l'Energie Nucléaire
SEM	Scanning Electron Microscope
SET	Strategic Energy Technology
SFR	Sodium Fast Reactor
SNEPT	Strategic Nuclear Energy Technology Platform
SNL	Sandia National Laboratories
SPERT	Special Power Excursion Reactor Tests
TEM	Transmission electron microscope
TIB	Total Instantaneous Blockage
TOP	Transient OverPower
TREAT	Transient Reactor Test Facility
TUCOP	Transient UnderCooling OverPower

UCLA	University of California at Los Angeles
ÚJV	Ústav Jaderného Výzkumu
UKAEA	United Kingdom Atomic Energy Authority
ULOF	Unprotected Loss of Flow
U.S. NRC	United Stated Nuclear Regulatory Commission
VHTR	Very High Temperature Reactor
VÚJE	Vyskumny Ustav Jadrovych Elektrarnf

Abbreviations

cw	Cold-worked
DCS-M-TT	Complementary Safety Devices - for severe accident Mitigation – Transfer Tubes
IVR	In-Vessel Retention
M/F	Melting/Freezing
SA	Severe Accident
SS	Stainless steel
V/C	Vaporization/Condensation

Symbols

Al	Aluminium
Al_2O_3	Alumina
B_4C	Boron Carbide
D	Diameter
ΔT	Temperature difference
K_{BB}	Experimental coefficient
Nd:YAG	Neodymium-doped Yttrium Aluminum Garnet;
Nu	Nusselt number
Pr	Prandtl number
Pu	Plutonium
Ra	Rayleigh number
Re	Reynolds number
SiC	Silicon Carbide
SiC_f	Silicon Carbide fibers
Ti	Titanium
U	Uranium
(U,Pu) C	Uranium-Plutonium Carbide fuel
UO_2	Uranium Oxide
PuO_2	Plutonium Oxide

We	Weber number
ZrO_2	Zirconium Oxide
Zr	Zirconium
Zry	Zircalloy

1 Introduction

1.1 Generation IV International Forum

The Generation IV (Gen-IV) International Forum (GIF [1]) was created in January 2000 by 9 countries and today includes 13 members, all of which are signatories of its founding document, the *GIF Charter*. Argentina, Brazil, Canada, France, Japan, the Republic of Korea, South Africa, the United Kingdom and the United States signed the GIF Charter in July 2001. It was subsequently signed by Switzerland in 2002, Euratom in 2003, and the People's Republic of China and Russian Federation in 2006.
GIF considers that nuclear energy is needed to meet future energy demand, and that international collaboration is required to advance nuclear energy into its next "fourth" generation of systems, deployable after 2030 (see Table 1).
The GIF recognizes six advanced nuclear power systems as most likely to be deployed first: the sodium-cooled fast reactor (SFR), the lead-cooled fast reactor (LFR), the very high temperature reactor (VHTR), the molten salt reactor (MSR) and the gas-cooled fast reactor (GFR).

Table 1: Overview of Generation IV systems [1]

System	Neutron spectrum	Coolant	Outlet Temperature °C	Fuel cycle	Size (MW)
VHTR **(Very-high-temperature reactor)**	Thermal	Helium	900-1000	Open	250-300
SFR **(Sodium-cooled fast reactor)**	Fast	Sodium	500-550	Closed	50-150 300-1500 600-1500
SCWR **(Supercritical-water-cooled reactor)**	Thermal/fast	Water	510-625	Open/closed	300-700 1000-1500
GFR **(Gas-cooled fast reactor)**	Fast	Helium	850	Closed	1200
LFR **(Lead-cooled fast reactor)**	Fast	Lead	480-570	Closed	20-180 300-1200 600-1000
MSR **(Molten salt reactor)**	Thermal/fast	Fluoride salts	700-800	Closed	1000

GIF defined four goal areas in its original *Technology Roadmap* (2002, [2]):

1) Sustainability
2) Economics
3) Safety and Reliability
4) Proliferation Resistance and Physical Protection

Safety and Reliability of the future generation of reactor designs are met by the achievement of specific goals:

1. **Generation IV nuclear energy systems will excel in operational safety and reliability.** The focus of this goal applies to safety and reliability during normal operation of all facilities employed in the nuclear fuel cycle, and thus, deals with the relatively likely kinds of operational events that set the forced outage rate, determine worker safety, and result in routine emissions that could affect workers or the public.

2. **Generation IV nuclear energy systems will have a very low likelihood and degree of reactor core damage.** This goal calls for design features that create high confidence that the possibility of core damage accidents will be very small for Gen-IV reactors. The goal deals with both minimizing the frequency of initiating events, and with provision of design features that ensure that the plants can successfully control and mitigate any initiating events that might occur without causing core damage.

3. **Generation IV nuclear energy systems will eliminate the need for offsite emergency response.** It is desirable that Gen-IV systems demonstrate, with high confidence, the capability of the safety architecture to manage and mitigate the consequences of severe plant conditions and that any potential releases of radiation will be small and have only insignificant public health consequences.

The Fukushima Daiichi nuclear power plant accident has emphasized the importance of designing nuclear systems with the highest level of safety and in particular the need for reliable residual heat removal over long periods as well as the necessity to exclude significant off-site releases in case of a severe accident. For the Generation IV systems, an additional set of questions has to be analyzed in detail and compared to the work on advanced light water reactors [3]. These relate in particular to:

• The use of non-water coolants in most Generation IV designs;

• Higher operational temperatures;

• Higher reactor power density;

• In some cases, the close location or integration of fuel-cycle or chemical facilities.

1.2 Gen-IV technologies investigated in the SAFEST project

To meet the Climate and Energy goals for 2050, the European Union adopted the policy of diversification of the energy supplies. In this context, a stress was put in ensuring the safe operation of the nuclear systems, CO_2-free emission plants.

Following the adoption of the Communication on Energy Technologies and Innovation, and the conclusions of the European Council of 22 May 2013, the European Commission reviewed its Strategic Energy Technology Plan (SET-Plan) with the aim to define an integrated roadmap that meets, among others, the energy policy objectives of security of supply, competitiveness and sustainability [4].

The research, development and deployment of innovative and competitive technology in the nuclear sector at a European scale are coordinated by the Strategic Nuclear Energy Technology Platform (SNETP) [5]. SNETP has set up a Task Force comprising research organizations and industrial partners to develop the European Sustainable Nuclear Industrial Initiative (ESNII) in support of the SET-Plan.

ESNII addresses the need for demonstration of Gen-IV Fast Neutron Reactor technologies, together with the supporting research infrastructures, fuel facilities and R&D work [6], [7]. SNETP has then prioritized the different Gen-IV systems and proposed to develop the following projects (Figure 1):

- **The ASTRID project,** a prototype sodium-cooled fast reactor (SFR) that will be built in Marcoule, France.
- **The ALLEGRO project,** a gas-cooled fast reactor (GFR) demonstrator to be constructed in the Czech Republic, Hungary or Slovakia.
- **The ALFRED project,** a lead-cooled fast reactor (LFR) demonstrator that will be built in Pitesti, Romania
- Additionally, **the MYRRHA research reactor project,** a lead-bismuth cooled accelerator-driven fast neutron multi-purpose research reactor, is also being developed. Since MYRRHA is based on the heavy liquid metal technology, it will strongly contribute to the development of LFR technology. MYRRHA will play the role of European technology pilot plant (ETPP) in the roadmap for LFR.

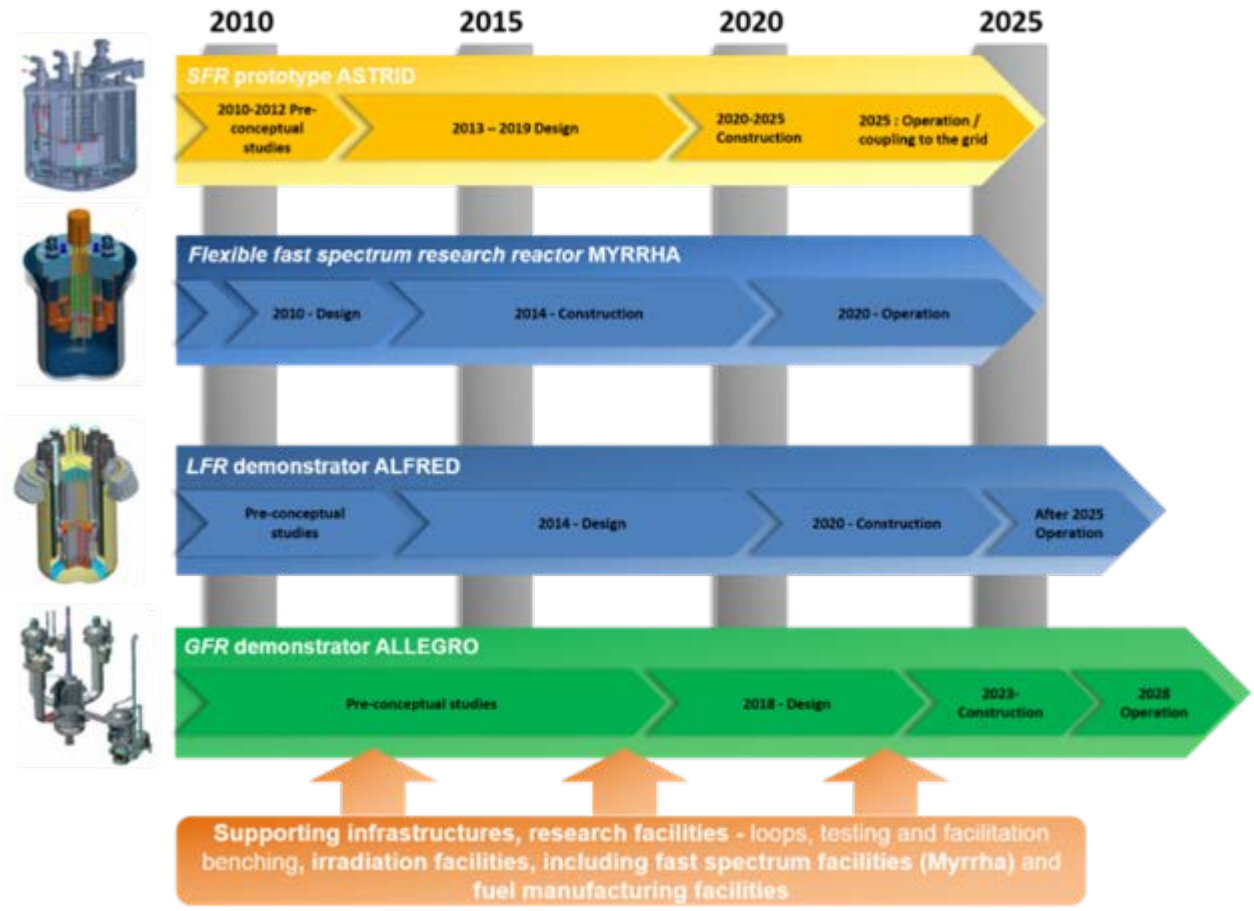

Figure 1: Gen-IV Fast Neutron Reactor technologies supported by ESNII [8]

ASTRID (Advanced Sodium Technological Reactor for Industrial Demonstration) has the goal to become the technological integration prototype of the SFR technology. The design of the reactor is led by the Commissariat à l'énergie atomique et aux énergies alternatives (CEA), in cooperation with national and international industrial partners. In particular EDF, Lab, PSI, KTH, HZDR, KIT, ENEA, JRC Karlsruhe, NNL, CIEMAT and the universities of Uppsala and Chalmers are part of ARDECO, ASTRID R&D European Co-operation [9]. Given the experience acquired with formerly operated SFRs, ASTRID must therefore demonstrate and qualify, on an industrial scale, the validity of the innovative options in the identified progress areas, in particular safety and operability. The recently started ESFR-SMART Horizon-2020 project, for instance includes tasks on severe accidents for a generic ASTRID-like SFR.

The Belgian Nuclear Research Center, SCK•CEN, leads the MYRRHA project.

The FALCON (Fostering ALFRED Construction) consortium [10] was signed in 2013 among Ansaldo Nucleare, ENEA and ICN to support the construction of ALFRED through European structural funds and to optimize the cooperation among the partners (joined by CV Řež in 2014). The consortium was renewed in 2016.

The ALLEGRO project [7] involves currently five participants (institutes and companies), which cooperation is regulated by a Memorandum of Understanding: MTA-EK Budapest (Hungary), ÚJV Řež (Czech Republic),

VÚJE (Slovakia) and associated members CEA and NCBJ Swierk (Poland). A GFR Centre of Excellence has been established for the project governance. It will cover four areas governed by the particular participants:

1) Safety concept and ALLEGRO design (VÚJE)
2) Helium technology and experimental support (ÚJV Řež)
3) Fuel laboratory (MTA-EK)
4) Industrial use of high temperature gas (NCBJ)

The ALLEGRO and MYRRHA projects are on the list of priority investments for the EU under the €315 billion Investment Plan launched by European Commission President Jean-Claude Juncker [11].

2 Defence in Depth applied to Severe Accidents

Gen-IV reactor design, as new nuclear power plant design, is based on the concept of Defense in Depth (DiD) [12] to meet the fundamental safety principles [13]. Following this approach, severe accidents are not anymore classified as "beyond-design basis accidents", but have an impact on the design of mitigating features aimed to avoid large releases of radioactive material and any long-term emergency plan deployment (5^{th} level of Defense in Depth). When possible, the mitigating strategy of In-Vessel Retention (IVR) is also applied to strengthen the radioactive confinement function.

In order to ensure the effectiveness of the mitigating devices a clear understanding of the severe accident sequence and of the phenomena affecting the device performance must be gained through dedicated R&D experimental programs, which also serve as database for the development and validation of the simulation tools used in support of the design.

3 Classification and identification of the phenomena occurring in a severe accident scenario

We can roughly classify the phenomena occurring during a severe accident in two main categories:

- Phenomena occurring inside the core, leading to core degradation;
- Phenomena occurring outside the core (but inside the main vessel) in the post-accident heat removal phase. These phenomena influence the corium in-vessel relocation and coolability.

The identification of the phenomena and R&D needs is mainly carried out exploiting the large research database available for the past experimental campaign on SFRs. SFR technology is the reference Gen-IV fast reactor technology within the ESNII, as it can rely on 30-year experience in R&D, construction, operation and licensing. A wide experimental database for severe accident is available, result of the R&D programs carried out mostly between the 1960s and 1990s in France, Germany, United Kingdom, United States and Japan, in support of reactor design and operation. The alternative technologies (LFR, GFR) do not have as detailed R&D plans on severe accidents yet. On the base of that, comparisons and considerations are made on the other two innovative ESNII technologies (LFR, GFR technologies) and, when needed, specific phenomena and R&D needs are addressed for the particular reactor design (ASTRID, MYRRHA, ALLEGRO).

Basic information about the core composition of the fast reactor technologies supported by the ESNII are listed in Table 2. An overview of the coolant properties of the ESNII reactors in comparison with light water is reported in Table 3.

Table 2: Main features of the ESNII reactor cores

	ASTRID [14]	MYRRHA [15]	ALFRED [16]	ALLEGRO [17], [18]
Thermal power	1500 MW	100 MW	300 MW	75 MW
Coolant	Sodium	Lead Bismuth Eutectic	Lead	Helium
Fuel	MOX (Pu enrichment :Inner core ~23.5% - Outer core : 20%)	MOX (Pu enrichment ~30%)	MOX (Inner core: ~22% Outer core: ~28%)	MOX (25.5%) / UO_2 (less than 20%) future upgrade to (U,Pu)C
Cladding	15-15 Ti cw austenitic steel	15-15 Ti cw austenitic steel	15-15 Ti cw austenitic steel	Austenitic steel/ceramic materials future upgrade to SiC/SiCf
Absorber material	Boron carbide	Boron carbide	Boron carbide	Boron carbide
Hexagonal wrapper	Stainless steel	Stainless steel	Stainless steel	Stainless steel / ceramic materials
Core catcher	Stainless steel/ refractory material	No specifications	No specifications	No specifications
Pressure	1 bar	1 bar (relevance of static pressure)	1 bar (relevance of static pressure)	70 bar

Table 3: Comparison among the thermo-physical properties of liquid metals and water

	Liquid Sodium [19] pressure = 0.1 MPa temperature = 450 °C	Liquid Lead [20] pressure =0.1 MPa temperature = 450 °C	Liquid LBE [20] pressure = 0.1 MPa temperature = 450 °C	Helium gas [21] pressure =7 MPa temperature = 260 °C – 530 °C	Saturated water pressure = 15 MPa [21]
Melting temperature, °C	98	327.4	125	-272	-1.1[1]
Boiling temperature, °C	883	1745	1670	-269	342
Vaporization heat, kJ/kg	3871	856.8	852	/	1000
Density, kg/m³	845	10520	10150	6.2-4.15	603
Specific heat capacity, kJ/kgK	1.269	0.1473	0.146	5.19	8.5
Thermal conductivity, W/mK	68.8	17.1	14.2	0.23-0.31	0.46
Kinematic viscosity, m² /s	$3 \cdot 10^{-7}$	$1.9 \cdot 10^{-7}$	$1.4 \cdot 10^{-7}$	$4.8 \cdot 10^{-6}$- $9.5 \cdot 10^{-6}$	$1.2 \cdot 10^{-7}$
Prandtl number	0.0048	0.0174	0.0147	0.13	1.27
Surface tension, mN/m	163	480	392	/	5.2

[1] https://www.engineeringtoolbox.com/water-melting-temperature-point-pressure-d_2005.html

4 Phenomena occurring in the core degradation phase

The main risk during the degradation phase of a fast reactor core is the generation of high energetic excursions, by the achievement of prompt-critical core configurations, which can induce excessive mechanical loads on the vessel. The main contributor to the reactivity insertion is fuel compaction: the more the damage progresses inside the core, higher is the risk of fuel compaction and strong reactivity insertion.
Furthermore, other issues are the integrity of all the core internals that can activate vessel bypass paths and the integrity of the absorber rods, when the damage is originated in protected conditions (the reactor is already shutdown and the absorber rods are inserted).

Passive mitigation devices inside the core aim at evacuating fuel outside the core, to solve the aforementioned issues (e.g. core transfer tube devices in ASTRID [22] and FAs with internal ducts, FAIDUS, in the JSFR [23]). These are bypass channels, connecting the core or the FAs with the lower plenum. Hence, the importance of carrying out experiments testing the fuel dispersion through confined channels.

We can then distinguish three investigation fields in the core degradation phase:

1) Pin failure: it is important to characterize the physical state of the materials in the initial phase of the core degradation.
2) Degradation in confined walls: phenomena at subassembly (S/A) scale, occurring within the pin bundle and at the wrapper wall. They influence the fuel dispersion.
3) Molten pool dynamics. It influences the fuel relocation and the damage propagation to the confining structures.

4.1 Phenomena causing pin failure

Several experimental campaigns were carried out in the past decades to study pin failures in sodium fast reactors, following transient overpower (TOP) by reactivity insertion and/or loss of cooling flow (LOF) events. Concerning reactivity insertion accidents (RIA), in-pile tests reproduced:

1) Slow TOPs (0.05 ÷ 0.5 $/s), corresponding to anticipated operational occurrences.
2) Medium TOPs (0.5 ÷ 1.0 $/s) and fast TOPs (> 1.0 $/s), reproducing typical reactivity insertions of a severe accident sequence.

These experiments aimed to determine failure criteria to be used for design purposes, and to investigate the post-failure phase characterized by the fuel dispersion and interaction with the sodium coolant.

The main contributions in characterizing the initiating phase of severe accidents in fast reactors came from the TREAT and CABRI (CABRI-1, CABRI-2) experimental test campaigns. Based on these databases, the mechanistic codes simulating the initiating phase of a severe accident in a sodium fast reactor were effectively validated.

4.1.1 TREAT experimental campaign

TREAT (Transient Reactor Test Facility) is an air-cooled, thermal, heterogeneous test facility designed to evaluate reactor fuels and structural materials under conditions that simulate various types of transient overpower and under-cooling situations in a nuclear reactor [24]. Fuel meltdown, metal-water reactions, thermal interaction between overheated fuel and coolant, and the transient behavior of ceramic fuel for high-temperature systems can be studied. A schematic of the TREAT transient test facility is shown in Figure 2.

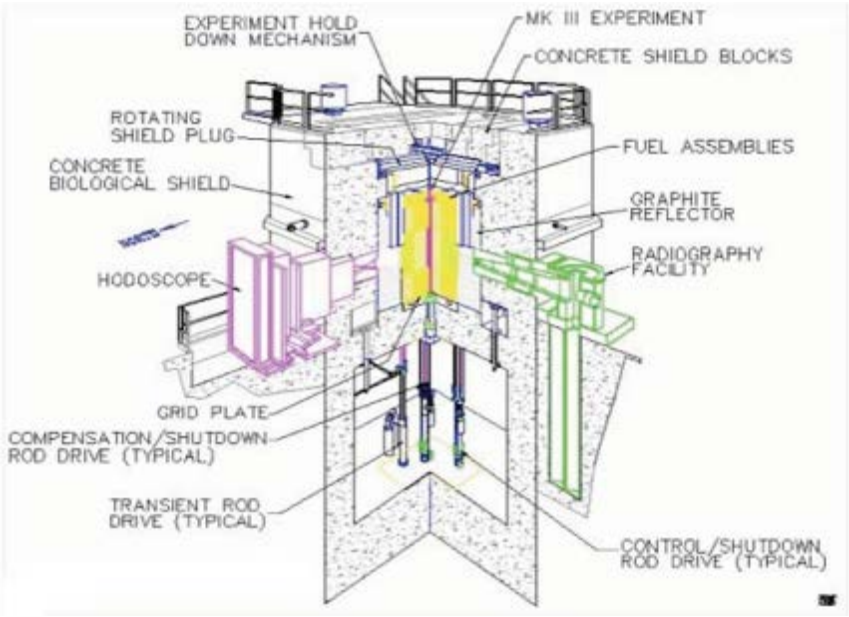

Figure 2: sketch of the TREAT facility [25]

TREAT is located at the Materials and Fuels Complex (MFC) at the Idaho National Laboratory (INL). It operated between 1958 and 1994.

TREAT was used primarily to test liquid-metal reactor fuel elements, initially for the operation of the Experimental Breeder Reactor-II (EBR-2), then for the Fast Flux Test Facility (FFTF), the Clinch River Breeder Reactor Plant (CRBRP), the British Prototype Fast Reactor (PFR), and finally, for the Integral Fast Reactor (IFR). Both oxide and metal elements were tested in dry capsules and in flowing sodium loops. The data obtained were used to establish the behavior of the fuel under off-normal and accident conditions, a necessary part of the safety analysis of the various reactors.

The F-series tests were done to study fuel behavior undercooling events in liquid metal fast breeder reactors (LMFBRs). These tests were performed in dry (no sodium) capsules to separate out effects of sodium on fuel behavior and, in F3 and subsequent tests, to permit visual observation [26].
They showed mainly the importance of the fuel enthalpy rate in determining the fuel ejection mode and the possibility of having pin disruption without fuel or clad melting, by the action of fission gas induced swelling, for high-burnup pins (> 60 MWd/Kg). In these tests, the power was increased on a 200 ms period

until constant linear powers of 820 and 2165 W/cm were achieved in F3 and F4, respectively. Nominal linear power and burnup for the F3 and F4 fuel were 295 W/cm and 9 at%.
Through the decade of the 1970s, the primary emphasis in TREAT experiments was supporting the FFTF and CRBRP safety analysis and licensing. For FFTF, the focus was on simulations of transient overpower (TOP) and unprotected loss of flow (LOF) accidents. The primary interest was determining the time and location of fuel pin failure, and characterizing the subsequent fuel motion. No strong fuel compaction was found that could cause the reactivity to diverge from the original input ramp [27].

The same comments can be thrown for LOF experiments (L-test series), implying that a smooth transition occurs in between the initiating and the transition phase of severe accidents. To carry out these tests [28] the Mark-II sodium loop was installed in the TREAT reactor, by replacing 2 central FAs (Figure 3). The test section consisted of a 7-pin bundle.
A preliminary test, L1, was conducted using a single fresh fuel pin. Fuel pin failure was not planned in this test, although the failure threshold was almost reached.
Test L2, the first of the three destructive tests, used fresh fuel pins. The following tests L3 and L4 used EBR-II-irradiated fuel pins having, respectively, "intermediate-power" (no central void) and "high-power" (fully developed central void) microstructure. Comparative data on the behavior of fresh and irradiated fuel were obtained. All tests used a power transient having a 2s-long preheat phase, followed by a constant-power phase in which flow coast-down took place.

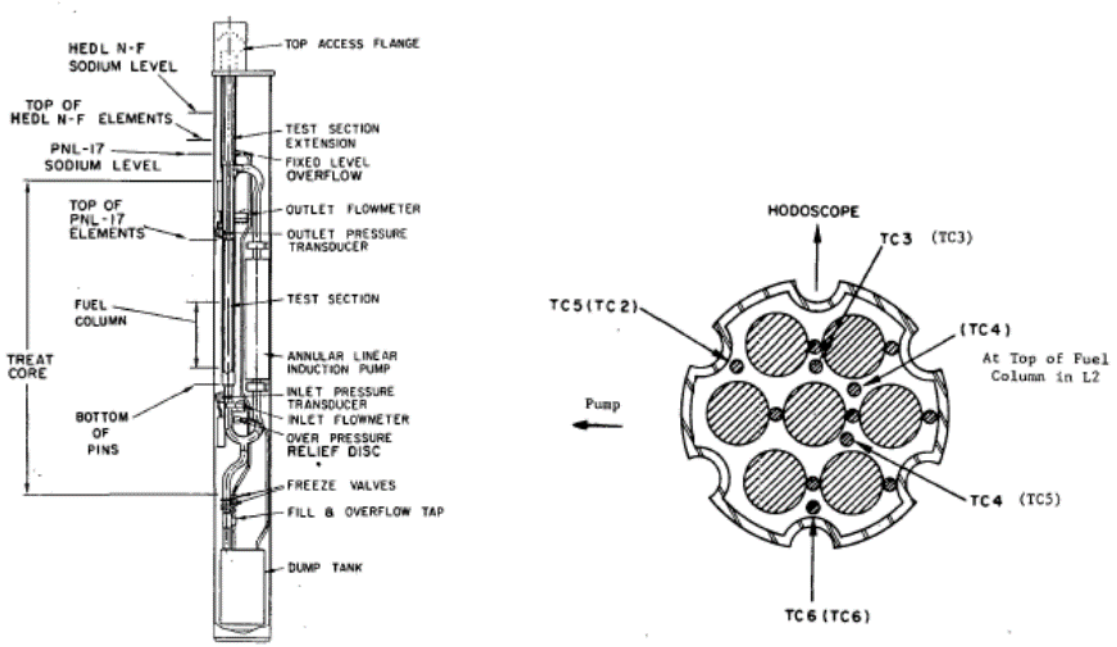

Figure 3: Mark-II sodium loop (left) and L2 test section cut (right) [28]

These tests provided interesting results on the pin disruption mechanisms and material relocation.

The fuel pins failed when the cladding melted, and the gas release was gradual. Considerable pre-failure bowing of the fuel pin occurred in all three tests that can potentially influence local coolant flow and temperature.
The majority of the molten steel moved downwards and froze in the lower part of the test section near the end of the original fuel column. As the fuel moved downwards, it re-melted the steel frozen beneath it.
The fresh fuel collapsed shortly after the cladding melted. In contrast, pre-irradiated fuel remained essentially in place after the cladding melted. This difference in behavior was most likely due to the swelling of the pre-irradiated fuel. Any eventual collapse of pre-irradiated fuel was most likely due to fuel melting. Fuel melted in all three experiments.
Solid flow blockages were formed near the bottom of the original fuel column in all three experiments. Frozen fuel tended to be porous in nature, while frozen steel was solid.

The PFR/TREAT collaborative program included 13 experiments on full–length pins conducted using UK designed bottom-plenum fuel pins between late 1980 and the end of 1983 [29]:

- 6 single pin capsule tests
- 7 pin bundle tests in flowing sodium

Fresh fuel was used only in two tests; the irradiated fuel was used in the remaining tests, with a burnup of 4 at% and 9 at% respectively. In each test, there was an axial relocation of fuel into a less reactive configuration. The results tended to validate predictions of time and location of failure, and showed that cladding melt-through is an important failure mechanism.

The tests included:

- Transient overpower (TOP) of 0.15 s period (fast) or 15 s period (slow);
- Transient undercooling with overpower burst (TUCOP) with cladding at different mechanical strength.

Additional transient overpower tests were carried out on the FFTF oxide fuel (RTF and TS series).
The TS-1 and TS-2 experiments were conducted to determine the time and location of failure of FFTF fuel pins subjected to hypothetical unprotected 0.05$/s transient overpower conditions. In both tests, the failure location was in the upper one-third of the fuel column.

4.1.2 CABRI experimental campaign

The CABRI experimental program [30] was developed in support of the R&D campaign for the French sodium fast reactor technology. It involved an international collaboration between CEA, KFK, UKAEA, PNC, and, up to 1985, U.S.NRC.

The TOP, TUCOP and LOF tests on sodium fast reactor fuel pins were carried out in the CABRI reactor between 1973 and 2001.

In comparison with the TREAT program, the CABRI-1 program aimed to investigate more in detail the fuel pin design chosen for the SNR-300 and Phénix reactor. Indeed the TREAT reactor could not reproduce the

operational and accidental conditions (faster and higher reactivity insertion) expected for the new reactors during a Hypothetical Core Disruptive Accident (HCDA) scenario.

A sodium test loop was installed in the center of the CABRI reactor (light water reactor, pool layout), which reached first criticality in 1977. The first campaign of experiments was carried out until 1987.

At the beginning of the CABRI-1 campaign (1973-1987, 32 tests) high and fast TOP tests (half-width ranging between 10 ms and 40 ms) were carried out, but the last part of the campaign was more focused on studying lower reactivity insertion rate (medium), as more realistic studies on the HCDA sequence showed the unlikelihood of having such fast reactivity insertions.

A test matrix was made to study the response of pins under TOP, TUCOP, LOF transients with pins at three different burnups (I=1 at%, G= 3 at%, H= 5 at%). I and H pins were irradiated in PHENIX (France), G pins in PFR (UK). The pins were then pre-irradiated in CABRI, before running the transients.

The outcome of the CABRI-1 test campaign was useful to identify new phenomena influencing the early fuel release and pin rupture, and for fuel performance code validation. It also contributed to steer the CABRI-2 campaign towards the investigation of alternative cladding material (15-15 Ti cw stainless steel), alternative pellet geometry (annular vs solid pellets) and the focus on milder overpower events.

In the CABRI-2 campaign, the pin linear power and burnup reproduced the PHENIX reactor irradiation conditions (and, in general, the conditions expected in a commercial size LMFBR). Two types of pins were tested:

1) OPHELIE-6: annular pellets at 5 at% burnup, to evaluate the effect the central void in mitigating PCMI failure with 20% cw stainless steel (SS AISI 316L). The burnup value is chosen for comparison with the H pins used in the CABRI-1 campaign (solid pellets) [31]
2) VIGGEN-4: solid pellets with 15-15 Ti SS and higher burnup (up to 12 at%, conceived for commercial size reactors)

12 tests were carried out, under different heating rates (slow, medium and fast TOPs) in different flow conditions to simulate pure TOP and TUCOP cases, taking into account the reactivity insertion following a ULOF in the initiating phase of the severe accident. Pure LOF tests were also run.
Differently from CABRI-1 program, also medium TOP tests were planned in CABRI-2 (Figure 4), in order to study the consequences of milder reactivity insertion following a ULOF. This choice was based on the more realistic predictions of the computational tools simulating a HCDA.

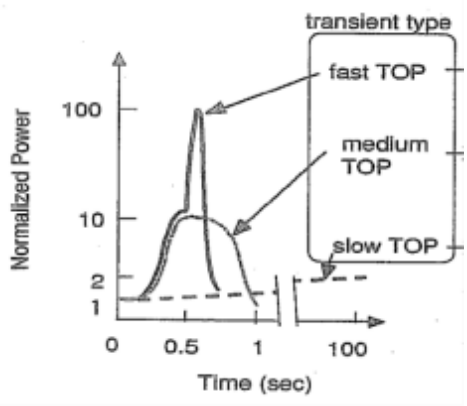

Figure 4: TOP transient tests in the CABRI-2 experimental campaign [32]

The CABRI campaigns were focused on the identification of the possible pin failure mechanisms and on the characterization of the in-pin molten fuel motion and ejection in the coolant subchannel, which influences the thermo-mechanical interaction between fuel and coolant and the material relocation.

The following pin failure mechanisms [31] were identified (see Figure 5):

TOP tests

1) Cladding thermomechanical failure in fresh pins;
2) Pellet Cladding Mechanical Interaction (PCMI) and burst failure by molten cavity pressurization in irradiated pins.

LOF tests

3) Fuel disruption by cladding restrain loss

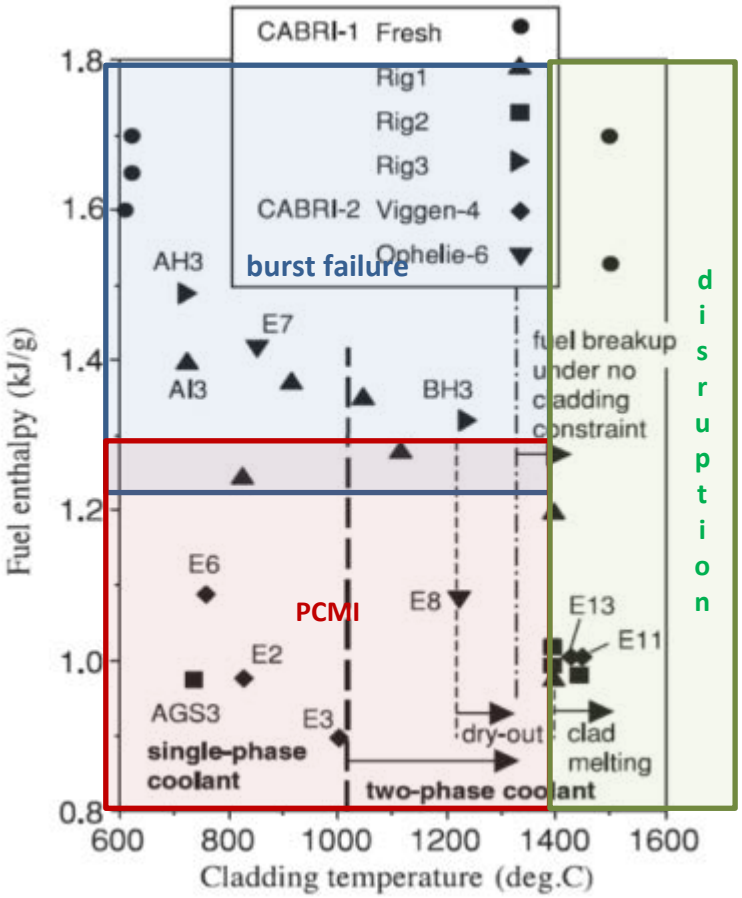

Figure 5: pin failure mechanisms in the CABRI tests, function of the fuel enthalpy and cladding strength (data refers to the breakup time) [32]

The mechanism leading to pin failure is influenced by the combination of the following parameters [33]:

1) irradiation power
2) burnup
3) smear density
4) amplitude and timescale of the power excursion
5) cladding strength

It is remarkable that in all tests carried out in the CABRI campaign pin failure occurred always after the onset of fuel melting in the central region, also because of the high centerline temperature of the fuel in steady-state conditions (pre-test peak linear power of irradiated fuel up to 310 W/cm). TREAT campaign showed that, at lower linear power, it is possible to have failure also without melting, at elevated burnup.

4.1.2.1 Pin failure mode: PCMI, burst failure by cavity pressurization, loss of cladding strength

PCMI failure during a transient overpower is caused by the combined effect of fuel thermal expansion and swelling. The main contributor between the two depends on the timescale of the transient and the temperature distribution inside the pellet. Intergranular gas swelling, leading to grain separation, relies on the gas diffusion from within the fuel lattice to the grain boundaries.
In the VIGGEN-4 pins, most of the retained gases were concentrated in the outer colder region. Gas diffusion to the grain boundaries was activated when this region reached 1600 °C – 1800 °C during the transient, but, during short power pulses, the process timescale is too large for the fission gas swelling to become relevant. The failure enthalpy reduces as the power excursion becomes milder and prolonged because the gas diffusion timescale becomes comparable with the excursion duration and a larger number of intergranular bubbles can migrate to the boundary grains.
Pin failure by PCMI occurs at medium-low enthalpies.
A low smear density, as in the case of annular pellets, provides additional void to accommodate the volumetric expansion and mitigate the effect of the fuel swelling. Solid pellets are therefore more likely to fail by PCMI.

In case of molten cavity pressurization, fuel melting in the central pellet region releases a large amount of fission gases that pressurize quickly the molten cavity. The large difference between the internal pin and the channel pressure causes the pin to burst.
The molten fuel ejection is driven by the difference between the internal pressure and the subchannel pressure and it goes much faster in case of burst failure than in case of PCMI failure, due to the high-pressure buildup in the pellet cavity. When injected in the channel the fuel interacts with the coolant (in SFR and LFR). This process contributes to the partial voiding of the sodium subchannels.

In case of PCMI failure (low enthalpies) or loss of the cladding restraint, the molten fuel is expected to be slowly released. In this case, subchannel blockages due to the formation of frozen fuel layers are possible.

In pure LOF scenarios (no reactivity feedbacks), the cladding melts when the fuel is still solid (this is true for ceramic fuel). After the cladding is lost, the pellets can either collapse in fragments or be disrupted by the gas swelling.

The enrichment in plutonium is also an additional variable to take into account in the pre-irradiation phase, because it influences the burnup distribution inside the pellet.

4.1.3 R&D needs

The CABRI experimental campaign contributed to the identification of the phenomena having an impact on pin failure, reactivity injection and fuel relocation and dispersal in sodium cooled channels.
The failure threshold values are anyway valid only for the specific pins used in the tests, hence, for the specific material composition. Considering the several phenomena influencing pin rupture the degree of prototypicality of the experiment is very important. The prototypicality of the in-pile experiments carried out between the 70's and the 90's is limited by the pre-irradiation inside thermal reactors. The well-known thermal neutron flux depression in the center of the pellet could enhance failure by PCMI against failure by melting. Therefore, experiments using appropriate filtering of the neutron flux should be repeated in the future.

In view of possible blockages by fuel fragments escaping after the cladding breakup, it is also important to register the size of the cladding opening, since it represents a maximum bound of the fuel size.

Contradictory data on the status of fresh and irradiated pellet after cladding loss seem to come out from the past test results. This point must be further investigated.

SFR

The design of SFR cores has evolved since when these tests were conducted. For ASTRID CFV core [34], a different geometry is considered (pin and spacer wire dimensions, heterogeneous core with fertile layer between two fissile layers, etc…) the effect of which on severe accident phenomenology must be experimentally verified. A new experimental campaign SAIGA [35], is planned in the IGR reactor, to investigate the degradation of the new CFV fuel elements. In particular, the impact of a smaller wire spacer and the presence of a fertile layer in between two fissile ones has to be investigated.

Three types of test will be carried out:

1) Instantaneous blockage (TIB)
2) Transient overpower (TOP)
3) Milder transient overpower with low sodium mass flow rate (TUCOP)

LFR

Concerning Heavy Liquid Metals, in-pile tests in a corrosive environment should be made to investigate the impact of corrosion on the safety limits. Considering the limitation on the operating power imposed by the long-term corrosion, a more extensive database is needed on low-power and high-burnup fuel pins. These pins seem to be more subjected to PCMI failure, because they retain most of the fission gases.
Furthermore, in Lead/LBE cooled reactors the corrosion limit may reduce the cladding maximum temperature below 600 °C, lower bound of the temperature range investigated in the CABRI tests.

Therefore, the existing database for TOP tests must be extended towards lower cladding temperature (down to the melting point of Lead/LBE) and lower linear power irradiation.

The G pins tested in CABRI-1 are an example of pins irradiated at low linear power, but they are partially representative of the irradiation status of a HLM pin because:

1) They were irradiated at higher nominal power in the CABRI reactor before being tested. The pre-test step of power brought the mostly intragranular gases to coalesce in bubbles, increasing the probability of PCMI failure.
2) They have a low burnup: 3 at%.

Loss of flow CABRI tests showed that the 15-15 Ti stainless steel loses its strength between 1100 °C and 1200 °C after sodium dryout, and pin disruption occurs above this temperature. The same conclusions may not be valid in a Lead/LBE system, because the coolant boiling point is higher than the cladding melting point and the cladding is still wet up to its melting temperature.
The mechanical properties and strength of the cladding up to its melting temperature must be then re-assessed for LFRs.

The status of fresh/irradiated pellets after cladding loss and the mechanical interaction with Lead/LBE in natural convection should be further investigated. Two scenarios remain open:

- The pellet breaks up in fragment;
- The stack of pellet remains in place.

In the second case, wettability and erosion/corrosion effect of Lead/LBE on the pellets should be studied.

<u>GFR</u>

If the ceramic material SiC/SIC_f will be selected as a possible cladding material for the ALLEGRO reactor, similar tests done in the past for the SFRs shall be repeated for ALLEGRO.

Thermodynamic calculations performed at CEA [36] have shown that in case of nitrogen ingress or injection in the primary circuit, the cladding can react with nitrogen (cladding nitriding) according to:

$3SiC + 2N_2 \rightarrow Si_3N_4 + 3C$,

if a temperature threshold ranging between 1200 °C and 1600°C is reached.

Similarly, water ingress can lead to active oxidation by steam above 1300-1400°C [37] according to:

$SiC(s) + H_2O(g) \rightarrow SiO(g) + CH_4(g)$
and/or $SiC(s) + 2\ H_2O(g) \rightarrow SiO(g) + CO(g) + 2\ H_2(g)$

Experimental tests, representative of accidental scenarios in GFR, should be carried out to confirm these phenomena and to assess the reaction rate.

Another phenomenon that can possibly lead to failure of the ceramic cladding is axial temperature gradient caused by cold heavy gas injection into the core [36] [38]. This effect is the strongest in case of N_2 injection, which is the gas of choice for heavy gas injection system in ALLEGRO.

Experimental tests with representative temperature gradients should be carried out to establish maximum allowed temperature gradient over the pin.

4.2 Phenomena at subassembly scale

The CABRI experimental campaign provided also useful information regarding the post pin-failure phase, concerning the interaction between fuel and coolant and material relocation and important to determine the reactivity feedbacks and the evolution of the accidental sequence.
The SCARABEE-N and MOL 7C test series gave an important contribution to the characterization of the damage progression inside a blocked FA. The two experimental campaigns examined different initiating events, but common phenomena can be identified in the degradation of the FAs. More recently the EAGLE in-pile tests at the IGR reactor [39] provided data on new devices at the subassembly scale (FAIDUS) to prevent the most energetic criticality events (see section 4.2.8 for more details).

SCARABEE test program

The SCARABEE in-pile test program was performed between 1983 and 1990 by the Institut de Protection et de Sûreté Nucléaire (IRSN) with the participation of French and foreigners partners [40]. The main objective of this experimental campaign was studying the consequences of a hypothetical total instantaneous blockage (TIB) at the entrance of a liquid-metal reactor subassembly at full power. 14 tests were run.
SCARABEE is the twin reactor of CABRI. The main advantages of SCARABEE in comparison with CABRI were the increased diameter of the experimental loop, which allowed testing of pin bundles up to 37 pins, increasing the degree of prototypicality of the experiment (see Figure 6). Furthermore, a high and relatively uniform linear power could be reproduced in the bundle, thanks to a higher driver core power and to the use of neutronic filters. The main disadvantage were that no fuel displacement-measuring device was available, like e.g. the CABRI hodoscope, and no rapid power transients could be achieved. Because of its characteristics, this reactor was then well suited to study the meltdown of small pin bundles in slow-power transients or transients resulting from cooling losses [40].

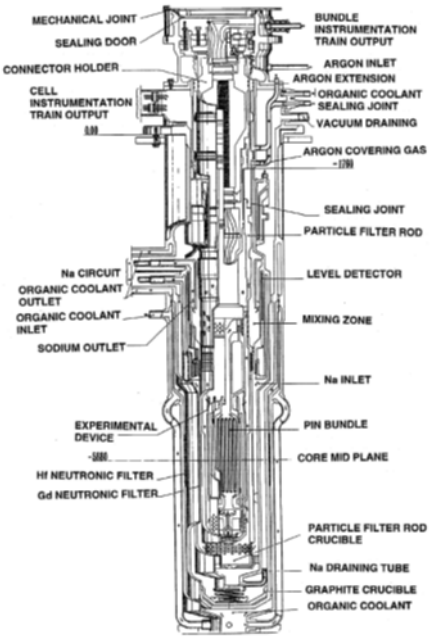

Figure 6: the SCARABEE in-pile section [40]

Anyway, the size of the experimental channel was not large enough to carry out integral tests fully representative of a whole TIB sequence. Therefore, five groups of experiments were performed, representing each sequential phase of the whole accident:

1) BE+, studying the phenomena in the blocked FA, up to the wrapper failure
2) BF, regarding the boiling pool dynamics and heat transfer
3) PI, focusing on the molten pool propagation in the interwrapper gap
4) PV, investigating the damage propagation in the neighboring FAs
5) APL, studying the phenomena following a loss of flow with pump coast-down

The experiments were run with fresh UO_2 fuel, in prototypical FA bundles.

Mol 7C test program

The Mol 7C experiment series provided important knowledge about the whole degradation process and damage extension originated by local blockages.
The experiments were carried out in the Belgian Reactor BR2, by SCK•CEN (Studiecentrum voor Kernenergie) and FZK (Forschungzentrum) to investigate the impact of local cooling disturbances in mixed-oxide fuel assemblies of liquid metal cooled reactors. The disturbances were simulated by porous blockages of steel and UO_2 inducing sodium boiling [41].

The tests were run for bundles of 30 pins (with grid spacers), with different burnup irradiation (from 0.1 to 10 at%). In all the tests loss of coolability and severe pin damage were observed but with different extension and timescale, depending on the burnup. For low burnup, only the blocked region of the pin bundle was affected, while for high burnup, a stepwise propagation to the whole bundle was observed. Delayed neutron detector response occurred within 30 s, enough time to avoid the damage extension to the neighboring FAs.

The in-pile test section and the initial blockage positions (axial and radial view) are shown in Figure 7.

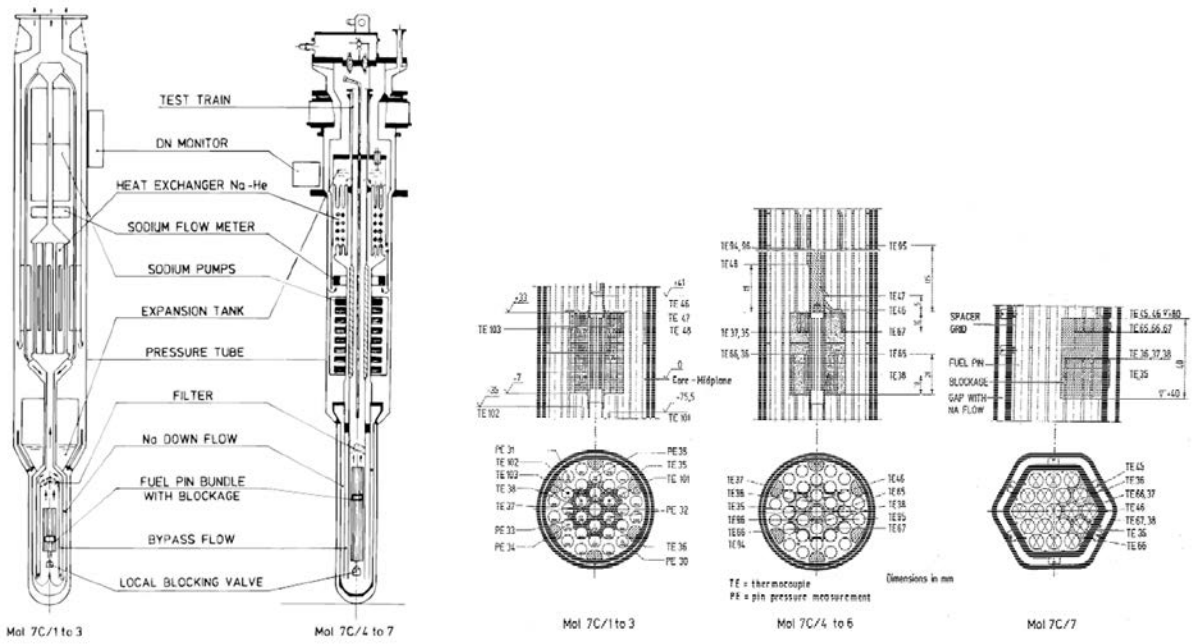

Figure 7: in-pile test section (a) and blockage positions (b) [41]

The outcomes of the CABRI, SCARABEE and MOL 7C programs, together with other relevant out-of-pile experiments are summarized in the description of the phenomena governing the fuel relocation and dispersion in a FA:

1) Chemical interaction between fuel and sodium
2) Fuel dispersion and relocation following pin breakup
3) Damage propagation in the pin bundle
4) Pressure drop buildup
5) Fuel dispersion through the interwrapper space
6) Molten fuel freezing
7) Molten steel freezing

4.2.1 Chemical interactions

The chemical reaction between the oxide fuel and the sodium, producing sodium urano-plutonate ($Na_3(U,Pu)O_4$) was well known from the operational experience of sodium fast reactors. This compound has a much lower density than the fuel oxide, generating an important swelling of the pellet. The MOL 7C test series showed the dependency of the formation rate of this compound on burnup and temperature. The maximum swelling rate was measured in the MOL 7C/4 test and corresponded to an increase of 50% of the original pellet diameter in 4 hours. This short-term swelling is not dangerous within the time needed to scram, but can influence the long-term behavior of a degraded pin during a severe accident sequence.

4.2.1.1 R&D needs

LFR

No relevant chemical reactions were observed between fuel, LBE and cladding up to the LBE boiling temperature at atmospheric pressure [42], [43], [44], [45]. Experiments under static pressure must be conducted, considering that the core is submerged. An increase of the Lead/LBE boiling temperature is indeed expected at higher pressure. The Lead and LBE saturation vapor pressure curves have to be validated for pressure higher than the atmospheric one [46].

GFR

Chemical interactions involving carbide fuel, liner, ceramic cladding have to be investigated in GFRs. Thermodynamics calculations [36], considering a W-5Re liner (with 95% W and 5% Re) and UC fuel in thermodynamic equilibrium, showed the formation of a liquid phase at 1880 °C (Figure 8a) . The system liner/cladding is stable up to 1845 °C (Figure 8b), temperature at which a liquid phase appears. When the temperature of the system increases, the amount of solid SiC almost remains constant and the amount of liquid does not increase very much up to 2400 °C (temperature bounding the calculation). Direct contact between the fuel (UC) and the cladding (SiC) may produce instead a liquid phase already at 1600 °C (Figure 8c). Some experimental data are still necessary on cladded fuel in order to assess the time scale at which such interactions can occur in realistic conditions.

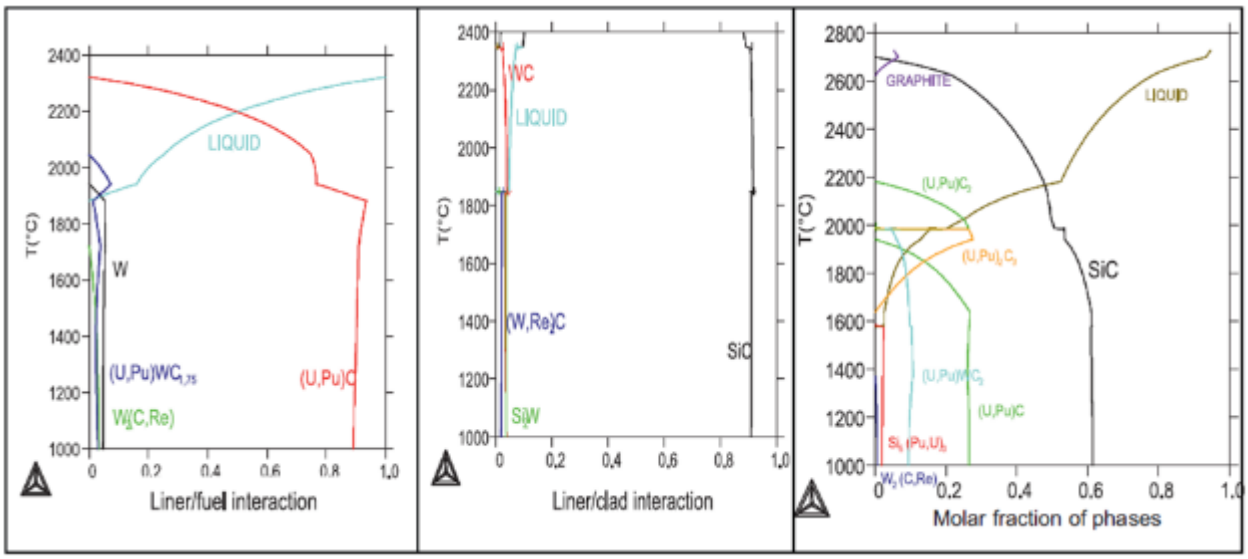

Figure 8: Molar fraction of compounds formed in case of interactions within the fuel assembly as a function of the temperature [36]: a) liner-fuel interaction, b) liner-cladding interaction, c) summary and interaction fuel-cladding

4.2.1.1.1 Chemical interactions between fuel and neutron absorber

SFR

It has been thought to use boron carbide as absorber for the mitigation of severe accident sequences, either from the upper neutron absorbers or from pellets dedicated to these mitigation measures. Preliminary work at CEA [47] and preliminary experiment at COMETA (UJV) [48] have shown that most of the B_4C can volatilize when interacting with UO_2. A major uncertainty for the criticality calculations is the quantity of available neutron absorber present with the degraded fissile material. No quantitative data exists on the volatilization rate and its effect on severe accident kinetics.

LFR

Chemical interactions between Lead/LBE and B_4C have to be investigated for events originating when the reactor is in protected conditions. If the cladding is lost, the absorber pellets are in direct contact with the coolant.

GFR

The issue of chemical interaction with absorber material (B_4C), which is possible at various stages of an accident sequence, must also be considered. One issue is the possibility of formation of volatile boron oxides, which would not remain to ensure neutronic absorption. Experiments are needed to determine the rate at which boron may escape from a molten fuel melt. The results must be coupled to modelling, in order to quantify the impact of these effects on accident energetics.

4.2.2 Fuel dispersion and relocation following pin breakup

Several factors influence the fuel relocation from the pin rupture zone [33]:

1) The amount of retained gas in the pellet
2) The fuel enthalpy and the enthalpy rate at the time of pin breakup
3) The cladding strength (restrained and unrestrained conditions)

4.2.2.1 Amount of retained gas in the pellet

The fission gas release from the fuel matrix to the gas plenum can occur:

- During pre-irradiation phase (steady-state operation);
- During the accidental phase, with increasing pellet temperature and upon fuel melting.

If the amount of gas released to the plenum is already very large in normal operation, the fuel has less possibility to be dragged upwards by the gas flow. During the accidental phase the cladding strength (restrained/unrestrained pins) and the enthalpy rate influence the gas behavior (see following sections).

4.2.2.2 Fuel enthalpy and enthalpy rate

The fuel enthalpy governs the fuel mobility, higher the enthalpy at pin failure, higher the mobility and the possibility to evacuate the fuel from the core.
Lower fuel enthalpies, slightly above the melting value, could cause the molten fuel to froth from the pin breakup point and re-freeze much earlier and closer to the breakup point, reducing the net subchannel flow area and forming blockages. The relocated fuel is almost solid, with a high viscosity, as it is a mixture of molten fuel, fuel chunks and grain-sized fuel particles.

High enthalpy molten fuel in contact with the coolant can instead fragment in droplets, which eventually will freeze, forming particles. The amount of fragmentation depends on the enthalpy of the fuel and on the coolant subcooling degree. The higher the fragmentation, the larger is the following fuel–coolant interaction (FCI). The pressure gradient generated by the FCI contributes to fuel relocation.

A high fuel enthalpy rate increases the fuel mobility as it favors a homogeneous mixing among the components (coolant, gas bubble, liquid fuel droplets) in the ex-pin motion.

When the enthalpy rate is low, the thermal and mechanical disequilibrium are instead dominant, introducing rate dependent phenomenon like momentum transfer (by drag forces) and heat transfer between the components. After the ejection in the subchannel, the flow regime can be either churn or annular, with either the gas or the molten fuel separated from the bulk mixture. The molten fuel can then freeze on the colder walls, forming a crust.

If the fuel enthalpy and enthalpy rate are low, the fuel relocates only within the active region, most likely reaching the border between the disrupted pin region and the intact bundle (unless the buoyancy force plays a role as in the case of HLMs). Blockages are foreseen to form at the boundary region.

If droplets or particles are released in the channel, the enthalpy rate after the breakup can influence the following relocation phase, through the FCI, which converts the fuel thermal energy into mechanical energy of the coolant. FCI is generally enhanced by high thermal energy exchange between the multi-components in the coolant channel.The heat exchange with the coolant can lead to important convection movements relocating the fuel, especially in case of coolant boiling. The convection movements are driven by pressure gradients in the channel. Phenomena influencing the pressure build-up at the interface with the coolant are:

1) coolant volume displacement due to fuel ejection
2) FCI (depending on the molten fuel droplets size and the mixing degree)
3) fission gas expansion
4) coolant boiling

In single-phase coolant channels, the pressure build-up in the coolant surrounding the breakup region is much higher than in two-phase channels, because of the low compressibility of the coolant.

4.2.2.3 Cladding strength

The cladding strength (expression of the mechanical behavior of the cladding) influences the size of the cladding opening at pin breakup and thus the delay between the cladding loss and the fuel release in the subchannel. If the pin breaks up with large openings, a large amount of fuel is released together with fission gases and it can be convected easily outside the core by the fission gases. On the opposite, in case of small breaches, fission gases are released before the fuel ejection and the following fuel ejection will be slow, as the pin is depressurized.

The cladding strength influences also the initial rip propagation. If the cladding is mechanically weak, the propagation is fast, especially if sustained by:

1) high fuel enthalpy increase rate after pin failure (if high, the gas diffusion is faster and the heat transfer from the fuel to the cladding is lower, limiting the cladding expansion)
2) high fission gas retention (potential for melt cavity pressurization and pellet swelling, which will induce mechanical stresses on the cladding)

4.2.2.4 R&D needs

A good prediction of material relocation governed by mass transfer processes is based on reliable equation of states (EOS) and thermophysical properties. Mixed fuel oxides, steel alloys are multi-components in which phase change processes occur within a range of temperatures. Within the melting/freezing (M/F) temperature range, mushy states (mixture of liquid and solid) can be defined to characterize the material behavior, in particular when new mixtures of fuel/steel/gas start forming as the pin starts degrading.
CEA demonstrated the importance of modelling the steel mushy state in the SIMMER III code [49] to better represent the lower steel plug formation in the SCARABEE experiments [50] (see the following sections). It should be assessed if the multicomponent modelling approach reproduces enough correctly the mass, momentum and energy exchanges or if mixtures must be modeled (e.g. foams formed by molten fuel fission gases).

LFR

In HLM reactors it is not likely to have significant amount of molten fuel released in the subchannels, because of the absence of large energetic excursion in the initiating phase of the severe accidents.
Nevertheless, low-priority experiments are needed to characterize molten fuel freezing in LBE and fuel-coolant interaction (see Par. 4.2.5.1).
Reactivity insertion and local heat fluxes to the wrapper wall are dependent on the buoyancy driven relocation of fuel debris. For large amount of particles, the validity of Eulerian-Eulerian models for the interaction particle-fluid (used for example in the SIMMER III code [51]) is questionable and must be assessed with experiments. Furthermore, reliable model predicting fission gas retention and release from the fuel pellet and the fuel fragment should be implemented and validated against experiments in the simulation codes. The gas retained in the fragments determines their density and relocation.

After pellet breakup the additional fragmentation of the initial pellet fragments due to the interaction with the coolant should be investigated (FCI, diffusion of Lead/LBE in the fragments).

4.2.3 Damage propagation in the pin bundle

In the SCARABEE tests, the pin bundle was already damaged few seconds after the total loss of flow event. The clad melting occurred at 5-6 s, following sodium boiling at 2-3 s (Figure 9). The disrupted bundle assumed soon a bottled-up configuration: a first blockage was generated at the bottom of the active length, by the molten steel re-freezing in contact with cold structural material. After fuel melting (8-11 s), a second blockage was generated at the top, at the boundary with the blanket region, due to either small FCI between molten fuel-sodium (if still present) or the expansion of the molten pool following the onset of steel boiling.

The tests showed that the presence of the blanket is an important limit for fuel dispersion. Due to its high thermal capacity the blanket acts as a heat sink, causing the molten steel to freeze and block at the outlet of the active region. If the blanket is removed, the upper steel structure above the active region melts rapidly and the molten pool can expand more than 20% of the initial active length (limiting the risk of reactivity insertion).

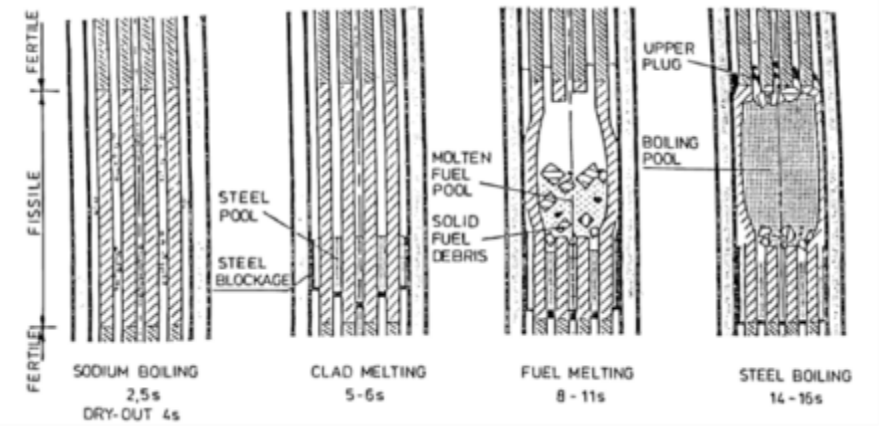

Figure 9: formation of a molten-boiling pool in the SCARABEE-N tests [40]

In all the MOL 7C tests, the degradation started in the blockage region. Differently from what observed in the TREAT experiments, but in line with the SCARABEE-N test series results, there was a net separation between the steel and the fuel degradation phases in fresh pins. The steel melted and refroze at the boundary with the intact and cooled region (blockage-free), forming a crust. The pellet stack did not collapse after the cladding loss (unless unsupported), and started melting later on, because the steel crust prevented sodium to enter and cool down the region. With high-burnup pins, fuel fragmentation was observed in the downward region of the blockage, where the high-velocity fission gas flow interacted with the unclad pellets. In the tests where the cavity extended farther than the blockage region, its growth was stepwise, alternating fuel/steel freezing and melting processes at the boundary of the cavity.

4.2.3.1 Role of fission gases in the damage propagation

The MOL 7C test series showed clearly that the risk of propagation of the original damage from the blockage region to the intact bundle and then the wrapper is much higher in case of high-burnup fuel, because of the presence of the fission gases. The fission gases released in the blocked region after pin failure accumulate in the blockage wake zone, voiding that region from sodium and causing further damage, by cladding dryout and melting. The propagation continues as the sodium flow gradually reduces, due to blockages caused by fuel particles or freezing of molten material relocating from the cavity to the intact bundle.
The amount of retained fission gases influences the pellet breakup in the blockage region. If this amount is relevant, at first the unrestrained pellet swells at temperatures much lower than the melting point and may breakup or melt, as the sodium flow area decreases under the pellet deformation.

4.2.3.2 R&D needs

The impact of fission gases on the heat transfer towards structures in blockage test should be further investigated, also for sodium cooled reactors, considering that no test with irradiated fuel is available in the SCARABEE experimental database.

4.2.4 Pressure drop buildup

In none of the MOL 7C tests the cooling flow decreased below 20% of the original value; flow reduction was mainly due to the molten cavity expansion from the blocked region to the rest of the pin bundle (by stepwise melting and freezing of fuel and steel). Fuel fragmentation and relocation to upward grid spacers or pin subchannels occurred when the fission (or the filling) gas pressure was high. The amount of fuel fragments forming secondary blockages by relocation was very limited, corresponding to 1/7 of the total molten fuel inventory (MOL 7C/6). Pin swelling by formation of urano-plutonate contributed to the pressure drop buildup in the post-transient irradiation phase.

4.2.4.1 R&D needs

LFR

The correct simulation of the pin bundle blockage formation by fuel debris and particles is very important for Lead and LBE reactors. Blockages represent indeed the main obstacles to the fuel dispersion. The blockage formation and growth mechanisms are investigated in the MYRTE EU project (HORIZON 2020) through a series of tests at KIT. A water mock-up with the dimensions of the MYRRHA fuel assembly is being designed at KIT in the KALLA facility [52]. Blockage formation at the inlet grid by lead oxides and its impact on the system pressure drops is also investigated in the MEXICO facility at SCK•CEN [53]. Within the MAXSIMA project, experiments were conducted to assess the risk of single pin failure in different positions (block of the central and the edge subchannel), by low-conductive blockage formation along the wire spacer pitch [54]. New experiments on heated blockages are foreseen in the future. No additional action is then required about this topic for HLM cooled reactors.

SFR (ASTRID)

The existing SFR database must be extended to take into account the new innovative heterogeneous ASTRID CFV core [34]. Its characteristics (narrow hydraulic channel between pins; heterogeneous fuel with a fertile layer between two fissile layers) can lead to different pin and bundle degradation sequences. To study these effects, CEA and the National Nuclear Centre of Kazakhstan are planning the SAIGA series of in-pile experiments in the IGR reactor [35].

4.2.5 Fuel-coolant interaction and wrapper failure

Molten fuel sodium interaction was experienced in the MOL 7C/7 test. It was localized in the cavity region. The cavity pressure was indeed lower than the sodium pressure in the bundle, therefore, upon melting of the cavity steel crust, sodium re-entered in the cavity region and a violent breakup was registered with a peak pressure of 45 bar. If low fuel mass is present inside the cavity an equilibrium in the energy exchange may be reached with the intact cooled region, without the steel crust to re-melt.

In case of total FA blockage, the interaction between fuel and liquid sodium re-entering the blocked FA (Figure 10) can generate an energetic event able to destroy the wrapper and spread the original damage.

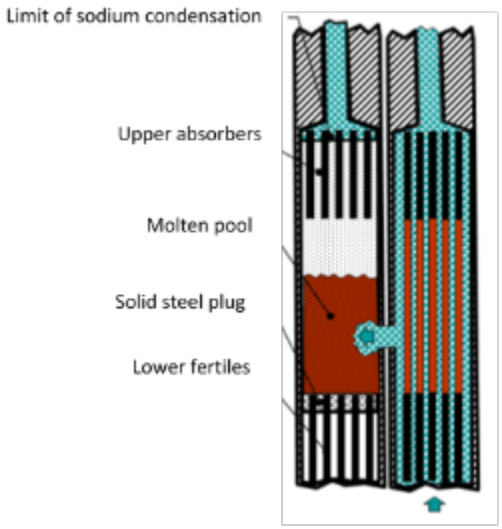

Figure 10: One sodium re-entry scenario [55]

Bird et al. [56] at Winfrith conducted tests in which sodium was mixed with 5 kg thermitic (UO_2-Mo) powder. They observed some pressurization which lasted longer as more sodium capsules where added to the melt. Armstrong et al. [55] [57] at Argonne have conducted 5 tests in which 3 to 7 g of sodium were injected into 30 to 60 g of molten UO_2. Some vapor explosions were obtained but the results are difficult to interpret since they destroyed the instrumentation. It seems that a sodium velocity of more than 5 m/s is necessary for it to penetrate inside the corium pool and lead to some vapor explosion.

Asher [57] conducted at UKAEA Harwell a series of tests in which 1.6 cm^3 of sodium was injected in 80 g of liquid steel (carbon steel and stainless steel). In some tests, energetic vapor explosions have been observed.

Chu et al. [58] conducted some tests within the FRAG series at Sandia National Laboratories, in which 23 kg of 509 °C sodium were injected into 20 kg of UO_2-ZrO_2. They showed that the debris size distribution is equivalent for sodium injected in corium and corium poured in sodium.

Fuel coolant interaction in a blocked sub-assembly by sodium re-entry in the molten pool was also investigated through the MFTF-B test series at UKAEA, since it was considered as the major risk of energetic events in the core. The MFTF facility at UKAEA consisted of a large vessel of 1.77 m^3 containing 1.3 t of sodium and operating up to 3.3 MPa and 600 °C. The UO_2 melt was produced by thermite reaction and reached a temperature of 3600 K. The setup for the B-test series is described in Figure 11 [59]. The sodium and the molten fuel reacted in a prototypical hexagonal wrapper (length: 1 m, flat-to-flat distance 185 mm, thickness: 4.8 mm). Three rupture disks were located at the wrapper top part. Sodium, contained in a storage tank mounted below the wrapper, was injected into the wrapper during the experiment.
Six experiments were conducted, changing the injection height of sodium (above/below the molten fuel pool), the sodium mass (4.5, 6.5 and 14 kg), the sodium subcooling degree (from normal operating temperature 474 °C to saturation, 884 °C) and the disk bursting pressure (0.5 and 1.0 MPa). It was concluded that FCI in one subassembly does not cause significant damage to nearby other subassemblies, especially with sodium at low sub-cooling degree. The amount of material entrained and discharged by the boiling sodium through the discharge disks ranged between 62% and 74% of the total inventory.

Finally, the CORECT test series [59] at CEA Grenoble showed that energetic interactions are possible. CORECT II test 18 was the most energetic of the series leading to a 70 bar pressure peak (18-35 kJ released corresponding to 10-20 kJ/kg of participating UO_2 debris).

The mechanical impact of the vapor bubble generated by such energetic events was studied in tests such as EXCOBULLE [60] at CEA Grenoble.

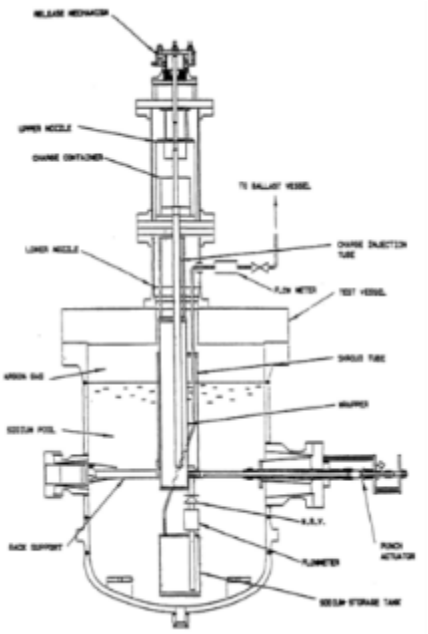

Figure 11: Experimental setup of the MFTF-B test series [61]

It can be considered that a sufficient database exists for the validation of codes in this sodium re-entry configuration so that no further experimental program is to be planned. This conclusion may be re-assessed in the future when the SCONE sodium-FCI code will have been tested against these experiments.

Structural damages due to FCI were also detected in the SCARABEE PI-A test, as the molten fuel from the blocked FA entered in contact with the sodium from the neighboring FA space [40]. In all the tests pressure events following FCI were mild and able to destroy only already eroded walls.

4.2.5.1 R&D needs

The fuel coolant interaction is present only in liquid-metal cooled fast reactors.

LFR

Whilst for SFRs a large database is available, no experimental database exists on FCI in Lead/LBE environment. In LOF scenarios, the cladding is lost before the fuel starts melting, because of the absence of positive reactivity feedbacks. Therefore, only fuel fragments are released in the coolant.
Even if some solid fuel fragments have a temperature higher than the boiling temperature of the coolant an energetic FCI cannot occur since it requires a liquid much hotter than the coolant, like molten fuel.
In case of RIAs, power excursions that are large and fast enough to cause extended fuel melting before the pin breaks up are unlikely. Nevertheless, it cannot be excluded that some molten fuel can be released in the subchannels. The possibility of FCI occurrence has to be investigated for Lead/LBE systems, but with lower priority than other phenomena.

4.2.6 Molten fuel freezing

In order to avoid the risk of strong reactivity insertion due to fuel relocation, design solutions meant to facilitate the fuel escape from the core are being proposed in Gen-IV sodium fast reactors. Bypass non-heated channels, connecting the core to the lower plenum are possible escape paths for molten fuel, unless blockages due to fuel/steel freezing form in the channel. The so-called “penetration length” is a

parameter that measures the efficiency of the fuel dispersal in a duct. It corresponds to the length that the molten fuel can travel in a duct, before stopping completely by freezing.

Several out-of-pile tests were carried out in a European framework, between the 80's and the 90's. The experimental programs investigating the freezing in subassemblies and, in general, in presence of structures (tubes or pin bundles) are listed below [61] :

1) FARO-BLOKKER (JRC-Ispra)
2) SMPR,LMPR,MFTF (UKEA)
3) GEYSER, SIGELCO, BULLAGE (CEA Grenoble)

The FARO furnace was designed to produce 100 kg of molten UO_2 at around 3000°C, by Joule heating. The main objectives of the FARO programme included studies on molten-fuel pools (FARO furnace), fuel impact and erosion on stainless steel structures (BLOKKER I test section), fuel freezing and blockage in channels and pin bundle (BLOKKER II test section - Figure 12b) and fuel jet stability and fragmentation of large masses in sodium (TERMOS test section).

The GEYSER tests were performed at CEA Grenoble. The installation consisted of a pool of liquid UO_2 at 3000 °C in which a steel tube was lowered, with inner diameter of 4 mm and outer diameter of 8 mm (Figure 12a) .The UO_2 was injected upwards inside the tube by a differential pressure between the pool and the tube outlet. The steel tubes were initially at room temperature (20 °C, except for Tests 7 and 8 in which the wall temperature was elevated to 1000 °C on the first 30 cm at the inlet). The differential pressure and the injection conditions were varied in different tests.

The tests were scheduled as follow:

- 13 tests involving molten UO_2 injection in tubes of different temperatures and diameters and four different injection pressures.
- 3 tests using molten UO_2 radial injection into a bundle (the MINIGRAPPE series, similar to the MFTF tests).
- 4 tests implementing molten UO_2 injection in a test section simulating the upper breeder zone of the core (ODAXIEU series).
- 1 test with boiling steel injection into a tube.

The main results can be summarized as follows:

1. Tube experiments: the penetration length lies between the lengths predicted by assuming either bulk freezing or conduction freezing.
2. Upper axial injections: the penetration length is about 30 cm and does not seem to depend strongly on the driving pressure (in the range between 3 to 10 bar) and on the initial steel temperature.
3. Bundle radial injections: full penetration (20 rows) was observed for a 10 bar driving pressure.

The BLOKKER II tests (Figure 12b) were conducted at JRC Ispra. In these tests, liquid UO_2 at about 3000 °C was injected into a steel structure from above. The structure contained four rectangular and one circular channels, with different hydraulic diameters, as shown in Figure 12b. A twisted section was also implemented, to simulate the flow of the melt in the inter-subassembly gap.
It was shown that the presence of the twist along the channel strongly reduced the penetration length.

Straight rectangular channels were found to have a greater draining capability compared to circular channels. The results on the penetration length were in line with the GEYSER ones.

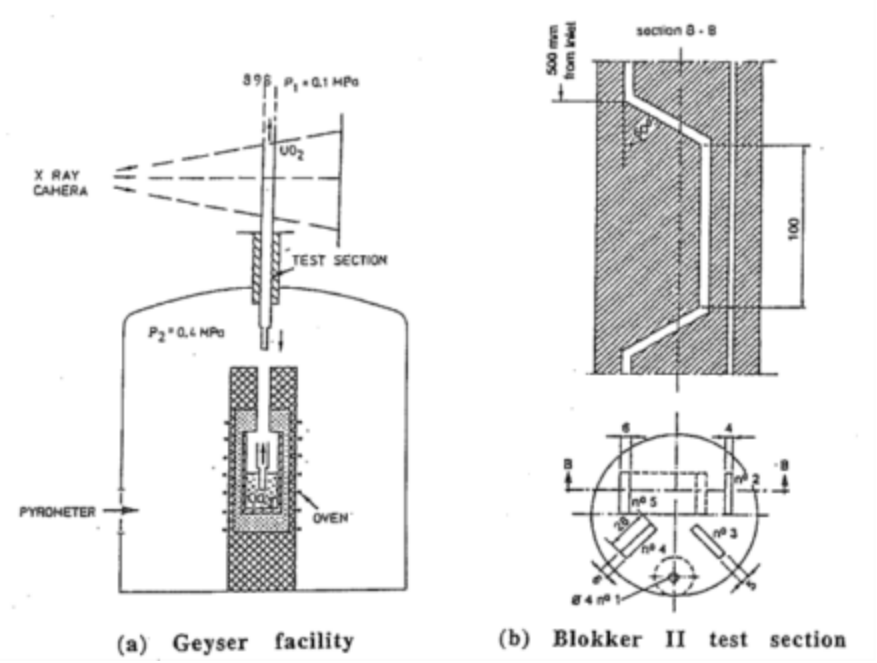

Figure 12: sketch of the (a) GEYSER experimental facility and (b) Blokker II test section [61]

From the post-test irradiation analyses of the GEYSER experiments, three different freezing zones could be identified along a pipe [62]:

1) An equally-axed crystal zone at the leading edge of the melt, originated most likely by a bulk freezing process;
2) A columnar crystal zone, oriented in the flow direction, result of a conduction-limited freezing, due to the presence of the wall;
3) A gross crystallization zone, occurring downward when the flow stops.

The three different zones are visualized in Figure 13.

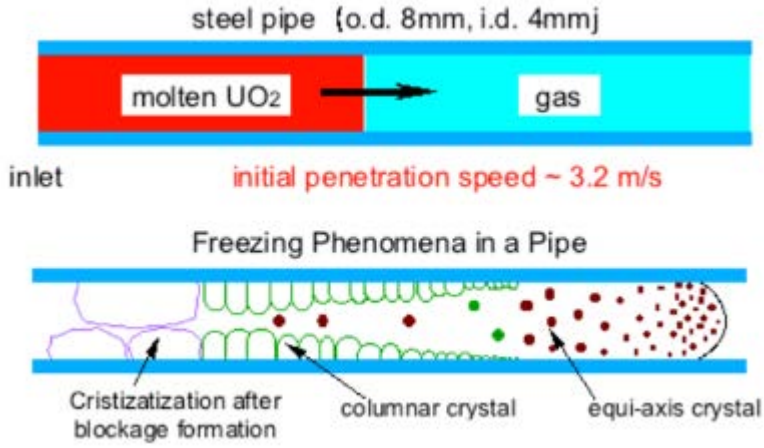

Figure 13: different crystallization during the penetration of molten UO_2 along a tube [58]

The microstructural differences explain why the experimental values of penetration length were in between the predictions of pure bulk or conduction-limited models. Moreover, the existence of significant thermal contact resistance, favouring the flow of molten fuel, has been observed and modelled [63].

4.2.6.1 R&D needs

SFR, GFR

No further actions are foreseen for molten oxide fuel except in relation with corium discharge tubes (Par. 5.1.1).

LFR

Molten fuel freezing in Lead/LBE occurs as soon as the molten fuel is released in the subchannel. The freezing mechanism should be studied in function of the fuel mobility. For high mobility, the molten fuel should be easily dispersed in Lead/LBE with predominance of bulk freezing, with generation of particles. For low mobility, the molten fuel could freeze in layers, at the very proximity of the failure, forming a crust on the still intact cladding.

4.2.7 Molten steel freezing

Steel freezing onto a structure is influenced by the medium in which the molten steel is flowing. Out-of-pile tests performed at Kyushu University [64] studied the freezing of molten stainless steel onto a wall in different media. Several tests were made, changing the wall material (stainless steel and copper), the medium (water and air) and the molten steel mass flow rate. Wood metal was chosen as the simulant melt (with properties similar to the stainless steel ones).

While only one freezing mode was observed for the experiments in air, freezing in water is characterized by several modes.

A series of simulation experiments at atmospheric pressure was conducted changing the coolant temperature and the volume and temperature of the melt. The penetration length and width were measured in the air-cooled experiments, whereas penetration length and the proportions of adhering frozen metal on the total one were measured in water coolant experiment. The melt flow and distribution were filmed by a high-speed video camera.

The experimental setup is shown in Figure 14. The length of the L-shaped metal structure is 80 cm.

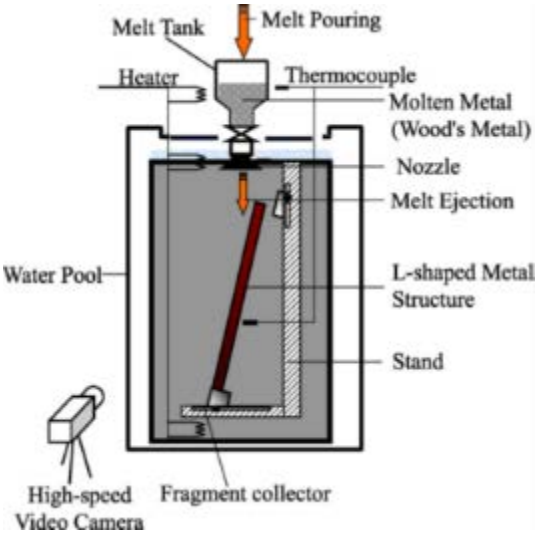

Figure 14: experimental setup of the molten metal freezing experiment [64]

In the case of the air experiment, and stainless steel wall, an elongated and thin crust adhered on the structure.

From the visual information gathered from the experiments in water, it was clear that only a fraction of the molten metal had frozen on the wall and a significant proportion of frozen metal broke up and fell down in fragments. The maximum proportion of adhered frozen metal was found to be 27% on a copper structure and 23% on a stainless steel structure.
The water experiments with stainless steel structure were carried with a melt mass flow rate of 110 g/s, with temperature ranging between 90 °C and 120 °C. The water temperature ranged between 50 °C and 60 °C. The mass of melt was 200 g in all the tests. For a melt temperature of 92 °C the test was repeated with a mass of 350 g.
The dependency of the penetration length on the mass of poured melt is much more relevant than the one on water temperature and melt temperature (Figure 15).

Mainly two dominant different freezing mechanisms (A, B - Figure 16) were identified in the water experiments, for different combination of water and melt temperature, on the base of the characteristics of the frozen metal adhered on the structure and the collected debris. A variant of the mode A, named mode C, was discovered for the maximum water coolant temperature (60 °C) and for high superheating of the melt (melt temperature above 100 °C).

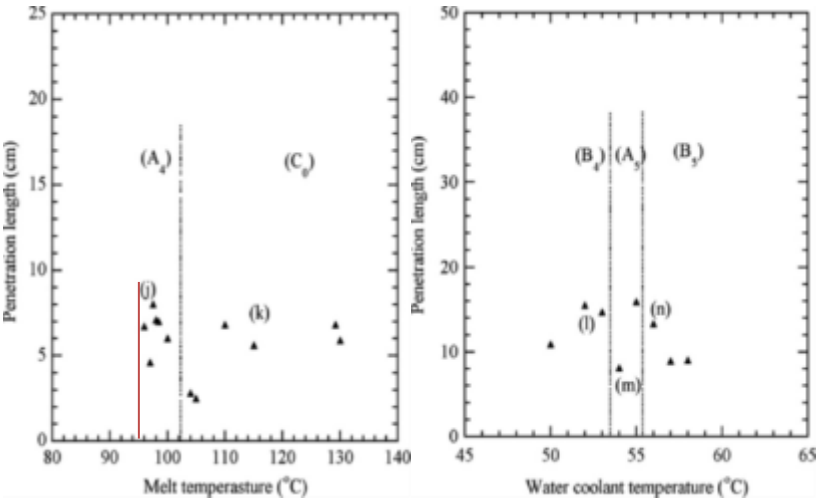

Figure 15 [64]: a) dependency on the penetration length of frozen steel on the melt temperature; mass of poured steel = 200 g. b) dependency on the penetration length of frozen steel on the water coolant temperature; melt temperature = 92 °C, mass of poured steel = 350 g

All the three freezing modes are characterized by an initial quenching with particle generation as the melt starts interacting with the water. Figure 16 describes the freezing process that leads to the full blockage of the steel melt, for the freezing mode A and B. Freezing mode C differs from freezing mode A just for the shape of the frozen steel fragments (see below). As the flow starts decreasing, the different melt temperature and the temperature difference between the melt and the wall influence the shape and size of the debris. Sheet-like debris are typical for the A mode, while larger size particles are typical for the B mode. As the flow reduces, the melt adheres to the wall and a frozen layer starts forming, which rapidly leads to the full blockage of the channel. In the A mode, the building-up of the frozen layer on the wall occurs in sheet-like layers and gradually extends to the whole section, whereas in the B mode, the adhesion starts all-at-once due to the enhanced viscosity caused by the large frozen debris. The freezing continues by layers piling-up on the original one. Downstream, the crust can detach in fragments (A) or in big pieces (B). In the mode C, the adhesion to the wall is in sheet-like layers as the A mode, but it is more rapid (without the typical cusp-shaped frozen crust).

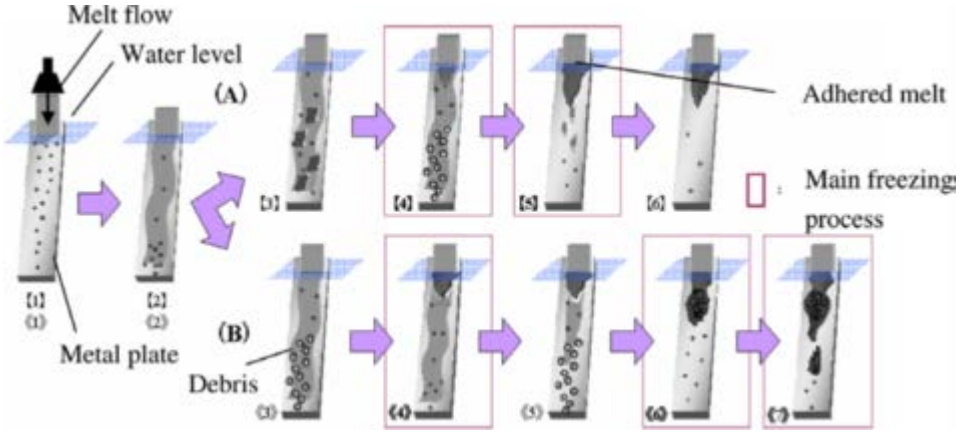

Figure 16 : typical phases of molten steel freezing mode A and B up to the full melt blockage [64]

The maximum penetration length of molten metal in the air coolant experiment was found to be 74 cm, whereas in the water coolant experiment it was found to be 17.4 cm, which is 4.25 times shorter than in the air coolant experiment.
In the air experiments, most of the frozen metal adhered to the structure while in the water experiments, this amount was limited to maximum 27%. Furthermore, in the water experiments, rapid cooling occurred as result of the efficient heat exchange between the water and the structure, resulting in a short penetration length and a large amount of debris, whereas, in the air experiments, cooling occurred mainly in contact with the structure and, as a result, longer penetration lengths were observed.

4.2.7.1 R&D needs

SFR, GFR
No further action foreseen except in relation with corium discharge tubes (ASTRID design, [22])

LFR
The results of the water experiments showed that steel onto a structure in a liquid mean can freeze in different modes, generating a combination of steel particles and frozen steel deposition on the wall. Furthermore, the penetration length reduction, compared to air experiments is relevant (4 times less). These tests are meaningful for Lead/LBE cooled reactors, where molten steel may freeze in contact with the coolant on the neighboring FA wrapper wall or in the upper intact bundle region (on cladding and wrapper wall), where it is relocated by buoyancy. Other experiments with Lead/LBE shall be performed injecting steel from the bottom, to simulate the buoyancy-driven motion of molten steel in Lead/LBE pools. For steel freezing in the pin bundle region, the wire spacers shall be taken into account, because they reduce the penetration length of the molten steel, as shown by the Blokker II tests with molten fuel (see Par. 4.2.6). Similar experiments in a pool test section shall be done to assess bulk freezing and the shape of the frozen steel.

4.2.8 Corium discharge

Molten fuel relocation out of the core reduces the possibility of severe re-criticality events. In-core channels with large hydraulic diameters such as control rod guide tubes (CRGTs) are potential discharge paths. The CAMEL C6 and C7 tests at ANL [65], [66] addressed corium relocation through CRGTs (Figure 17). In these tests, approximately 2 kg of molten uranium dioxide (UO_2) was generated by thermite reaction and injected into a tube that simulated the CRGT of the Clinch River Breeder Reactor design. The experimental results showed that as soon as the molten UO_2 was injected into the tube, it vaporized liquid sodium in the tube and the coolant vapor pushed liquid sodium out of the tube. Such coolant-void development is an effective phenomenon for corium discharge, since if a large quantity of liquid coolant stays within the discharge path, corium discharge would be inhibited by inevitable corium freezing. However, due to the limited amount of molten UO_2 in the CAMEL tests, there was insufficient information on corium discharge through in-core channels.

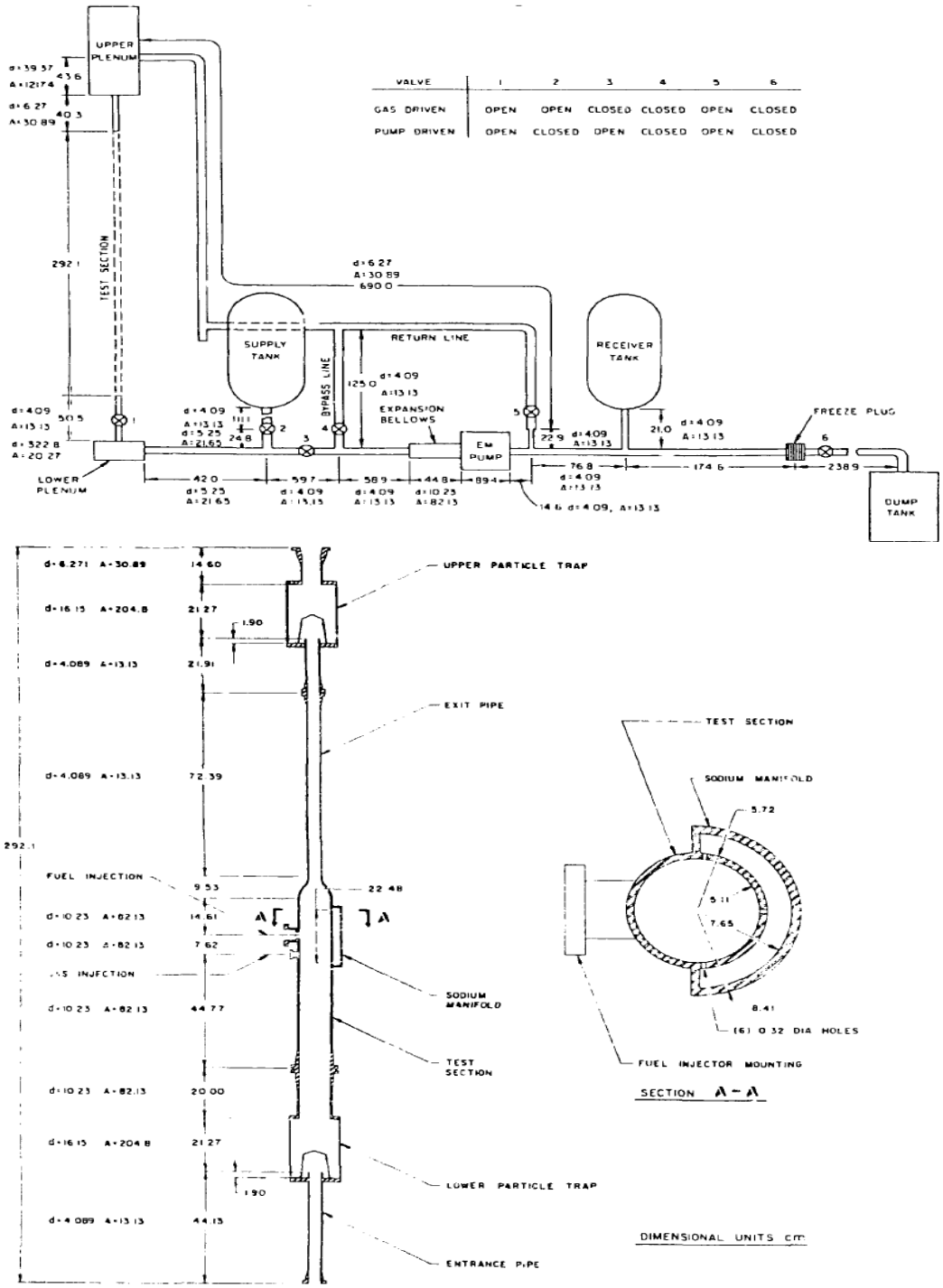

Figure 17: schematic of CAMEL loop (top) and test section (bottom) [66]

In order to clarify fundamental mechanisms that dominate corium discharge through in-core coolant channels, Kamiyama et al. [67] conducted an experimental study using simulant materials, including a low-melting-point alloy and alumina (Al_2O_3), at the MELT facility (Figure 18) of JAEA and at the EAGLE out-of-pile test facility (Figure 19) of the National Nuclear Center of the Republic of Kazakhstan (NNC/RK). These experiments showed that the discharge path could be entirely voided by the vaporization of a part of the

coolant at the initial corium-discharge phase, followed by coolant vapor expansion and corium penetration into the voided channel (Figure 20). These experiments covered mainly the corium discharge in Fuel Assembly with Inner Duct Structure (FAIDUS) designed for JSFR, rather than through CRGTs, but it can be concluded that the inhibitory effects of the liquid sodium on corium discharge were limited in in-core coolant channels. However, due to the existence of internal structures such as flow regulating mechanism in CRGT, there remain uncertainties on corium relocation.

To enable corium discharge, molten corium has to break through such internal structures without forming a blockage. Hence, in order to improve the experimental database, JAEA has recently started a new experimental program using EAGLE out-of-pile and in-pile test facilities of NNC/RK.

It can be concluded that a sufficient database on this matter will be created through existing experimental programs, including EAGLE tests. However, additional experimental needs and test conditions specific of the ASTRID reactor will be clarified through the future assessment of corium relocation. These additional tests are needed because of the particular features of the CFV core design, in particular of the two fissile zones separated by a fertile zone and design of the corium transfer tubes (DCS-M-TT [22]) through the core supporting structures.

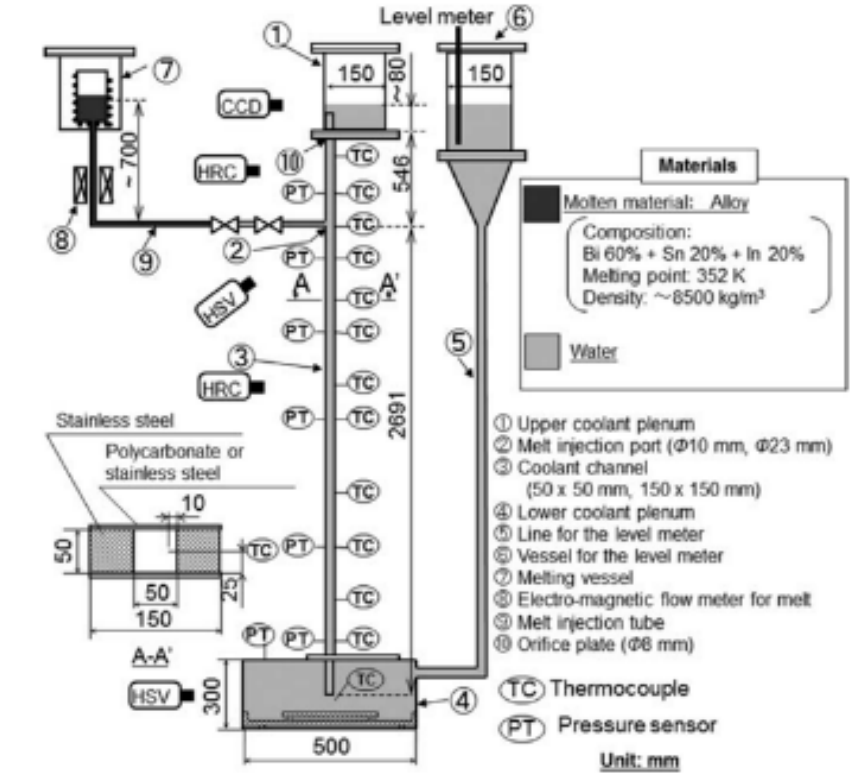

Figure 18: Schematic of MELT facility [67]

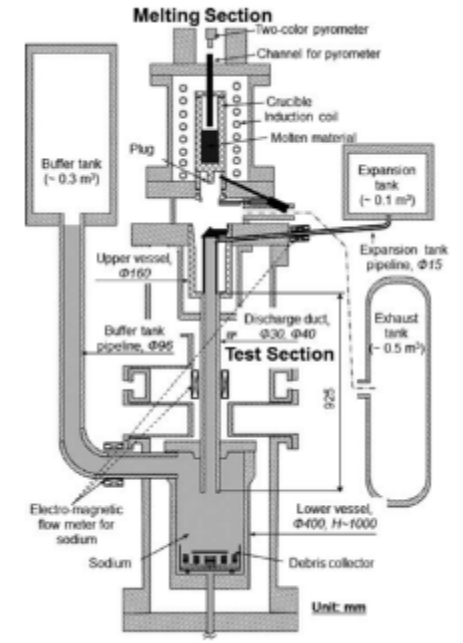

Figure 19: Schematic of EAGLE out-of-pile test facility [67]

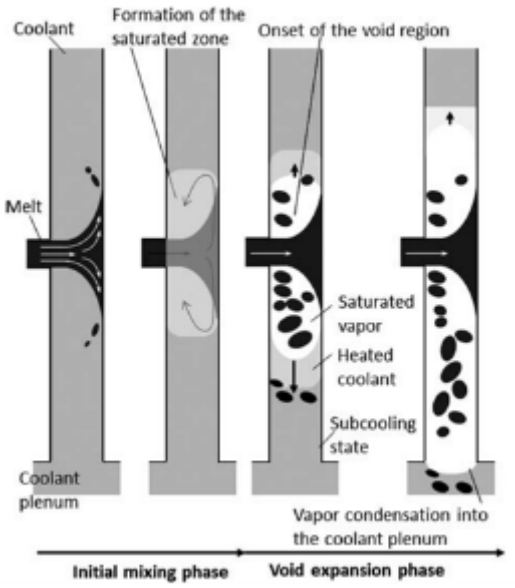

Figure 20: Schematic of a mechanism for corium relocation through a discharge tube [67]

4.2.8.1 R&D needs for ASTRID

The Corium discharge process is influenced by the core internal design. For ASTRID a validation of the engineered corium relocation process (powered by fuel coolant interaction) for large scale experiment will be needed, while small-scale in-pile experiments to validate the corium discharge from the core area to the lower plenum are already planned and close to those performed for the Japanese FAIDUS concept [68].

4.2.8.1.1 PLINIUS2-TR

Experiments performed in the PLINIUS2 facility (see Par. 6.2.2), on corium transfer, in the ASTRID corium transfer tubes (DCS-M-TT [22]), will aim at demonstrating the operation of these tubes at a scale close to 1. Molten corium will be introduced in a sodium-filled tube and will relocate to a zone simulating the lower plenum.

4.3 Molten pool dynamics and wrapper failure

When a molten pool is formed in a disrupted pin bundle, it can extend radially to the neighboring FAs by failure of the confining walls (thermal or mechanical failures). An estimation of the heat flux distribution along the wrapper wall and the pressure build-up is then needed to predict wrapper failure.
The density difference influences the pool configuration and the heat fluxes towards the wrapper wall.

The dynamics of a two-component and two-phase boiling pool was investigated in the SCARABEE BF test series with the support of preliminary out-of-pile tests on a two-component boiling water pool, carried out in the SEBULON facility (CEA) [69].
From the SEBULON test, it was possible to characterize the behavior of a two-phase boiling pool and explain in general the axial distribution of the heat flux along the wall. Extrapolation to different pool size, power level, fluids were also possible.
Figure 21 shows a representation of the two-phase boiling pool developed in the SEBULON test [69].

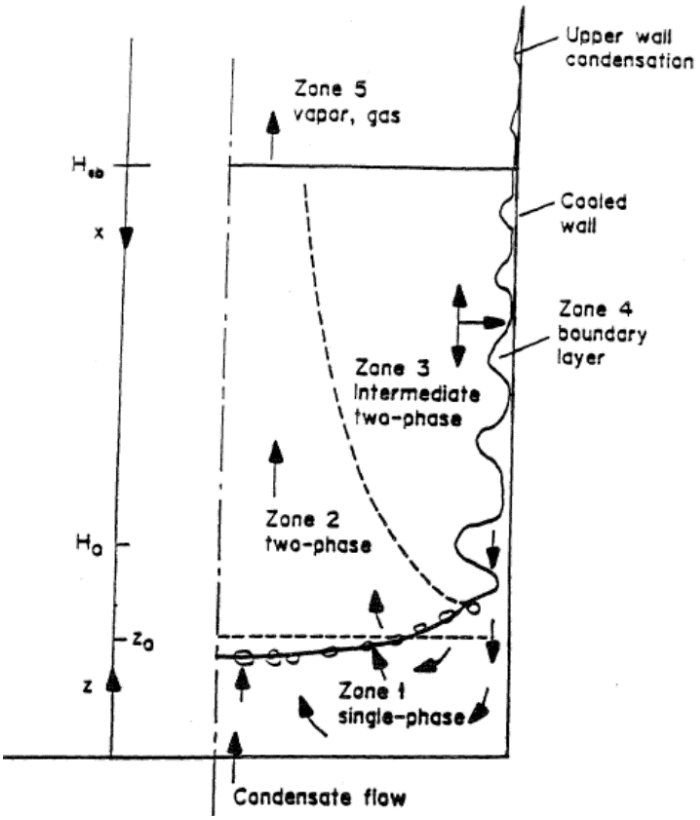

Figure 21: mixed UO_2-steel boiling pool characterization [69]

Zone 1 is a single-phase zone, which is fed by the condensed liquid draining along the wall boundary layer. The height of this region increases as the power decreases.
The actual boiling pool consist of two zones, zone 2 and 3, characterized by different dynamics. Zone 2 is the inner part of the pool, where an upward two-phase flow establishes, while in zone 3, the outer part, close to the wall, the flow direction is unstable (oscillating in the axial and radial directions, in tight connection with the oscillations in the boundary layer zone).
Zone 4 is the boundary layer, which, differently from a classical two-phase flow regime, has an oscillating behavior. Liquid waves propagate downwards toward the single-phase region, interspersed by a very thin liquid layers regions (below 1 mm). In the wake zone of the waves there is evidence of vapor condensation from the boiling pool (subtracted from the dispersed vapor). Both condensation and convection contribute to the heat transfer at the pool walls. Condensation at the wall becomes the dominant heat transfer mechanism at high power.

Zone 5 is the top vapor region, where the vapor flows out of the pool. The mass flow rate corresponds to the difference between the steel vapor generation rate in the pool and the steel condensation rate on the lateral walls.

4.3.1.1 Heat transfer along the pool wall

The MESCLA model [70] prediction of the average heat transfer towards the wall was in good agreement with the experimental results of the SEBULON and SCARABEE tests, under the assumption of homogeneous boiling in the whole pool and 1-D geometry:

$$\mathrm{Nu} = 0.0388 K_{BB}\,\mathrm{Ra}^{0.4}$$

where:

Ra is the Rayleigh number
K_{BB} is an experimental coefficient, which depends on the material or mixture of the pool.

The ZEBUL model [71] can also predict the axial distribution of the heat flux, which depends on the material distribution in the pool.
The comparison study between the measured heat flux, the predictions of the ZEBUL and MESCLA models and the AFDM code (nowadays SIMMER code) of the BF3 SCARABEE test helped in understanding the mixing process between steel and fuel.
The molten steel, which generates before molten fuel, deposits at the bottom of the pool. Above the steel pool a molten fuel pool is formed, separated by fuel debris and crust from the steel pool (Figure 22). In the boiling region of the pool, fuel and steel are not homogeneously mixed and some uncertainties remain on the influence of the stainless steel on the heat transfer towards the wall. The AFDM gave a representation that is coherent with the experimental observation on wall heat fluxes and temperature distribution in the pool [40]: the residual molten steel tends to deposit on the walls, enhancing the wall heat transfer and limiting the temperature increase in the center of the UO_2 pool, below the saturation point.

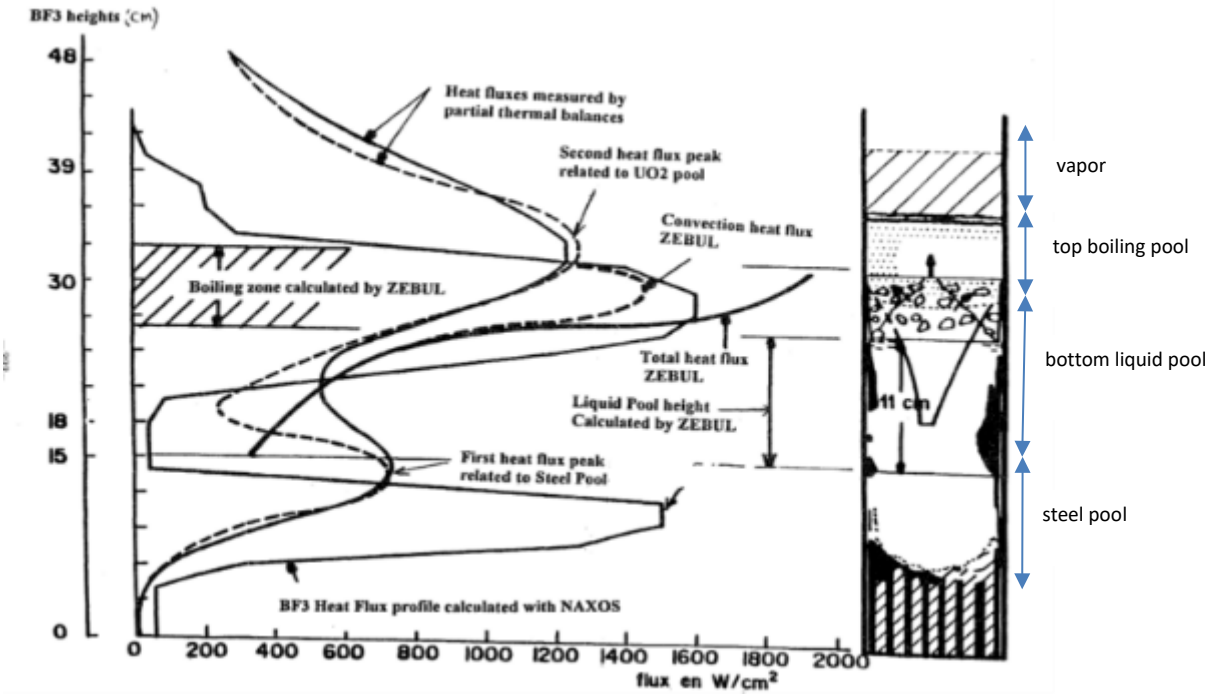

Figure 22: Heat flux distribution along the wall of the SCARABEE-BF3 test section [69]

4.3.2 Wrapper failure

In the SCARABEE-N experiments no ablation of the wrapper occurred in contact with the molten fuel, but a crust of fuel was formed. The steel behind the crust gradually melted and drained down so that the wrapper was gradually replaced by the fuel crust. This process occurs for heat fluxes below 1000 W/cm^2 and up to a minimum thickness below which the wrapper collapses by mechanical stresses. The wrapper melt-through revealed to be a strongly non axial-symmetrical phenomenon [70], even when the experimental device internals were axial-symmetric.
No mechanical rupture was observed, because no strong pressure build-up was registered in the blocked FAs. With irradiated pins the situation may be different; if the fission gases cannot escape from the blocked FA the pressure may increase considerably, once they expand in the FA bundle.

4.3.2.1 R&D needs

No further experiments are needed for this topic, but further code development is needed to represent the wrapper melt-through.

4.3.3 Fuel dispersion through the interwrapper gap

In the SCARABEE-N test series the interwrapper flow did not play any role in removing the fuel, because the molten steel released in the interwrapper space formed tight blockages in the interassembly space (hydraulic diameter equal to 12 mm), by re-freezing onto the upward intact cold wrapper walls.

4.3.3.1 R&D needs

SFR
No further actions must be taken for sodium cooled reactors.

LFR
Similar tests should be performed with Lead/LBE. After the wrapper is lost, molten steel is expected to propagate radially only if the internal FA pressure is higher than the interwrapper space pressure, otherwise it should escape axially from the FA by buoyancy. The steel freezing mechanism in the interwrapper gap may be different from the sodium case, because no strong FCI is foreseen to occur in the interwrapper space between fuel particles and coolant, and the steel remains always mixed with the Lead/LBE, leading to possible combined bulk and wall freezing.

GFR
In case of a FA blockage in gas cooled reactors, the freezing mechanism should not differ from the one observed in the SCARABEE-N tests.

4.3.4 Molten pool radial propagation to the neighboring FAs

The SCARABEE tests showed that, if the interwrapper space is blocked, the molten fuel pool can enter the neighboring intact bundles, under certain conditions: partial loss of flow in the neighboring bundles and heat fluxes at the neighboring wrapper wall reaching 1000 W/cm^2. The propagation is rapid and leads to the total blockage and destruction of the bundle. The process is stepwise. The incoming melt first blocks in the first row of pins, by freezing on the cladding walls; the blockage is initially tight, but it is weakened when the cladding starts melting and then it is broken by the pressure spikes caused by the interaction between the molten material and the sodium. When the blockage is removed the melt propagates farther

and freezes on the cladding wall of the second pin row. The drop of the sodium flow, due to the blockages, accelerates the bundle degradation that becomes completely blocked in less than 1 s.

4.3.4.1 R&D needs

SFR, GFR

No further actions are foreseen, except for ASTRID design to take into account the effects of the subassembly geometry with possibility of having a fertile layer between 2 molten fissile layers, for which the planned SAIGA experiments [35] can provide some insights.

LFR

In Lead/LBE cooled reactors a molten-boiling pool cannot form without strong energetic excursions of power. Permanent voiding by fission gases is not realistic, because even in presence of a FA blockage at the top of the active length, a minimum residual porosity guarantees the gas escape.

4.4 Summary of the phenomena occurring in the core degradation phase

The phenomena described in Chapter 4 are listed in Table 4.

In column 2 the main investigation field is presented. Relevant phenomena addressed in Chapter 4 are gathered under each field (column 3). The specific phenomena to be investigated with experiments are found in column 4. Past and operating relevant experimental campaign and facilities are reported in column 5.

Table 4: List of phenomena occurring in the core degradation phase

Nº	Investigation field	Phenomenon	Need for R&D	Past/Operating/ experimental facility (Owner Institution)
1	pin failure by overpower	transient pellet swelling, inner cladding corrosion (JOG), fuel melting, cladding cracking	Needs: 1) Prototypical neutron flux distribution 2) LFR: database extension at lower cladding temperature values (HLM reactors – minimum value 200 °C) and lower linear power 3) LFR: experiments in Lead/LBE environment to investigate any short-term corrosion assisted failure 4) GFR: experiments with cladding ceramic materials (SiC/SiC_f) 5) Need for data on the cladding breach dimension 6) SFR: testing of new pin concept (ASTRID)	TREAT (INL) EBR-II-TOP (INL) CABRI (CEA) IGR-SAIGA (NNC)

2	Pin failure by loss of cooling	Cladding mechanical degradation, burst and creep failure, corrosion	1) LFR: assessing cladding mechanical degradation up to cladding melting in wetted conditions. 2) LFR: experiments in Lead/LBE environment to investigate any short-term corrosion assisted failure. 3) LFR: Need for data regarding the cladding breach dimension, to be used for representative experiments for fuel-coolant interactions, and to determine possible fuel particle sizes escaping from the breach. 4) GFR: experiments with metallic and ceramic cladding materials.	TREAT (INL) CABRI (CEA) IGR-SAIGA (NNC)
3	GFR: pin failure by cladding nitriding	Cladding embrittlement due to the reaction with nitrogen	Representative experiments of GFR accidental scenario, to determine the reaction rate.	
4	GFR: pin failure due to axial thermal stresses	High axial temperature gradient of the fuel pin caused by injection of cold gas into the core	Experimental tests with representative temperature gradients to establish maximum allowed temperature gradient over the pin.	
5	Pellet status after cladding loss	Fragmentation LFR: Lead/LBE interaction with the fuel pellet (corrosion/erosion)	Need for an assessment of both fresh and irradiated fuel. LFR: experiments in natural circulation.	TREAT (INL) CABRI (CEA)

6	Chemical reactions	Fuel-clad-coolant interactions	LFR: Experiments to be extended at temperatures higher than the LBE boiling point at atmospheric pressure. GFR: phase diagram characterization of the system fuel-liner-cladding at high temperatures.	Crucible tests performed at JRC-Karlsruhe and at Chalmers University (SEARCH and MAXSIMA EU projects)
		Absorber-fuel interactions	SFR, GFR: volatilization rate of B_4C in contact with molten fuel.	
		Absorber-coolant interactions	LFR: interaction experiments above steel melting point.	
7	Impact of fission gases on the damage propagation	Degradation of the heat transfer towards structures due to fission gases	Validation of simulation codes, by SCARABEE-type tests with irradiated fuel.	
8	SFR, LFR: Fuel coolant interaction	1) Vaporization/Condensation (V/C) 2) Melting/Freezing (M/F) 3) Flow characterization	SFR: Extension to low subcooling degrees of sodium and larger masses of corium. The main risk in this phase comes from sodium re-entering into blocked fuel assemblies.	FARO-TERMOS, BETULLA (JRC) MFTF-B (UKAEA), CORECT (CEA), EXCOBULLE (CEA)

			LFR: a series of tests should be planned to study the FCI caused by a local release of molten fuel or fuel particles in Lead/LBE with temperature higher than the Lead/LBE boiling temperature.	CABRI-TPA2 (CEA) MELT (JAEA) SOFI (IGCAR) PLUTON (IPPE) PLINIUS2 (CEA, planned) DROP-Na (CEA, planned)
9	EOS functions and thermo-physical properties of materials in a degraded core	Thermophysical properties of steel mushy state and mixture fuel-gas-steel	SFR: Code development	CABRI (CEA) ACRR (SNL) TREAT-SLSF(INL) SCARABEE (CEA)
		LFR: - Lead/LBE saturation pressure curve - stainless steel behavior in Lead/LBE at high temperatures	Validation at pressure higher than the atmospheric one Experimental data are missing in the range of temperatures between the sodium boiling temperature at atmospheric pressure and the steel melting point.	
		GFR: EOS functions for ceramic materials		

10	Molten fuel freezing	Molten fuel freezing mode	SFR, GFR: No further actions LFR: experiments aimed to study the impact of Lead/LBE on the freezing process.	THEFIS, SIMBATH (FZK) GEYSER, SIGELCO (CEA) FARO-BLOKKER II (JRC) CABRI-EFM1(CEA) ACRR-TRAN (SNL) MOL 7C (SCK•CEN) SHOTGUN, LID, GAPFLOW (ANL)
11	Molten steel freezing	SFR,GFR: no further action, except for ASTRID corium discharge tubes (see issue n°14) LFR: Steel relocation and freezing mechanisms in Lead/LBE	Freezing on structures in Lead/LBE and bulk freezing must be investigated.	SCARABEE, GEYSER (CEA) THEFIS (KIT) Wood tests at Kyushu University
12	LFR: Relocation and mixing of fuel debris in Lead/LBE	Fission gas distribution in the pellet fragments Further fragmentation due to the interaction with the coolant (FCI, diffusion of Lead/LBE in the pellet fragments)	Validation of models predicting the gas release when the pellet breaks up in fragments Out-of-pile experiments with injection of fuel /simulant particles in Lead/LBE at different temperatures.	

13	LFR: Validation of models predicting blockage formation by particles in the pin bundle and grids	Mechanical blockages	Experiments in different flow regime for several matrix shapes (loop).	KALLA (KIT) MEXICO (SCK•CEN)
14	SFR, GFR: Corium discharge	Corium discharge through transfer devices	Qualification experiments of the transfer devices.	IGR (NNC)
15	SFR: Boiling pool dynamics and propagation	Heat transfer Flow regime Mixing fuel-steel	ASTRID: the design should take into account the possibility of having a pool with a fertile layer in between two fissile layers.	SCARABEE-N, SLOSH, SEBULON (CEA)
16	Wrapper failure	Wrapper melt-through	Improvement of code simulation capability.	SCARABEE (CEA) MFTF-B (AEA) EXCOBULLE tests (CEA)

5 Phenomena occurring in the post-accident phase

The post-accident phase is characterized by the corium and core debris relocation in the reactor plenum. All the phenomena identified influence the vessel integrity and the design of severe accident mitigation devices, such as core catchers and post-accident heat removal systems.

Several investigation fields can be identified in the post-accident phase:

1) Fuel-coolant interaction in the plenum
2) Phenomena related to the core catcher design
3) Debris bed coolability
4) Post-accident decay heat removal

Corium coolant interaction in the plenum is mainly relevant for SFRs, because in LFRs only fuel debris and particles are expected to exit the core region, as the coolant maintains its liquid phase. The size distribution of debris and particles coming out of the core region is mainly determined by the core degradation phase, even if a finer fragmentation might be possible when the particles encounter cold LBE. No energetic events are expected to happen, because of the low temperature of the debris and the high boiling point of Lead/LBE.

The R&D needs for the core catcher design vary for each reactor design (ASTRID, MYRRHA, ALLEGRO), therefore dedicated sections have been foreseen for each project.

5.1 Fuel Coolant Interaction in the plenum

Caldarola [72] and then Berthoud et al. [59], [73] published in the past summary papers on sodium-UO_2 interaction experiments, which served as a basis for the state of the art on the fuel-sodium interaction knowledge.

A vapor explosion (or energetic fuel-coolant interactions, FCIs) is a process in which hot liquid (fuel) transfers its internal energy to colder, more volatile liquid (coolant). The coolant vaporizes at high pressure, expands and does work on its surroundings. From the works of Board & Hall [74], the energetic fuel-coolant interactions could be distinguished in subsequent stages:

1) premixing (or coarse mixing), due to a hydrodynamic fragmentation of the molten fuel in the sodium, which is characterized by a metastable film boiling regime
2) triggering, when due to instabilities of the vapor film surrounding the droplets, saturated sodium comes directly into contact with the droplets, increasing the local heat transfer and the pressure buildup, followed by the fine fragmentation of the melt
3) propagation, the explosive vapor formation propagates throughout the mixture region
4) expansion, the sodium vapor expands against the surroundings

However, for subcooled sodium it is difficult to separate a premixing phase, as there is rather a succession of small explosions, than one explosion following an actual fragmentation phase. The small explosions limit the melt quantity that could penetrate in sodium [75]. For sodium close to saturation, the above-mentioned 4-phase description is expected to occur [76].

Corium fragmentation and heat transfer is greatly dependent on sodium boiling regimes. The Betulla II experiments [77], in which small drops of melt where injected in sodium pools, showed that a violent transition boiling regime (growth/collapse of vapor bubbles) can be identified as the most probable cause of melt fragmentation. Further tests lead Schins [78] to conclude that a film boiling regime occurred, explaining the measured elevated pressure pulses during the interaction.

However, Le Belguet recent bibliographic review [79], [80], [81] showed that only a limited number of experimental data existed to derive film boiling laws, mainly coming from the unique experiments conducted by Farahat [82], [83], in the 1970s (Figure 23).

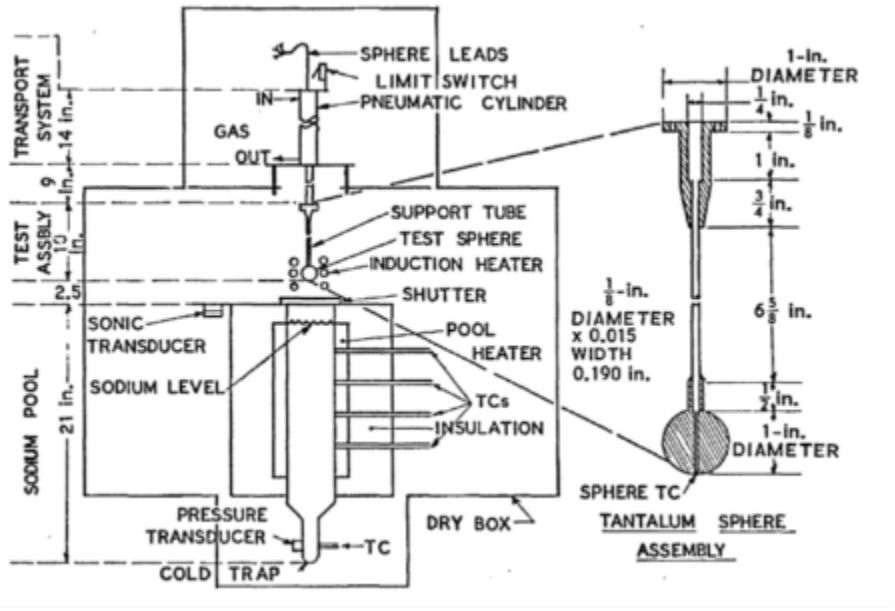

Figure 23: Schematic view of Farahat experimental device [83]

5.1.1 Jet fragmentation

Several configurations were experimentally studied that could be valid also for the jet fragmentation process in ASTRID severe accident scenarios.
Corium fall in a sodium pool is a rather academic configuration, which is useful for code validation. It could occur in scenarios in which the discharge tubes have been emptied of their initial sodium content (which has vaporized) so that corium may flow in the empty tube and enter sodium in the lower plenum volume (Figure 24).

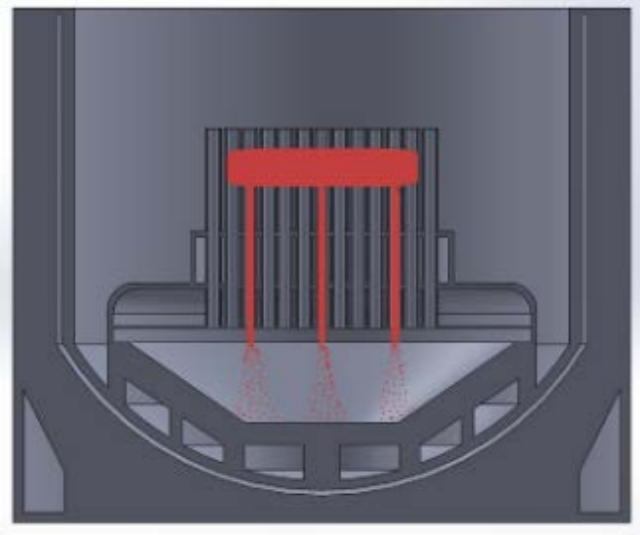

Figure 24: Potential scenario of corium fall in ASTRID sodium pool

The major experimental programs on this configuration were FRAG [58], [84] at Sandia National Laboratories and FARO [75] at JRC Ispra. Smaller scale tests were also conducted in the Betulla facility [77] at JRC Ispra, as well as at Argonne National Lab with metallic melts [85].

In FRAG [55], [86] at SNL, about 20 kg of a 30 wt% steel, 70% $(U,Zr)O_2$ melt were poured in 23 kg of sodium (~30 cm deep) between 250 °C and 650 °C depending on the test. Fine fragmentation was observed with large debris bed porosity (e.g. 56% in FRAG4 test).

In the Betulla I test [77], up to 2.4 kg of molten UO_2 or steel were spilled into a sodium pool at temperatures between 350 °C and 700 °C. The jet was always fragmented and particle median size (Figure 25 left) was between 0.15 and 1 mm, which was similar to previous experimental data.

In FARO-TERMOS [75] at JRC Ispra, only two experiments were conducted in which 100-kg, 50-mm diameter UO_2 and 140-kg 80-mm diameter molten jets have been poured in a 2.5 m deep 400 °C sodium pool. Planned experiments at higher temperatures were not performed, due to early termination of the experimental program. A series of pressure peaks were recorded when the melt entered the pool. The jet was totally solidified and a stratified debris bed was formed with finer particles at the top (median size around 0.1 mm) and coarser (median size around 1 mm) at the bottom and middle. No compact molten mass was found, indicating a complete fragmentation in this case. The debris bed porosity ranges from 58 to 62 %. The observed results are consistent with those of FRAG experiments.

In the MELT facility at JAEA, a series of small-scale sodium experiments on FCI were conducted using a few kilograms of melt [87]. In the preliminary experiments, molten aluminium (Al) (melting point: 660 °C, density: 2.7×10^3 kg/m^3) was poured into a sodium pool (depth: 1 m, diameter: 0.1 m) through a nozzle. An X-ray system was used for the visualization of molten Al behavior in sodium. The initial temperatures of molten Al and sodium were approximately 1200 °C and 400 °C. The molten Al jet instantaneously collapsed, accompanied by local sodium-vapor expansion, and as a result, penetration of the jet was limited within a short distance from the sodium level (Figure 26). The Al debris (Figure 27) also showed that the jet was totally fragmented. The particle median size was approximately 2 mm, which was relatively larger than a typical median diameter of UO_2 debris quenched in sodium [75], [77]. Schins et al. [77] suggested that thermal fragmentation induced by a violent transition boiling was the most probable mechanism for the fragmentation of molten UO_2 in sodium, and also that a delayed thermal stress

shrinkage arose on the UO_2 during its quenching, thus leading to the cracking of the UO_2 debris particles. The results observed by X-ray might evidence such thermal fragmentation. However, experimental evidence on the fragmentation mechanism is still limited, because of insufficient information by visualization. In the future experiments at the MELT facility, the use of molten stainless steel (a prototypic material), was planned to enrich experimental database on fragmentation, including jet penetration length and debris bed formation, as well as the fragmentation mechanism.

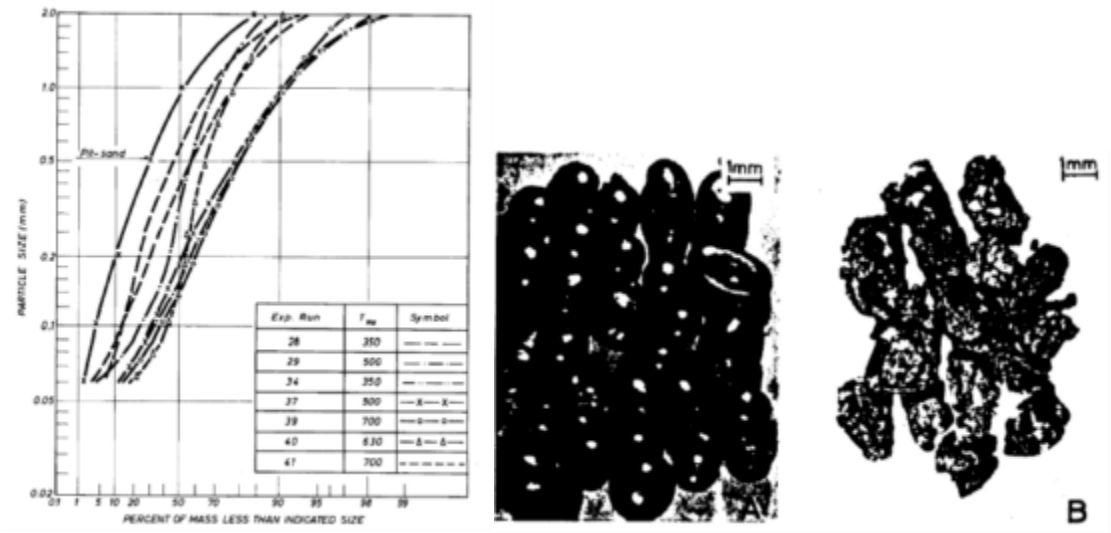

Figure 25: BETULLA I data [77] Left: UO_2Particle size distribution – Center: smooth UO_2 particles – Right: Fractured UO_2 particles

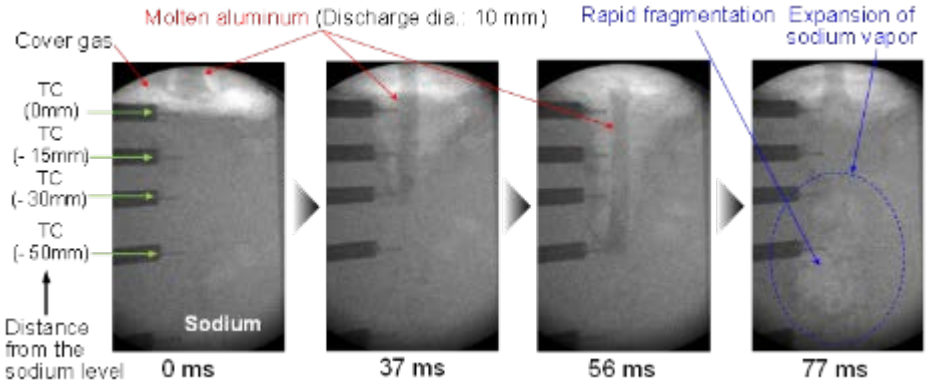

Figure 26 : Molten Al behavior visualized by X-ray [87]

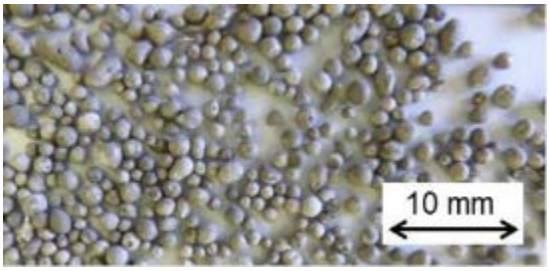

Figure 27 : Typical example of Al debris

A second series of experiments was devoted to the drop fragmentation. Indeed, as the interaction proceeds, and especially in case of vapor explosions, drops are fragmented into smaller droplets.

At ANL, Armstrong et al. [55] studied the fragmentation of 10 g scale drops of molten uranium dioxide and steel in sodium between 200 and 600°C. Smooth round debris were found for UO_2 with a median size around 0.2 mm. Pressure spikes were recorded with higher energy at higher sodium temperatures.

Mizuta et al. [88], [89] conducted similar interaction experiments with 1 to 15 g UO_2 drops in 150 g of sodium between 200 and 300°C. The observed particle size distribution is similar to the one of Armstrong ANL tests as well as to those from TREAT and SPERT in-pile tests [89] with median sizes between 0.2 and 2 mm (Figure 28). Mizuta [89] established an empirical lognormal law for the lowest envelope (labelled most pessimistic curve in Figure 28) of the experimental size distributions:

$$P(D < d < D + dD) = 2.317\ exp\left(\frac{-(Log\ D - 2.267)^2}{0.9442}\right) dD$$

Mizuta also analyzed the particle shapes. Larger particles had a round shape (they must have been formed in liquid state) and exhibit a central void (due to contraction at solidification). Some of them were formed by the agglomeration of two smaller particles. Small particles had a more irregular shape, but most of them had a smooth surface and a central void.

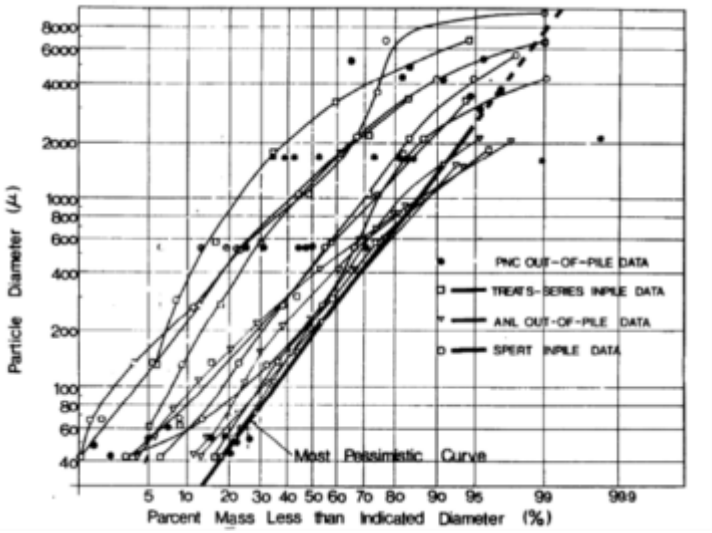

Figure 28: Particle size distribution from different UO_2 drop-in-sodium tests and in-pile tests [89]

At CRIEPI, Nishimura et al. [90] conducted experiments in which molten aluminum drops were poured into liquid sodium. One interesting result was that the median diameter was higher than in tests with oxide melt (in the 1-10 mm range). This is consistent with the results from MELT tests with aluminum.

Zhang et al. conducted a series of small-scale sodium experiments where a single molten steel droplet (5 g) was poured into a sodium pool [91]. Based on the results of these experiments, it was suggested that under high Weber number (We>500) or high superheat (ΔT>200 °C) conditions, the fragment sizes of steel droplets were comparable to those of molten steel jets tested by Schins et al. [77].

5.1.2 Vapor explosion

Fuel Coolant Interaction deals with the rapid heat transfer that appears when molten fuel drops are in contact with coolant (sodium for SFRs). For finely dispersed melt, the exchanges may become so large that the rapid formation of sodium vapour may create a shock wave.

The FARO furnace and TERMOS test section [75] were built at JRC Ispra in the 1980s to study FCI with sodium from 400°C almost to boiling point. It followed a smaller scale experimental program at the BETULLA facility. Unfortunately, these SFR programs were terminated in 1990 and only two tests with largely sub-cooled sodium were performed before FARO/TERMOS was adapted for Light Water Reactor FCI experiments. It is nevertheless necessary for the validation of a sodium FCI code to have experimental data for large masses of corium interacting with hot sodium. FARO-KROTOS experiments showed that, at least for water FCI, coherent molten fuel jets were only found for large-diameter long-duration jets, large-scale confirmatory experiments will be needed.
These cases could occur after the pour of large masses of overheated corium in the lower plenum and/or in the case of Unprotected Loss Of Heat Sink (ULOHS) accidents.

5.1.3 R&D needs for FCI

SFR (ASTRID)
Two R&D approaches for code development can be followed to solve the issues related to FCI:

a) Development of a mechanistic FCI model for Corium-Sodium Interaction, as it is currently done for the Corium-Water Interaction case with computer codes [92] such as MC3D or TEXAS. CEA has launched the development of SCONE [93], a corium-sodium interaction tool that must be validated on experiments.

b) Use of a lumped parameter approach to estimate the thermodynamic parameters of the energy exchange, the jet fragmentation length and the resulting debris bed characteristics. This approach requires the determination of empirical correlation from a series of experimental data, or from mechanistic calculations.

For the ASTRID safety case, the list of issues to be solved with proposed experiments is presented in the following sections.

5.1.3.1 Jet fragmentation

This issue concerns the possibility of a (partially) non-fragmented coherent jet to reach the core catcher sacrificial material and ablate it. It will be necessary to validate that, even at the highest sodium pool temperatures (after huge masses of corium have been poured in the lower plenum) all the corium is still fragmented. In case non-fragmented jets cannot be ruled out, core catcher sacrificial material ablation by a corium jet must be studied, in particular the so-called “pool effect” which reduces ablation efficiency after a few jet diameters have been ablated [94].

One type of separate effect experiment needed to validate any molten fuel-coolant interaction code, like the SCONE code, is the drop fragmentation experiment of a corium droplet in sodium. It could be considered as a transposition to sodium of the MISTEE experiments [95].

The experimental database of jet fragmentation lacks especially tests on large-scale prototypic jets in sodium at high temperatures, as FARO-TERMOS tests were limited to 400°C. The database on drop fragmentation shows the same limitation in the sodium temperature (maximum temperature of 600 °C). The risk of non-fragmented jets impinging on the core-catcher must be further investigated by experiments with larger-diameter and longer-duration jets of molten fuel.
A preliminary R&D experimental program has been drafted for PLINIUS-2 in support of ASTRID safety (see Par. 6.2.2). It includes 5 experimental campaigns between 2020 and 2025. PLINIUS2-FR experiments [96] will investigate the jet fragmentation. Main accent will be put on the performance of a series of medium-scale experiments (in a 25-30 cm diameter test section compatible with X-ray imaging). In a second step, confirmatory experiments at large scale (in the 1-m diameter sodium test section) will be necessary. These experiments dedicated on premixing will be conducted without any artificial trigger. Corium subcooling will be one of the major parameter of this series.

5.1.3.2 Vapor explosion in the lower plenum

The issue of possible energetic vapor explosions due to corium relocation and their yield will be solved by using the SCONE code.
There is a need for specific experimental configurations in which melt is provided below the sodium surface as at the exit of the discharge tubes (CRGTs for JSFR, DCS-M-TT for ASTRID).
This configuration was not been studied in the past. Indeed, for the past SFRs, no discharge path was designed so that molten corium rapidly enters the lower plenum. From the past experimental database, some tests which were devoted to FCI in the case of melt ejection from a subassembly to a sodium full neighbor may provide some partial insights: JEF at CEA Grenoble [97] AF2 at CNEN [98], Gabor experiments at ANL [99], [100] , MFTF-SUS experiments at UKAEA Winfrith [59].
Medium scale experiments with explosion triggering, enabling X-ray visualization of the premixing phase (initial condition of the explosion) are required to validate the SCONE code. Transposition to reactor scale shall be qualified thanks to experiments at a larger scale (order of magnitude of the corium discharge tube diameter, with hundred-kilogram prototypic corium).
In particular, it will be necessary to investigate possible pressure buildup by the explosive FCI. As it is expected that low sodium subcooling favor vapour explosions, experiments at high sodium temperature[2] are necessary.

PLINIUS2-EXPLO campaign [96] will carry out vapor explosion experiments, based on the experience of the PLINIUS-FR campaign (see Par 5.1.3.1).

Film boiling heat transfer regime plays an important role in the molten fuel-sodium interaction. However, the current heat transfer model is not fully validated because of the few experimental data available [79], [80], [81] . In particular, data are missing on sodium film boiling heat transfer for low sodium undercooling, for flowing sodium and for high pressures, both for stable and unstable film configurations.

[2]Calculations are underway to determine the maximum temperature that can be reached during corium discharges in the ASTRID lower plenum during corium transfer.

5.1.3.2.1 Influence of the discharge point on FCI: the EAGLE program

An alternative corium transfer technique must be implemented, compared to the delivery in the gas above the sodium free surface: corium must be directly injected below the sodium pool free surface, as in the EAGLE out-of-pile tests [101] (Figure 29 left) with an induction furnace and a sodium filled duct, or, in the case of water, in the MFMI facility [102] (Figure 29 right), in which the corium is produced by thermitic reaction in an underwater test section which is deliberately broken by pressure increase.

The EAGLE out-of-pile program investigated the issue of molten corium poured below the sodium surface. In the tests [101], approximately 10 kg of molten alumina (2200 °C) was injected into a sodium pool (400 °C, diameter 0.4 m, depth 1.3 m, inventory 140 kg) through a tube (inner diameter 40 mm to 63 mm), whose exit was positioned below the sodium surface (Figure 18). During the injection, pressure buildup was observed in a sodium pool, but quite lower than the pressure observed in the CORECT test series (70 bar pressure peak) [59]. Such mild pressure buildup might be attributed to the fact that high subcooling degree still remained maintained in the bulk of the sodium pool through the injection of alumina. In the future EAGLE program, in order to investigate the corium cooling in a flattened sodium pool (namely, reactor core inlet plenum of JSFR), a new series of tests is planned, where molten alumina will be injected into a restricted volume of sodium pool. In the new tests, the bulk of the sodium would be heated to its boiling point during the injection of alumina, since the mass ratio of alumina and sodium (M_f/M_c) can be raised to approximately 1, which is rather larger than in the past EAGLE tests (M_f/M_c = 0.07). To reinforce the experimental evidence on the corium cooling, in-pile tests using IGR of NNC/RK are planned as well. It is considered that low subcooling conditions increase the risk of energetic FCIs. Hence, although the scale is limited to 10 kg of corium pouring, these EAGLE tests will provide insights on vapor explosion in sodium.

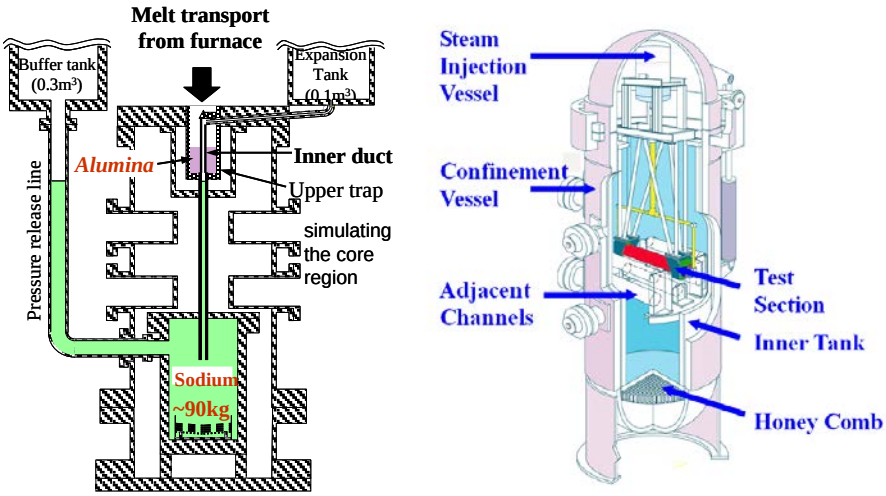

Figure 29: scheme of the EAGLE out-of-pile (NNC for JAEA) [left] and MFMI (AECL) [right] facilities

5.1.3.3 Size distribution of the debris bed

Experimental activity will concentrate in the sieving and microscopic analyses of the debris formed in the FCI tests. This is a prerequisite to study the debris bed coolability.

5.2 R&D in support of the core catcher design in SFR (ASTRID)

5.2.1 Core catcher ablation by corium jets

Postulating that corium jets are not totally fragmented when they reach the core catcher surface, introduces the issue of jet ablation. Due to its high temperature compared to steel melting point, it appeared that a steel plate could be perforated by a high temperature metallic corium jet. This is the major reason why protective materials (zirconia-based) have been selected to be installed in ASTRID in-vessel core catcher.

Experimental research started in the 1970s with Yen and Zehnder [103] and the ANL simulant material experiments by Swedish et al. [104], [105] in which water jets ablated several solidified targets in ice, octane, p-xylene or olive oil.

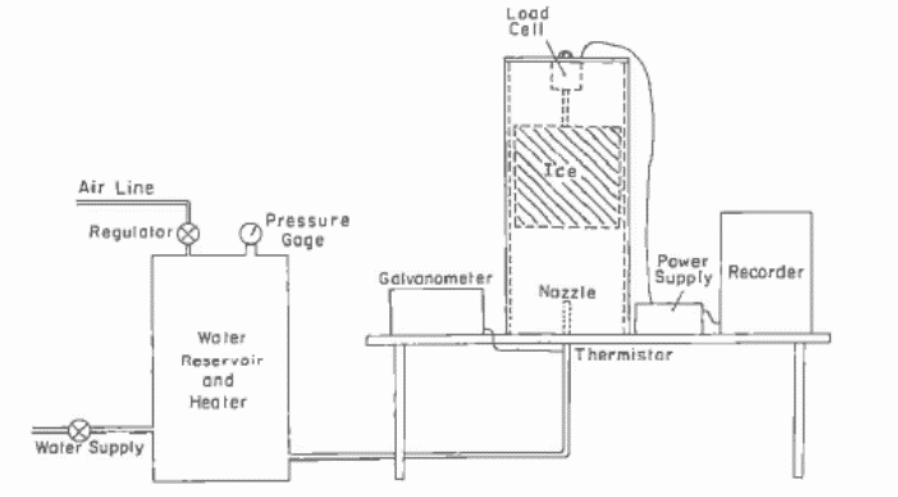

Figure 30: Yen and Zehder facility: water jet impinging ice from below [103]

At JRC Ispra, the Blokker I test series [106] studied the ablation of an inclined steel plate by an UO_2 jet (Figure 31). A 1-2 mm thick crust have been found, while a few mm were ablated by pours up to 100 kg of molten uranium dioxide.

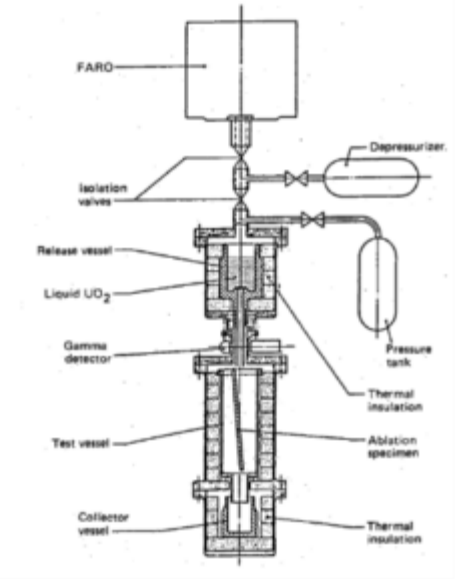

Figure 31: The FARO-Blokker I test arrangement [106]

Saito et al. [94] conducted jet ablation tests with molten salts in the MELT-II facility at JAEA (Figure 32). These experiments showed the limiting role of corium crust at the jet-plate interface and led to the proposal of the famous Saito correlation, giving the Nusselt number for turbulent heat transfer by a jet with the simultaneous occurrence of jet freezing and substrate melting:

$$Nu = 0.00333\, Re \times Pr$$

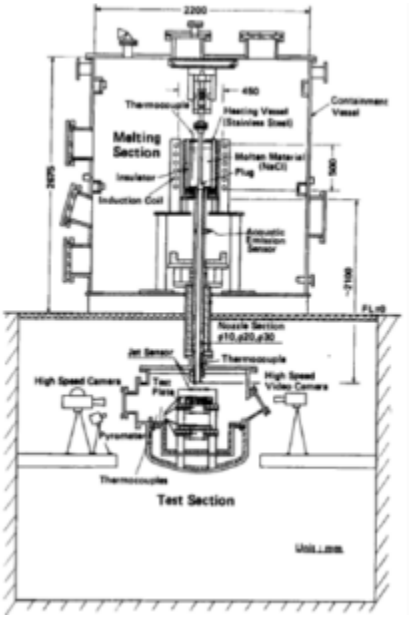

Figure 32: MELT II facility for jet ablation experiments [94]

Hole ablation was also studied in UKAEA Winfrith facility [107] using UO_2-Mo thermite.

Furthermore, jet ablation by corium jets was investigated in the context of LWR severe accident research. For instance, Sehgal et al. [108] performed simulant material experiments with water and ice (from fresh and salted water). At FZK, the KAJET facility was used to perform jet ablation tests with alumina and iron jets on concrete samples (Figure 33). Ablations of the order of 1 cm/s have been observed which verified the Sehgal correlation [109].

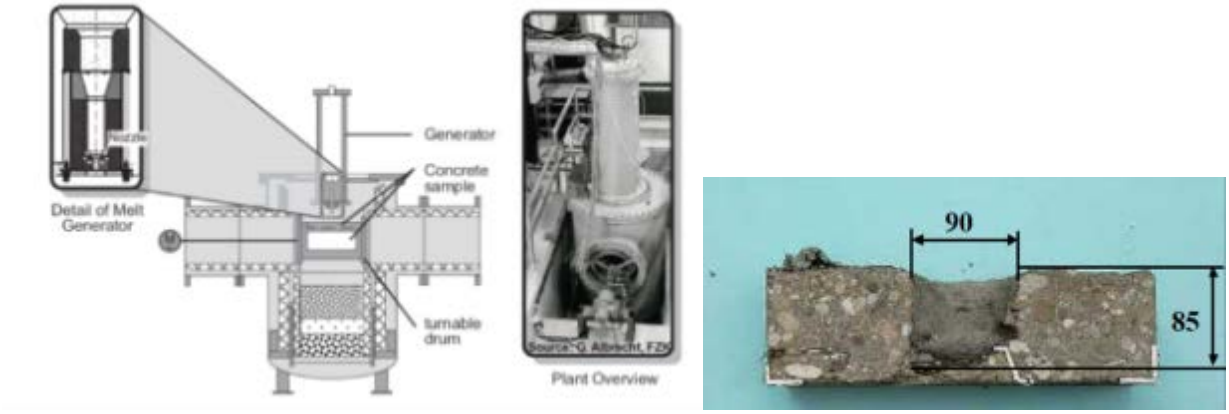

Figure 33: KAJET facility - Left: Scheme – Center: Photograph of facility – Right: Typical concrete sample after ablation

5.2.1.1 R&D needs

The physics of jet ablation is quite well understood and modelled. There are two remaining issues:

- stability of fuel crust
- pool effect

The latter is a deceleration of jet ablation which occurs when the hole depth is of a few times its diameter. The presence of a molten pool in this hole limits the heat exchanges (Figure 34). Although the pool effect was evidenced in Saito et al. [110] it is still not satisfactorily modelled and more work is thus needed. In the Saito et al. tests [110], lighter jets (NaCl, Al_2O_3) ablated heavier plates (tin, stainless steel), while the density of prototypic corium jet would be larger than that of ablated plates (stainless steel, zirconia-based material). Such difference might affect the stability of crust and pool effect. In addition to separate effect experiments with low temperature simulants, work with prototypic corium is needed due to the impossibility of simulating corium crust behavior.

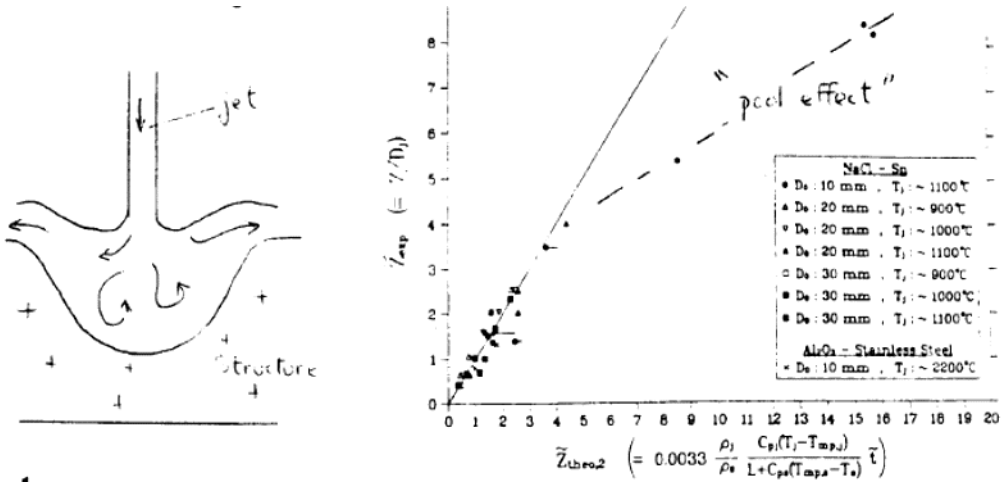

Figure 34: Pool effect: Left: schematic view – Right: Observed deviation in Saito [110]

5.2.1.1.1 PLINIUS2-IMPACT

Experiments on the impact of a corium jet on the core catcher ceramic materials will be carried out in the PLINIUS2-IMPACT. These experiments have to be performed if PLINIUS-FR (see Par. 5.1.3.1) confirms the possibility of a coherent jet reaching the core-catcher. These tests will run without sodium, to concentrate on the jet ablation processes.

Preliminary experiments with simulant materials at MOCKA facility in KIT are planned within the ESFR-SMART European project [111] to study oxide and metal jet impingement on sacrificial material, as well as separate effect tests with water/ice (HAnSoLO facility at the University of Lorraine) [112].

5.2.2 Corium interaction with sacrificial materials

It is planned to install a protective layer on the core catcher to protect it from molten core impact and to delay the requirement of core catcher lower face cooling. For the ASTRID conceptual design phase 2, CEA is considering the use of stabilized zirconia ceramics. IGCAR is also considering the future use of yttria-stabilized-zirconia; these choices have to be confirmed. In particular, sacrificial material ablation (both rapid ablation by impinging jets and slow ablation by molten pool) and sacrificial material long-term behaviour in sodium during normal operation must be considered. CEA is about to adapt its PWR Molten Core Concrete Interaction code TOLBIAC-ICB [113] into a Corium-Sacrificial Material Interaction Code (TOLBIAC-SFR) that will require experimental data for validation.

Joint activities are foreseen between the selection of core catcher materials and the cooling of the core catcher.

5.2.2.1 Corium-sacrificial material mixture properties

The VITI facility is part of the current PLINIUS platform and has been already used to study the interaction of corium with sacrificial materials [114] especially HfO_2 and Al_2O_3.

The working chamber volume is of about 70 L. It is possible to work either under low vacuum or under inert gas atmosphere. The maximum absolute pressure in the working chamber is $2.5x10^5$ Pa. Induction heating is used to reach temperatures above 2000°C with limited thermal gradient. The induction coil couples with a graphite susceptor, which heats the crucible by thermal radiation. The radiation losses are attenuated by a dedicated thermal shield. The maximum electrical power of the induction generator is 24 kW and its frequency is 23 kHz. The temperature of the studied material mixture and the temperature of the external crucible wall are measured by bichromatic pyrometers (λ_1 = 0.92 and λ_2 = 1.04 µm). The facility is represented in Figure 35 and Figure 36, for the aerodynamic levitation configuration.

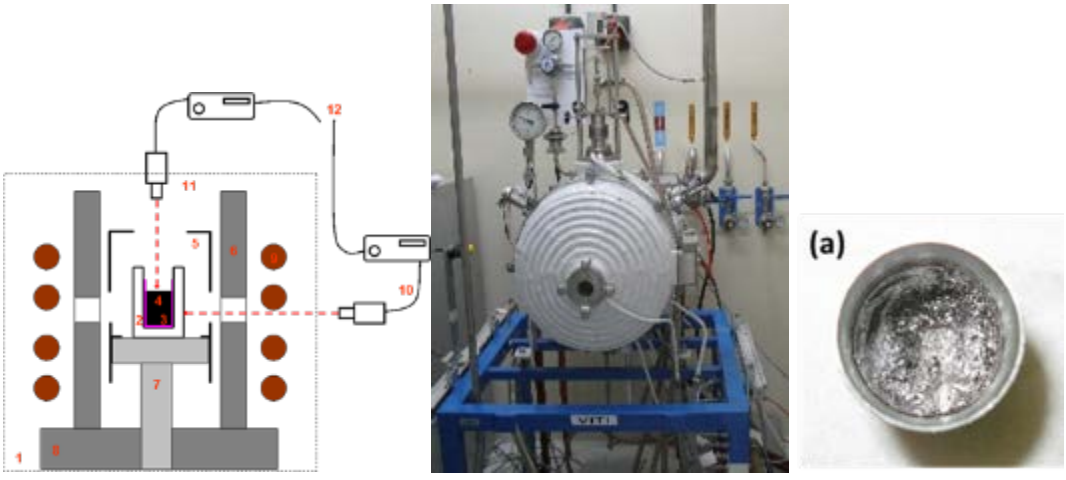

Figure 35: VITI Facility - Left :Scheme of VITI furnace: (1) VITI tank, (2) Crucible, (3) Protective coating (option), (4) Mixture, (5)`Graphite susceptor, (6)Thermal shield, (7) Support for crucible, (8) Support for thermal shield, (9) Inductance coil, (10) Pyrometer, measurement of $T_{mixture}$, (11) Pyrometer, measurement of $T_{crucible}$, (12) Data acquisition Centre: Photograph of VITI - Right: Typical crucible used in VITI

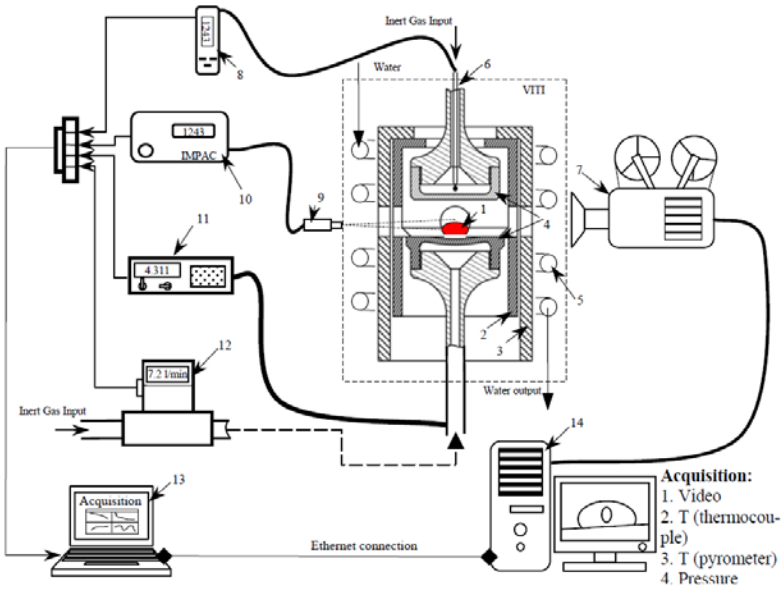

Figure 36 : VITI facility – Aerodynamic levitation configuration: (1) sample droplet (2) susceptor (3) thermal shield (4) diffusers (5) inductor (6) Type-C Thermocouple (7) fast camera (8) Analogue-Digital Converter (9-10) pyrometer (11) lower diffuser pressure sensor (12) flowmeter (13) Acquisition system (14) PC

5.2.2.2 Behavior of sacrificial materials in sodium

Core catcher sacrificial materials will be in potential contact[3] with sodium, since the core catcher in French and Indian reactors are located in the main reactor vessel. Their long-term corrosion behavior in liquid sodium in the conditions of the cold plenum has to be then assessed, in order to assure that the safety related components would still be efficient when required. The CORRONA facility [115] is lab-scale test setup devoted to the studies of corrosion phenomena in liquid sodium and its modeling for the long term prediction, by performing static corrosion in controlled conditions [116] [117](Figure 37 left). Before and after the interaction with sodium, microscopic observations are performed to characterize the corrosion phenomena (Figure 37 right) and to quantify corrosion kinetics versus exposure time when regular extractions of specimen is achieved. Experiments have been launched with zirconia.

Preliminaries results for ceramics indicated that the actual composition (including impurities), fabrication process parameters and the microstructure play a major role in the observed behavior in liquid sodium. In addition to tests performed in CORRONA with various alumina samples for duration from 100 h to 2000 h and with different oxygen content in sodium, similar tests must be carried out with the material selected for ASTRID and CFBR.

[3] These core-catcher materials will likely be installed in some type of casing. Anyway, local ruptures cannot be excluded so compatibility with sodium is indeed an issue.

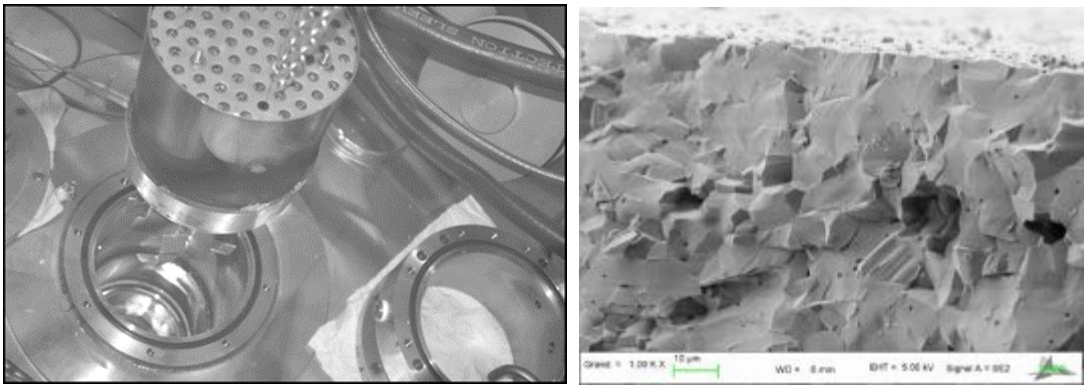

Figure 37: CORRONA Facility - Left: View of open sodium pot – Right: Micrograph of 99.7% alumina sample after 1000 h in sodium

5.2.2.3 Corium-sacrificial material interactions at various scales

The VULCANO facility (Figure 38) is dedicated to study medium masses (25-50 kg) of prototypic corium and its interaction with various materials. In the LWR severe accident program, VULCANO has been used to study the interaction of corium with concrete [118] and with ceramic materials [119].

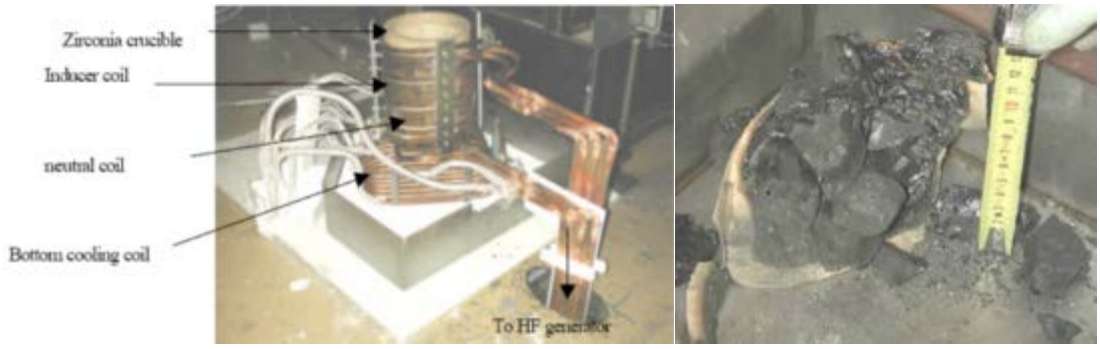

Figure 38: VULCANO facility - Left: crucible + induction coils; Right: solidified corium and ablated ceramic crucible [118]

5.2.2.4 R&D needs

This VULCANO facility is considered for performing experimental R&D on the sacrificial material melting and dissolution transients during contact with corium. Since these tests will be dedicated to the corium-sacrificial material interaction, it will not be necessary to add sodium during the test.

The facility will also be useful to study, with prototypical materials, the natural convection in presence of two immiscible liquid phases (oxide and metal) and in particular the effect of metal segregation on heat transfer.

The results of these experiments will be needed for the validation of TOLBIAC-SFR code. As there is a size effect, mainly due to the stability of crusts, the future PLINIUS-2 platform (see Par. 6.2.2) will be useful to complement these medium mass tests by a few large mass (300-500 kg) tests.

PLINIUS2-CC (Core Catcher) is an experimental setup without sodium aiming at studying the behavior of a corium pool interacting with ceramics. This experiment will be conducted without sodium but with induction heating simulating the decay heat[4] during several hours.

Preliminary experiments with simulant materials at LIVE facility in KIT are planned within the ESFR-SMART European project [111].

5.2.2.5 Corium pool thermal hydraulics

If a non-fragmented jet reaches the core-catcher or if the debris bed re-melts, a corium pool is formed where decay heat is dissipated. Convective heat transfer from this pool determines the loads to the core catcher structure.

Baker et al. [120], [121] presented a review of early experimental data on natural convection in volume heated liquids. They led to famous experimental correlations as those of Kulacki & Emara [122] or of Fieg [123]. At CEA Grenoble, the BAFOND facility [124] (Figure 39) provided results that lead to an extension of Fieg's correlation [123] to the following range:

$2<Pr<7$; $10^{12}< Ra_H<10^{16}$; $1<H/D<3$

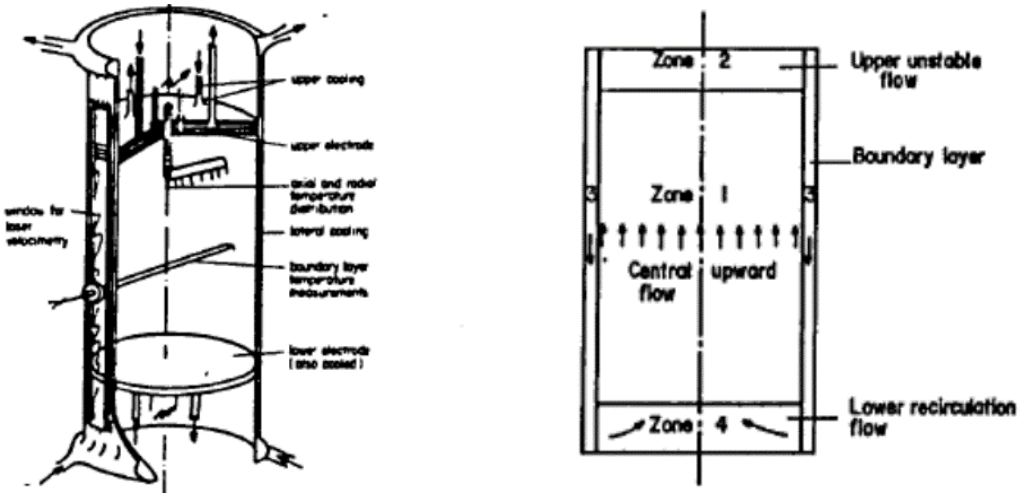

Figure 39: The BAFOND facility : Left- Sketch – Right: Simplified modelling [124]

More recently, the LIVECERAM test [125] at Karlsruhe Institute of technology (KIT) simulated the dissolution of sacrificial material by a molten pool with molten salts. The test results clearly showed that dissolution of solid refractory material can occur in a non-eutectic melt. Dissolution stops when the liquid is saturated in refractory species for the instantaneous interface temperature. The final steady state (when ablation has stopped) corresponds to a uniform interface temperature distribution equal to the

[4]The other test configurations being transient, decay heat is negligible compared to thermal inertia and does not need to be simulated during the experiments.

liquidus temperature corresponding to the pool composition (although heat flux distribution is not uniform). As the pool composition is also uniform in the final steady state (due to convective mixing and absence of mass transfer at the boundaries), the convection in the pool is governed by thermal natural convection and the heat flux distribution is similar to what would be obtained for a single component pool.

5.2.2.6 R&D needs for corium pool behavior in proximity of the core catcher

The LIVECERAM tests must be confirmed by experimental data with prototypic corium and core catcher materials, in particular for the development and validation of TOLBIAC-SFR code[5].

Another issue is related to boiling pools, as steel might reach its boiling point during some post accidental core catcher scenarios. The SEBULON experimental facility [126] was used at CEA Grenoble to study the thermal-hydraulics of boiling pools, following earlier works summarized by Greene et al. [127].

The need for further experiments on boiling pool thermal-hydraulics is subject to the results of future TOLBIAC-SFR calculations that will indicate whether, with the selected materials, boiling pool configuration are possible.

5.3 R&D in support of the core catcher design in GFR

There has been a broad agreement inside the GFR community to implement an ex-vessel core catcher as a part of severe accident mitigation measures. However, no comprehensive design is available. ÚJV has recently started with first evaluation that should lead to first conceptual design of a core catcher for ALLEGRO.

5.3.1 Location and type of the core catcher

One of the most important challenges in the conceptual design of ALLEGRO core catcher is the actual location of the device. Modern GFRs features a leak-tight closed containment as a part of the design, which keeps certain residual pressure in case of LOCA accidents to ensure effective core cooling.

In case of severe accidents with corium ejection from the RPV, pressure inside the closed containment will be already close to the maximum design pressure and further pressurization by vapor and gases from cooling of corium in the core catcher is undesirable. The above-mentioned arguments support the placement of the core catcher outside the closed containment.

[5] Since the phenomenon has similarities with concrete ablation by corium simulated by molten corium concrete interaction codes such as TOLBIAC-ICB this code will be adapted to SFR core catcher configuration.

On the other hand, the control rod driving mechanisms are typically located below the RPV, similarly to BWRs. If the core catcher will be located outside the closed containment, more complicated ways of corium localization after the ejection would be needed.

A list of needed computer simulations to be further proven by mock-up experiments to support the design studies will be prepared.

5.4 R&D in support of the core catcher design in LFR

LFR (MYRRHA)
There are still on-going evaluations concerning the need of implementing a core catcher in the MYRRHA reactor.

5.5 Corium coolability

5.5.1 Debris bed formation and shape

The issue of debris bed formation and shape is considered as sufficiently studied in the past and has not priority. The EDULCOREE experiments [128] at CEA Grenoble were carried out with about 100 kg of copper balls of various diameters falling into a water pool and a similarity law based on the Froude number corresponding to the ball terminal velocity was applied. When the height of fall is relevant, there is a quite clear threshold at 300 µm, above which the pile obtained is not levelled at all and is very similar to that obtained with falls in air. We can conclude that, above 300 µm for copper, the particle falls too quickly in the fluid to be significantly affected by radial forces. Transposed to the UO_2-Na case, this situates the levelling threshold at D = 100 µm approximately. (For D < 70 µm the UO_2 will be perfectly levelled whereas for D > 110 µm the angle of repose tends to be the same than that obtained in air). Consequently, for D > 110 µm, the nature of the fluid, water or air, seems no longer to have any significant effect.

With increasing masses, homothetic piles up to the limiting case of a pile with an angle of 30° were obtained.

When the height of the fall is small, in every case leveling is poor because the fluid has not time to acquire velocity. Tests carried out with powders having different particle size ranges produce piles with various slopes where the finer particles are located on the periphery with small angles.

Kyushu University and JAEA carried out a series of water experiments dedicated to debris sedimentation behavior, using particles with different densities, sizes and so on [129]. Effects of these parameters on maximum particle dispersion angle, particle fall time, bed heights, and bed shapes were investigated under an isothermal condition. Simulation results using discrete element method (DEM) showed a reasonable agreement with the experimental observations.

On this issue, the work performed at KTH Stockholm in the DEFOR facility [130] for BWR severe accidents is also noteworthy. DEFOR experiments with oxidic corium simulants provided data on melt jet fragmentation in water and quenched particle size distribution at different melt jet diameter and superheat, water pool depth and water subcooling. Formation of cakes and agglomerates at high jet temperature/diameter and insufficient water depth was demonstrated and quantified in term of mass fraction of agglomerated debris, which can be more complicated to cool down. Interpretation of DEFOR experimental data for the case of oxidic melt fragmentation in molten sodium is a very challenging task because of the large differences of material properties of water vs sodium.

If the coolant pool depth is too small and/or the jet diameter is too large, no significant jet fragmentation happens, jet reaches the coolant pool bottom and melt spreads. Melt spreading on the bottom of shallow water pools was studied at KTH in the PULIMS experiments with the same oxide corium simulants as in DEFOR. Large experimental database on underwater melt spreading was accumulated from PULIMS tests, but the experiments also demonstrated regular spontaneous steam explosions in stratified configuration of melt spread covered by shallow water pool. This configuration previously was considered relatively safe one, i.e. incapable to generate strong steam explosion. New SES facility better instrumented for stratified steam explosion studies was build and SES experiments demonstrated quite energetic and systematic steam explosions. Similarly to DEFOR, PULIMS and SES data and conclusions are complicated to extent to the case of sodium coolant having very different properties in comparison with water.

5.5.1.1 R&D needs

SFR

Particle sedimentation in liquid metal pool and debris bed build up from the solid particles are quite well understood and modelled. There are the following remaining issues on melt fragmentation and debris bed formation:

- Insufficient data from sodium and prototypic corium experiments increase priority of material scaling of melt fragmentation and debris formation in water vs sodium. Such scaling approach would be very beneficial for SFR safety studies. Supporting experiments and studies for scaling confirmation can be useful.
- Formation of agglomerated debris (cake), which can be less coolable than the particle debris bed, is expected between the two bounding cases: molten pool and particle debris bed. Understanding the conditions for cake formation and prognosis of cake properties, such as open and close porosity, size and morphology, can be important for safety analysis.
- Further efforts are welcome to address melt spreading in SFR core catcher and risk of stratified vapor explosion in sodium.

LFR

Similar experiments carried out for the SFR shall be repeated for heavy liquid metals (HLMs). Additionally, due to the small density difference between oxide fuels and Lead/LBE (their density vary roughly between 11000 kg/m^3 and 8500 kg/m^3 [46] in all the possible expected conditions) the mobility of core debris significantly increases. Three bounding cases shall be investigated:

1) Core debris gathering at the free surface of the Lead/LBE pool
2) Core debris suspension
3) Core debris deposition at the vessel bottom head

The real debris distribution is a combination of the identified configurations. The risk of deposition at the vessel bottom is less likely for lead cooled fast reactor, because of the higher density of lead, compared to LBE.

5.5.2 Debris bed levelling promoted by sodium boiling

Under the influence of sodium boiling, the debris bed can be (partly) fluidized, leading to particle spreading and to the so-called levelling of the debris bed.

The ETABUL [128] experiments at CEA Grenoble in the early 1980s studied this phenomenon with heated copper balls in water. Leveling kinetics was found to depend on two parameters, particle heating power and pool subcooling. The limiting angle of repose, less than 2° for initial debris bed angles ranging from 14 to 23°, was always the same whatever the power applied, but the time to reach it depends on the power. The leveling rate also reduces with the subcooling degree (~2.4 times slower with 60°C subcooling than at saturation).

Gabor et al. [131] conducted similar experiments, including UO_2 debris. In all cases in which variations in bed depth, material type and particle size were tried, the beds tended to level.

Kyushu University and JAEA more recently carried out a series of experiments dedicated to levelling (Figure 40) using different approaches (Figure 41) to simulate sodium boiling (in water): gas injection, bottom heating of the debris, and depressurization-induced boiling with a large range of particles (sphericity, material, size) [129]. These experiments confirmed that the smaller the particle size and density, or the larger the equivalent power density, the easier leveling occurs or the faster leveling proceeds. It was also more difficult for levelling to proceed in beds with non-spherical particles than with spherical particles.

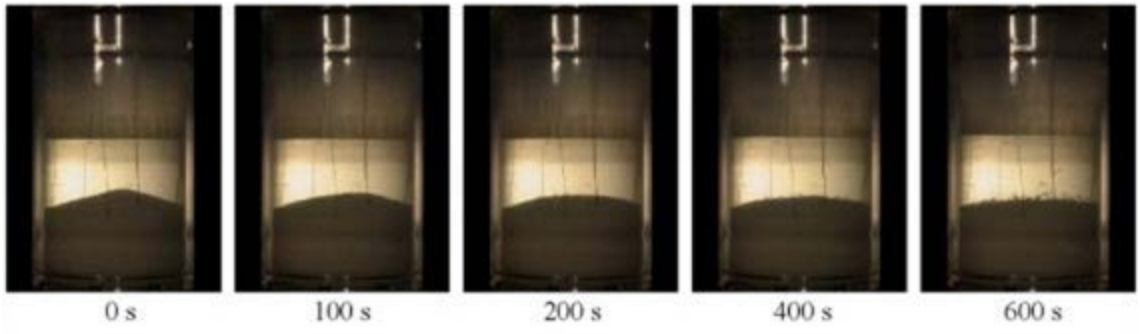

Figure 40: Typical levelling of a debris bed [129]

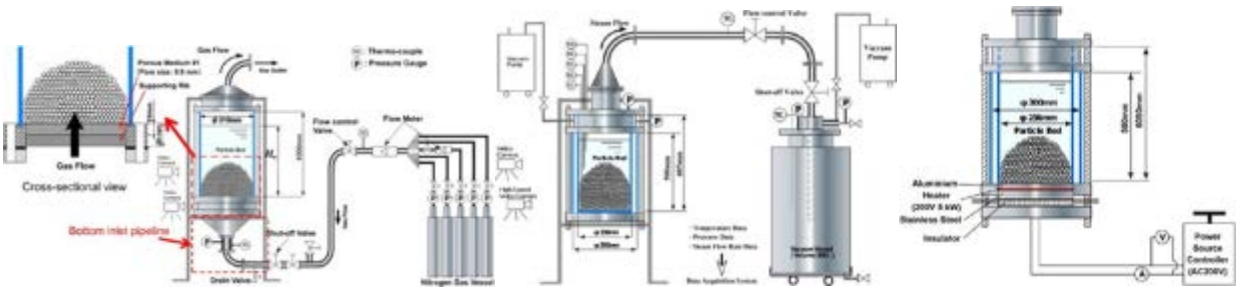

Figure 41: Three debris levelling experimental approaches to simulate sodium boiling [129]. Left: gas injection Center: water pool depressurization Right: Bottom heating

Some debris bed levelling experiments have also been conducted at KTH-NPS Stockholm on the PDS facilities [132] with air injection. The most important experimental finding from PDS-2 and PDS-C is that the bulk of the debris bed volume is immobile most of the time. Only the topmost layer of the debris is responsible for the spreading of the bed. The moving layer thickness is in the order of few diameters of the particles.

For SFRs like ASTRID, the safety case assumes that it will not be possible to demonstrate that the debris will never remelt, and that the heat loads from a melt will be conservative compared to those of a debris bed. Moreover, there is an important existing database on debris bed coolability. Therefore, the focus for the long-term core catcher configuration lies on the molten pool configuration. The remaining issues concerning debris bed lies more with the transient behavior of a debris bed, in particular with the shapes it may have with respect to criticality issues, and its remelting (in relation with the ablation of the core catcher sacrificial material).

5.5.3 Debris bed coolability

Out-of-pile debris bed coolability experiments for sodium fast reactors started in the 1970s with Gabor et al. [131], [133]at Argonne, Dhir, Catton et al. [134], [135], [136] at UCLA, Squarer et al. [137] at Westinghouse R&D, Hu & Theophanous [138] at UCSB and Barleon & Werle [139] at KfK. They were complemented by a series of 13 in-pile experiments in the Annular Core Research Reactor (ACRR) at Sandia [140].

These experiments lead to the development of several 1-D models relating the Dryout Heat Flux to several parameters.

5.5.3.1 R&D needs

SFR

Transposition of experiments in water to sodium cooling is quite important but difficult especially since sodium large thermal conductivity and high wettability are too far from water properties. Nevertheless, it is interesting to note the current hot topics in debris bed heat removal by water, since they should also apply to sodium case:

- Large influence of 2-D effects increasing the Dryout Heat Fluxes compared to 1-D cylindrical geometries (COOLOCE tests [141] at VTT and POMECO tests [142] at KTH);
- Large influence of distributed debris sizes compared to monodisperse sphere beds, leading to a smaller Dryout Heat Flux than that obtained for a monodisperse bed of the Sauter average diameter [143]

Due to the significant existing database, and as long as ASTRID safety case does not aim at demonstrating debris bed coolability but will consider molten pools, there is also no need for further experiments on this issue.

LFR

Similar experiments can be reproduced to investigate the debris levelling in Lead/LBE at the vessel bottom head. Additionally, debris coolability issues shall be investigated if the debris collect at the LBE free surface level. The debris spreading at the free surface influences the efficiency of top cooling system. It can be influenced by the natural circulation in the pool and by the LBE surface tension.

The overall natural circulation in the pool and the debris bed spreading itself can be affected by the presence of vapor bubbles. Separate effect studies with bubble injection are needed.

GFR (ALLEGRO)

Direct corium cooling is probably not possible in ALLEGRO due to resulting excessive pressurization of the close containment, if the core catcher will be located inside the close containment.

There is a need for supporting studies and experiments of indirect corium cooling possibilities. Some of the results are already available from EPR and VVER-1200 core catcher development processes.

A research program has recently started with aim to test innovative sacrificial materials (SM) for fast reactors, with special attention to GFRs. This initiative is connected with the need of more efficient indirect corium cooling mentioned above. The innovative sacrificial material should (as a part of the advantages) decrease viscosity and melting temperature of the resulting corium-SM mixture.

Experiments in several small-scale devices in JRC-Karlsruhe and larger-scale experiments in the new IS cold crucible in Řež are envisaged (see Chapter 6).

5.6 Post-accident heat removal

The capacity to remove the heat in order to maintain the debris configuration and to ensure the structural integrity of main vessel depends upon the kind of convection path developed in the coolant between the source and heat sink. These issues are well enough described [144] to ensure effective post-accident heat removal (PAHR) mechanism. Nevertheless, design-specific validation is needed as CFD codes still, alone, cannot prove the effectiveness of natural convection heat removal in a new geometry.

Some generic configurations concerning natural convection caused by vertical and downward facing heated surfaces have been studied in sodium, e.g. by Sheriff and Davies [145], [146] at UKAEA Risley, or Le Rigoleur & Tenchine [147] at CEA. Correlations have been proposed from these experiments, in link with the larger database for water.

Then, it was necessary to consider a hole in the core support plate in the actual plant design for Superphénix, to achieve satisfactory DHR performances. Recently, PATH facility (Figure 42) at IGCAR Kalpakkam [148], [149] has been used to study post accidental heat removal in PFBR (India's Prototype Fast Breeder Reactor) in a 1:4 scaled mockup filled with water.

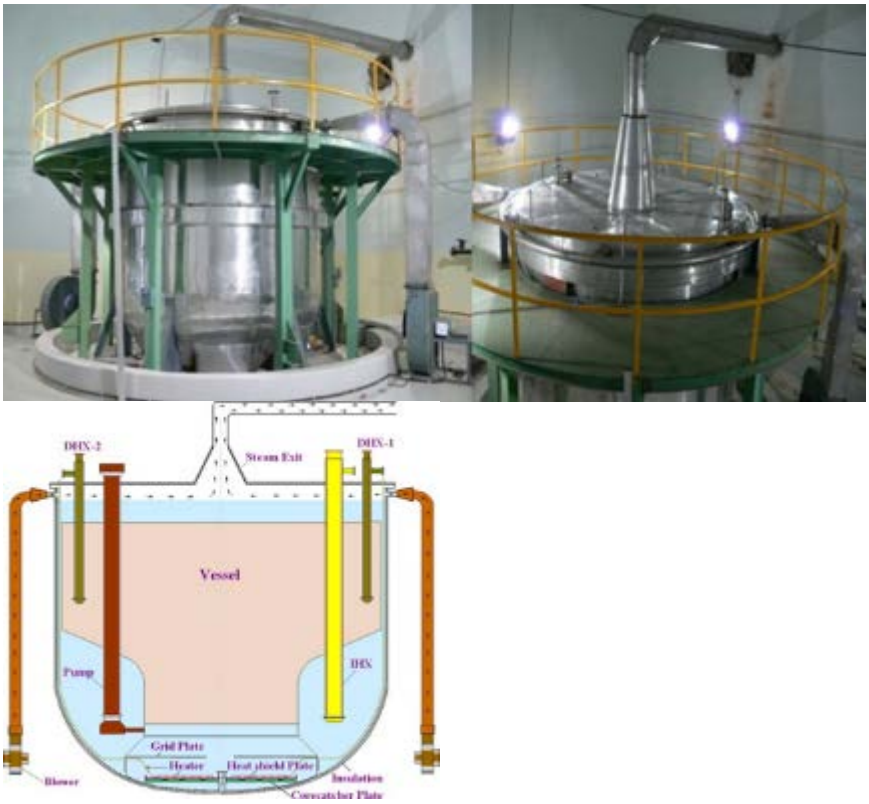

Figure 42: PATH facility. Left and center: photographs – Right: sketch

5.6.1.1 R&D needs

SFR (ASTRID)

Concerning PAHR in ASTRID, decay heat is removed from the core catcher (both core catcher plate lower side and top of debris bed/pool) by natural convection mode to a decay heat exchanger.

Due to the complexity of convection loops from core catcher to Decay heat Exchangers, it seems necessary to conduct specific experiments. A comprehensive test program in simulant fluid (water) as well as a few confirmatory experiments in sodium are necessary for ASTRID.

LFR (MYRRHA)

Considering the possible pathways for debris dispersion in LFRs, mentioned in Par. 5.5.1.1, the MYRRHA reactor will be equipped with two severe accident cooling systems, which are the Reactor Vessel Auxiliary System (RVACS) and Reactor Top Cooling System (RTCS), shown in Figure 43 [15], [150].

The RVACS working principle consists in flooding the reactor pit with water, which removes the core debris residual heat from the vessel by natural circulation. The main issues for the system functioning are the correct start-up of the system with natural circulation onset and the possible heat transfer degradation due to the incondensable gases (mainly nitrogen) initially present in the reactor pit.
The RTCS preliminary design consists in the direct cooling of the core debris at the LBE free surface, by a spray system. The effectiveness of this system depends strongly on the particle distribution at the LBE surface and on the heat transfer regime. Furthermore, interactions between coolant, fuel and steel at the LBE free surface shall be studied. Alternative heat transfer mechanisms are also investigated for the RTCS.

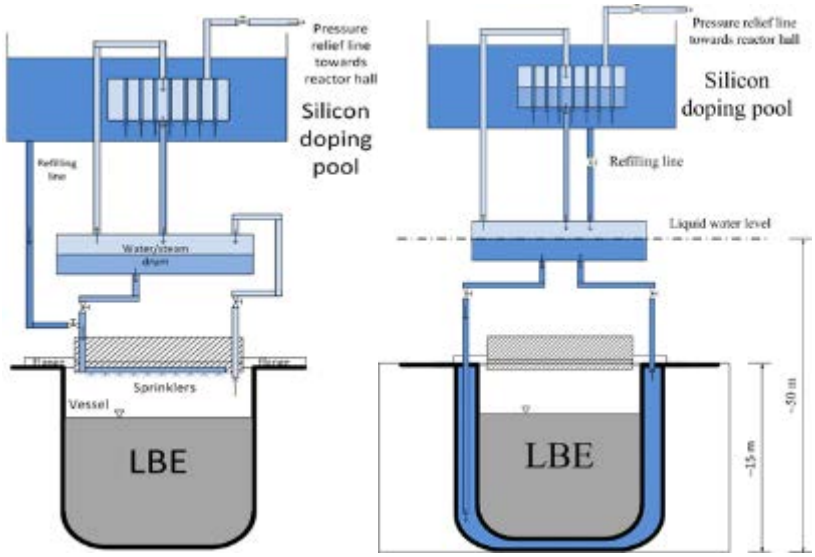

Figure 43: preliminary design of MYRRHA Reactor Top Cooling System (left) and Reactor Auxiliary Cooling System (RVACS) [150]

GFR (ALLEGRO)
Development of the core catcher cooling system has not yet started. The design of the system depends on the selected solution of the actual core catcher.

5.7 Summary of the phenomena occurring in the post-accident phase

The phenomena described in Chapter 5 are listed in Table 5.

In column 2 the main investigation field is presented. Relevant phenomena addressed in Chapter 5 are gathered under each field (column 3). The specific phenomena to be investigated with experiments are found in column 4. Past and operating relevant experimental campaign and facilities are reported in column 5.

Table 5: List of phenomena occurring in the post-accident phase

Nº	Investigation field	Phenomena	R&D needs	Past/Operating facilities (institute owner)
17	SFR, LFR: Fuel coolant interaction	SFR: Jet and drop fragmentation SFR: Sodium vapor explosions SFR, LFR: Debris initial size distribution	Mechanistic simulation of the FCI. Experimental database extended to: 1) Large masses of corium to study non-fragmented corium jets. 2) Low sodium subcooling degree, to assess the consequences of sodium explosions (non ULOF sequences). 3) Direct injection of jets into the lower plenum in confined volumes (exit location of the transfer devices). 4) Injection of particles in Lead/LBE for different temperature gradients.	FARO-TERMOS (JRC), BETULLA (JRC), MELT (JAEA), FRAG (SNL), IGR (NNC)
18	SFR, GFR: Core catcher ablation by corium jets	fuel crust stability corium pool heat transfer	1) Experiments aimed to study the crust stability when a coherent molten jet impinges on a ceramic material surface. 2) Experiments aimed to study the effect of a corium pool on the heat transfer towards the core catcher.	AEA (UKEA), KAJET (FZK), LIVE (FZK), BAFOND (CEA), FARO (JRC), MELT (JAEA) MOCKA (KIT)

19	SFR, GFR: Sacrificial material testing	Corium-sacrificial material interaction 1) Melting and dissolution of sacrificial materials 2) Natural convection 3) Heat transfer to the core catcher Sodium-sacrificial material long-term interaction	Large-scale experiments Investigation of natural convection in presence of immiscible phases (metal and oxide). Investigation of the impact of metal segregation on heat transfer.	LIVE (KIT) VULCANO (CEA) CORRONA (CEA) VITI (CEA)
20	SFR, LFR: Debris coolability	SFR: 1) Debris bed levelling at the vessel bottom head 2) Self-levelling by sodium boiling 3) Dryout heat flux in function of the debris size distribution	Experiments to be used for transient cases (critical geometry). Debris re-melting and core catcher material melting. Enough experimental data.	EDULCOREE, ETABUL (CEA) DEFOR (KTH) Experiments at Kyushu University

		LFR: 1) Influence on vapor bubble on natural circulation and debris bed spreading 2) Debris distribution on the free surface 3) Debris bed levelling at the vessel bottom head • debris leveling by LBE boiling	Bubble injection experiments Tests on the stability of natural convection/circulation. Effect of the gas/vapor bubbles on natural convection/circulation. Experiments aimed to show the impact of Lead/LBE surface tension, Lead/LBE natural circulation on the debris spreading. Experiments aimed to show the impact of residual heat, natural circulation and gravity on the levelling of initial debris bed configurations.	TALL, BUTRA (KTH)
21	Post accidental heat removal	SFR (ASTRID): Natural convection pathway from the core catcher to the DHR	Prototypical experiments needed.	PATH (IGCAR)

	by natural convection	MYRRHA RTCS: Direct heat transfer between debris and coolant	1) Experiments investigating the interaction between coolant and core debris and frozen steel and effects on the natural circulation loop. 2) Experiments with different fuel particle size and density to characterize the heat transfer regime.	
		MYRRHA RVACS: Natural circulation onset Heat degradation by incondensable gases	Experiments aimed to investigate the impact of different heat flux distribution along the vessel on the natural circulation onset. Experiments aimed to verify the correct purging of incondensable gases and to evaluate the heat transfer degradation along the vessel.	

6 Experimental facilities of the SAFEST consortium

The SAFEST experimental facilities can perform experiments in specific fields of severe accident research and corium behavior for main types of light water reactors. The partners of the SAFEST project will carry out experiments, develop and validate numerical models aiming at adequate description of the investigated phenomena and upgrade the SAFEST facilities to be able to address the future research needs.

The next sections describe the facilities of the SAFEST consortium, grouped per owner institute. The descriptive chapters refer to the Deliverable 2.1 “European corium experimental research roadmap” of the WP2 of the SAFEST project [151].

In Chapter 7, a general assessment on the possibility of exploiting the SAFEST facilities to tackle the R&D issue identified in Table 4 and Table 5 is presented.

6.1 Experimental facilities at KIT

The LACOMECO experimental platform at KIT includes the following facilities.

6.1.1 QUENCH

The QUENCH facility is the only operating experimental facility in EU for investigations of the early and late phases of core degradation in prototypic geometry for different reactor designs and different cladding alloys. This includes analysis of the relocation of cladding and fuel and the formation and cooling of in-core debris beds to gain information on the characteristics of the created particles. The main objective is the study of Zircaloy oxidation and H_2 production on quenching by water and rapid cooling by steam, with variation of pre-oxidation conditions.
The main component of the QUENCH test facility is the test section (Figure 44) with the test bundle. The facility can be operated in forced-convection mode and a boil-off mode. The system pressure in the test section is set to 0.1 and 0.5 MPa absolute. The test section has separate inlets at the bottom to inject water for reflood (bottom quenching) and synthetic air (80% N2 + 20% O2) in case of air ingress test. The argon, the steam and gases not consumed, and the hydrogen produced in the zirconium-steam reaction flow from the bundle outlet at the top through a water-cooled off-gas pipe to the condenser where the steam is separated from the non-condensable gases.
The test bundle is approximately 2.5 m long and is made up of 21 (Figure 44), 24 or 31 fuel rod simulators depending on cladding size and bundle geometry (quadratic or hexagonal). The fuel rod simulators with Zr-alloy claddings are held in position by five grid spacers, four are made of Zry-4 and the one at the bottom of Inconel 718. The rods can be electrically heated or unheated. All test rods can be filled with Kr or He at a pressure between 0.2 and 5.5 MPa absolute.

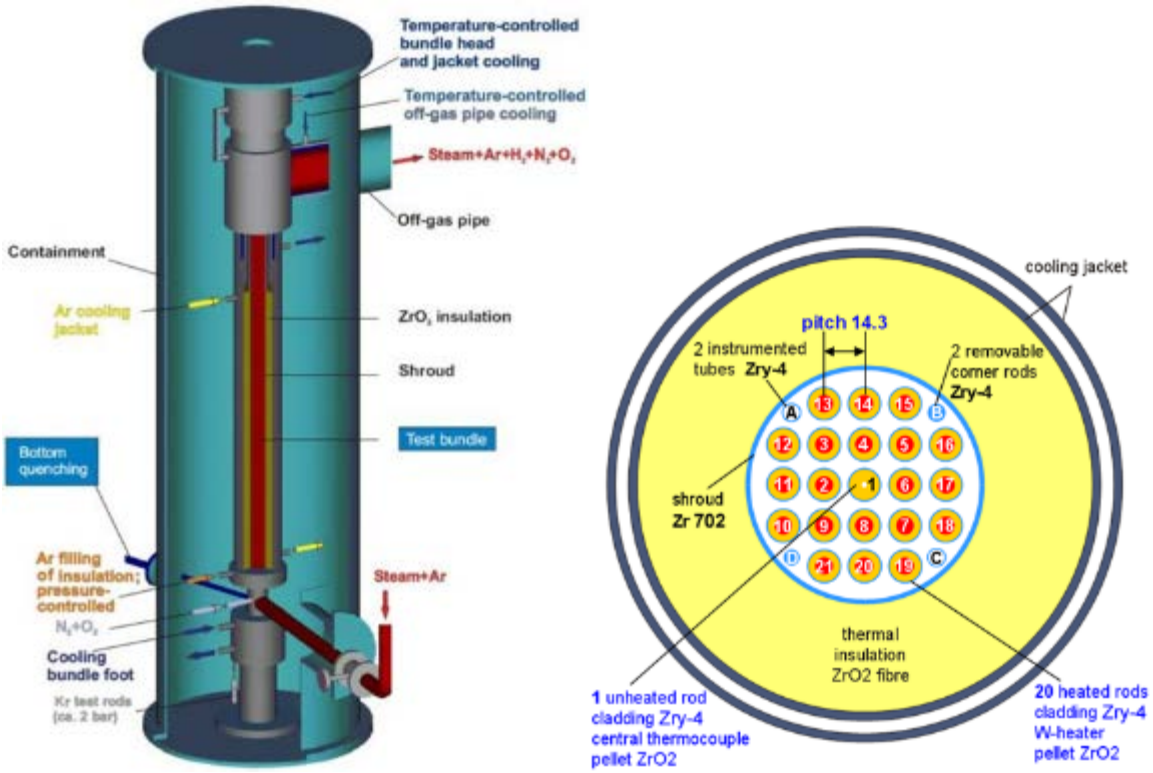

Figure 44: Sketch of the QUENCH facility (left); layout of the QUENCH test section (right)

6.1.2 LIVE

The LIVE test facility at Karlsruhe Institute of Technology concentrates on the investigation of the whole evolution of the in-vessel late phase of a severe accident. This includes e.g. formation and growth of the in-core melt pool, characteristics of corium arrival in the lower head, and molten pool behavior after debris re-melting in large-scale 3-D geometry, with emphasis on the transient behaviour.

The main part of the LIVE-3D test facility is a 1:5 scaled semi-spherical lower head of a typical pressurized water reactor, (Figure 45). The diameter of the test vessel is 1 meter. The top area of the test vessel can be covered by an insulated or a cooled lid. The test vessel is enclosed in a cooling vessel to simulate the external cooling.

The melt is prepared in an external heating furnace designed to generate 220 l of the simulant melt.

The maximum temperature that can be reached in the heating furnace is limited to 1100 °C. In addition, the heating furnace is equipped with a vacuum pump, so it is possible to extract the residual melt out of the test vessel back into the heating furnace.

The volumetric decay heat is simulated by means of eight heating planes in the test vessel. Each heating plane consists of a spirally formed heating element with a distance of ~40 mm between each winding. The heating elements are shrouded electrical resistance wires and are located in a special cage to ensure the correct positioning. To realize a homogeneous heating of the melt, each plane can be controlled

separately. In the case of homogeneous heat distribution, the maximum heating power is limited to ~29 kW. The maximum temperature of the heating system is also limited to 1100 °C.
To investigate both the transient and the steady state behaviour of the simulated corium melt, an extensive instrumentation of the test vessel is realized. The temperatures of the vessel wall inner surface and outer surface are measured to be able to calculate heat flux distributions.
Additionally, up to 80 thermocouples are positioned within the vessel to measure the temperature distribution in the melt pool and in the crust.
To get detailed information about the crust formation, three thermocouple trees are installed at the vessel wall at different heights. A precise crust detection lance can detect the crust front and measure the crust/melt boundary temperature as well as the melt pool vertical temperature profile. Two video cameras and one infrared camera are used to visualize the convection of the melt pool [152].

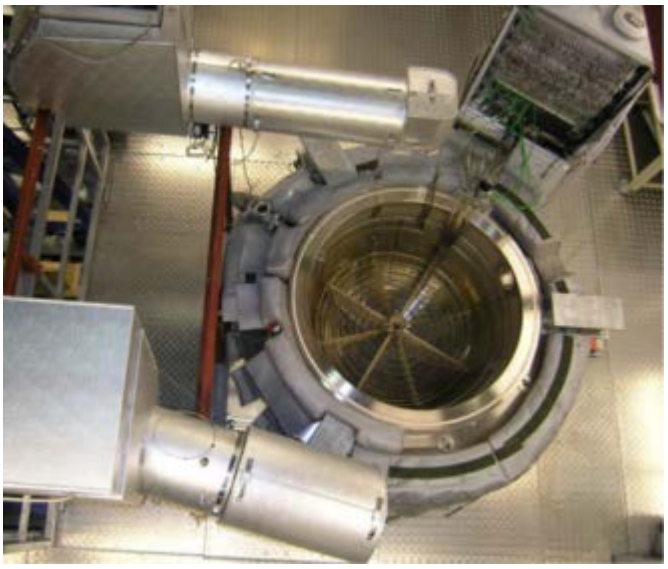

Figure 45: LIVE experimental facility

Up to now, the LIVE test facility was mainly devoted to the study of the corium behaviour in the lower head, mostly for Gen II-III reactors but also for Gen IV (LIVE-CERAM test [125]). Several experiments have been performed to investigate the melt pool transient and steady-state behavior under different heating and cooling conditions.
Comprehensive experimental results have been obtained regarding melt pool temperature, heat flux distribution through the vessel sidewall, crust thickness and crust properties. Furthermore, experiments to investigate the temperature distribution of a debris bed in the lower head in dryout condition and the global melting process of the debris bed after relocation of liquid melt have been performed.
Besides this, it is planned to upgrade the LIVE test facility in order to study the quenching of debris beds in the lower head.

6.1.3 DISCO

DISCO (Figure 46) is the only operating facility available worldwide for integral direct containment heating and FCI investigations. It is designed to perform scaled experiments that simulate melt ejection from the RPV to the reactor cavity after the RPV failure under low system pressure during severe accidents in LWRs. These experiments investigate the fluid-dynamic, thermal and chemical processes during melt ejection out of a breach in the lower head of an LWR pressure vessel at pressures below 2 MPa. The main components of the facility are scaled about 1:18 linearly to a large PWR. The model of the containment pressure vessel has a height of 5.80 m and a total volume of 14 m³, Figure 46. The volumes of the reactor cooling system (RCS) and the reactor pressure vessel (RPV) are modelled by a vertical pipe. A disk holding 8 pipes (46 mm inner diameter, 255 mm length) separates the two partial volumes. This arrangement models the main cooling lines with respect to the flow constriction between RCS and RPV. The RPV model, mounted at the lower end of the pipe, serves as crucible for the generation of melt by a thermite reaction between iron oxide and aluminum. The total volume of the RCS/RPV vessel is 0.08 m³. The breach in the lower head is modelled by a graphite annulus at the bottom, which is closed with a brass plate. This plate melts when the thermite reaction reaches the bottom. The reactor pit is made of concrete and is installed inside a strong steel vessel. The main cooling lines are modelled by eight horizontal steel cylinders with a scaled annular space around each of them, modelling the flow path leading into the equipment rooms. The equipment rooms are modelled according to the reactor design being investigated.

Figure 46: DISCO experimental facility

Standard test results are: pressure and temperature history in the RPV, in the cavity, in the reactor compartments and in the containment vessel; post-test melt fractions in all locations with size distribution of the debris, video film in the sub-compartments and containment and pre- and post-test gas analysis in the cavity and the containment. The gas analysis allows determining the amount of produced, burned and remaining hydrogen.

6.1.4 MOCKA

The MOCKA facility (Figure 47) is designed to study the erosion of the concrete by the molten corium, in a 3-D large-scale geometry with simulant melt masses of up to 3 tons. The melt is generated in a thermite reaction and the decay heat is simulated by adding the thermite briquettes and Zr into the melt from the top.
To allow sufficient time and material for the erosion process, the cavity of the cylindrical crucible is fabricated as a massive concrete structure.
The experimental focus is on the cavity formation in the basement and the risk of a long-term basement penetration by the metallic part of the melt. Several types of concrete can be tested.

Figure 47: MOCKA test facility

Up to 3200 kg of melt is generated by ignition of the specific thermite mixture in a concrete crucible. After completion of the chemical reaction, the melt separates into the lighter oxide melt on top and the heavier metal melt at the bottom. The initial temperature of the melt is more than 1800 – 1900 °C and the melt has sufficient overheat over the liquidus temperature to show significant effects also in transient tests.
Even if MOCKA is mainly devoted to corium concrete interaction studies for LWRs, it can be used for Gen IV-relevant issues such as jet ablation, as planned within the ESFR-SMART project [112].

6.2 Experimental facilities at CEA

6.2.1 PLINIUS platform

The current PLINIUS experimental platform (Figure 48) at CEA is composed of four facilities devoted to the corium behaviour and physical properties studies:

- VULCANO is a rotating plasma arc furnace able to melt about 80 kg of corium at temperatures of up to 3000 °C (in- or ex-vessel corium) and to pour the melt according to different configurations. It studies corium spreading, interaction and solidification phases.
- VITI has been developed to perform viscosity and surface tension measurements on corium by aerodynamic levitation up to 2500 °C. Samples of a few milligrams of corium can be implemented. It is also used for small mass experiments for properties estimation or material compatibility tests, and it can be employed to study molten core concrete interactions.
- KROTOS facility is dedicated to steam explosion phenomenon studies. About 5 kg of corium at more than 2850 °C are dropped in water. Thermal, optical and pressure instrumentation, along with fast imaging, constitute the instrumentation. The KROTOS facility for corium-water interaction tests has been transferred from JRC Ispra (Italy) and has been rebuilt at CEA Cadarache within the PLINIUS platform.
- RESCUE facility is a 4 m high mock-up dedicated to improve understanding and check the efficiency of In-Vessel Melt Retention safety systems.

Figure 48: Facilities composing the PLINIUS platform. From the left: VULCANO, VITI, KROTOS, RESCUE

6.2.2 PLINIUS-2 platform in support of ASTRID and SFR design

CEA has decided to launch the design of a new corium platform [153]: PLINIUS-2 (Figure 49). This new experimental platform will replace the current PLINIUS prototypic corium platform. Its main advantage will be the possibility to use corium and sodium, as well as an extended mass range.
It will consist of a furnace, and of several test sections, installed in 3 separated halls. The furnace will be installed in an airtight enclosure that can be moved, between experimental series, over the experimental halls above the selected test section. Cold crucible induction technology is the most widely used for prototypic corium melting (RASPLAV [154], SICOPS [155], COMETA [156], SOFI [157], TROI [158], and VESTA [159]). Very high temperatures can be reached with this technology, which also prevents any significant melt pollution thanks to the formation of a self-crucible.

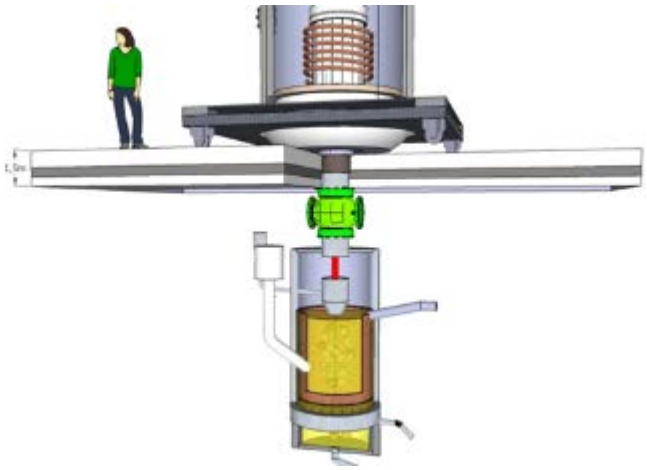

Figure 49: Conceptual view of PLINIUS-2 FCI experimental layout with furnace (top)

A complementary melting or pre-heating process has been selected: Self-propagating High-temperature Synthesis (SHS) reaction. This process is based on an oxidation-reduction reaction that is strongly exothermic. Temperatures can reach 3000 K in a few seconds. This approach is routinely used to produce prototypic corium at ANL [160] and has been used for instance in the MFMI facility [102] with specific corium compositions. Urano-thermic reactions have already been tested in the PLINIUS/VULCANO facility [161] and have been selected as the corium melting technique for a newly started French national project on LWR corium cooling.

The design of the Fuel Coolant Interaction (FCI) test section (Figure 50 left) reproduces the major outlines of the FARO TERMOS test section [75] since this program was terminated before necessary experiments with high temperature sodium interacting with large masses of molten UO_2 could have been carried out. The test vessel will be protected by thermal insulation in order to withstand hot sodium. A dedicated sodium loop is being designed (Figure 50 right). It will be necessary to fill the section with sodium, to heat it to the necessary temperature. After the test, the sodium will be recycled after filtering of possible debris. Great care is being given to the capabilities to perform meaningful post-test observations and analyses. Asides from the large scale (250-500 kg, ~1 m diameter) test section, it will be necessary to build for commissioning tests a medium scale (<50 kg, ~25-30 cm) facility. This facility will indeed be available for medium-sized experiments throughout the platform lifespan. In particular, it will be dimensioned in order to be compatible with X-ray visualisation of FCI.

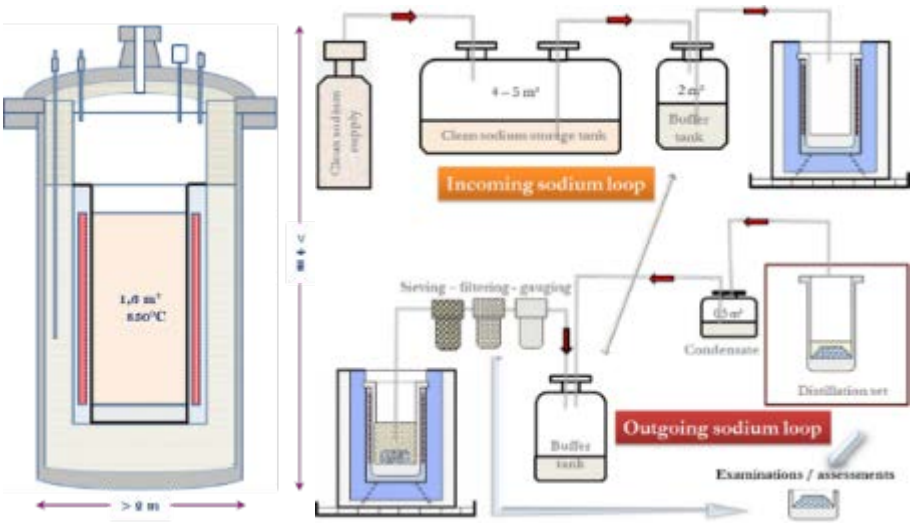

Figure 50 : Preliminary conceptual design of sodium test section (left) and loop (right)

An alternative corium transfer technique to deliver in gas above the sodium free surface must be implemented, as explained in Par. 5.1.3.
The building of the PLINIUS-2 facility is being designed (Figure 51) and optimized to conduct experimental programs providing security requirements, in particularly in the presence of sodium and water in separated halls. The building is structured on two levels with three corium experimental halls in the basement and a corium furnace hall at ground level.

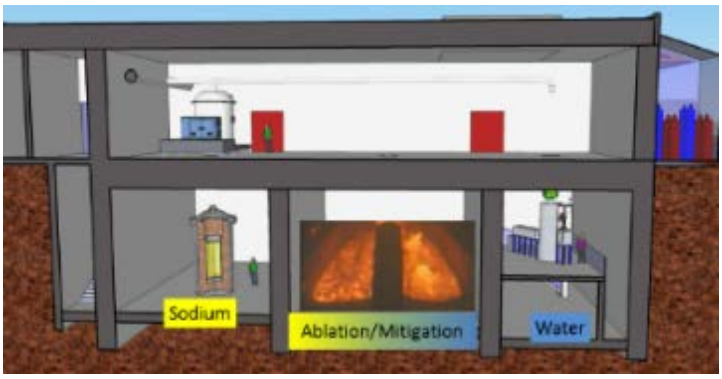

Figure 51 : Conceptual design of PLINIUS 2 building

It has been decided to launch the PLINIUS2 project for a new experimental infrastructure dedicated to the resolution of corium issues for both LWRs and Sodium Fast Reactors during the next decades.
It will cover Gen II-III and Gen IV corium needs, allowing experiments varying from 5 g of corium up to 500 kg involving water or sodium coolants, concrete, metal, ceramic, sacrificial, neutron poison, etc... It will be built on the CEA Cadarache site and will be operated as an international user facility hosting test sections for national and international partner programs.
It has been decided that the processes will rely on evolutionary technologies based on proven techniques based on the worldwide experience of corium experimental facilities. Preliminary studies have been launched with a focus on the regulatory aspects linked to the joint use of corium and sodium. These studies, performed in 2012-2013, led to the decision to make the investment. The design studies have started in 2014 [162] and the facility should be available for experimental programs in 2021 [22].

6.3 Experimental facilities at KTH

The SWECOR (Swedish Corium Research) experimental platform at KTH is a unique platform of experimental facilities to study different phenomena of corium-water interaction, jet fragmentation and debris formation and coolability. The platform integrates several facilities using corium simulants.

6.3.1 DEFOR

DEFOR is a large-scale facility (Figure 52) positioned inside reinforced containment and devoted to the study of melt jet fragmentation in water and formation of solid debris with up to 80 kg of simulant corium melt. The protective containment is certified and tested for 5 bar internal pressure.
DEFOR facility (Fig. 4) is composed of a 45kW medium-frequency (up to 50 kHZ) Induction Furnace (IF) for melt generation, a melt delivery funnel, and a coolant tank with glass windows for visual imaging of transient melt-coolant mixing and debris formation. The simulant-material melt is generated in a SiC crucible or in a double crucible of SiC as a back-up for a Zirconia crucible. The liquid melt is delivered to the funnel by tilting the crucible. The delivery funnel is conical with a replaceable discharge nozzle up to 25 mm in diameter. The test section is an open rectangular tank (2 m tall, with cross section 0.5 x 0.5 m).

Figure 52: DEFOR facility

6.3.2 SES

SES (Steam Explosion Stratified facility, Figure 53) is an experimental facility for the investigation of Fuel Coolant Interaction (FCI) in stratified melt coolant configuration and underwater liquid melt spreading. The SES facility can be used to obtain insights on: (i) energetics of steam explosion, (ii) melt spreading dynamics, and (iii) development of melt-coolant premixing layer.
The facility consists of 45kW medium-frequency (up to 30 kHZ) generator, induction furnace (IF) with a SiC crucible for melt preparation, melt delivery, funnel, impact pale, and a water pool (SES test section). The SES test section is an open stainless steel rectangular container: 0.8 m deep, 1x1 m wide, positioned 800 mm above the ground on the supporting frame. The lateral walls are 4 mm thick and equipped with four

(400x600 mm) Plexiglas windows allowing visualization of the melt delivery and spreading. The bottom of the test section is a 10 mm thick stainless steel plate.

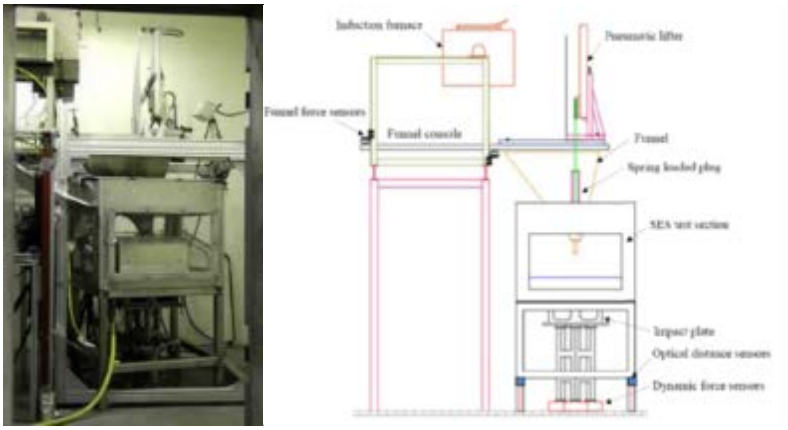

Figure 53: photo and layout of the SES facility

Interactions between molten binary oxidic melt mixtures at temperatures up to 1600 °C and masses up to 80 kg with large shallow water pool at temperatures up to 95 °C can be studied in the SES facility. The facility can be configured to provide melt spreading under water or in a dry section with subsequent flooding.
The melt is delivered into the funnel directly from the crucible by tilting the induction furnace.

6.3.3 POMECO

POMECO test facilities at KTH (Figure 54) are dedicated to the coolability quantification of debris beds formed in a hypothetical severe accident of light water reactors (LWRs), when the molten corium is relocated into a water pool, fragmenting and forming a particulate debris bed on the water pool bottom for both in-vessel and ex-vessel scenarios. It could also be used to study the effects of impure water on debris cooling.
The POMECO-FL investigates two-phase flows in a porous media.
POMECO-HT is capable to use about 30 liters of electrically heated corium debris simulants for the study of the debris coolability and dryout heat flux at natural and forced convection of water in the porous media. The facility features flexibility of reconfiguration and a maximum heat flux of 2.1 MW/m^2, which enables coolability investigation on various beds of a broad range of particles with either top-flooding or bottom-fed schemes. The facility is also well instrumented with two differential pressure transducers installed to measure the pressure drops. The bed can be quenched from the top by an overlying water pool and from bottom by using downcomers or forced injection of water.

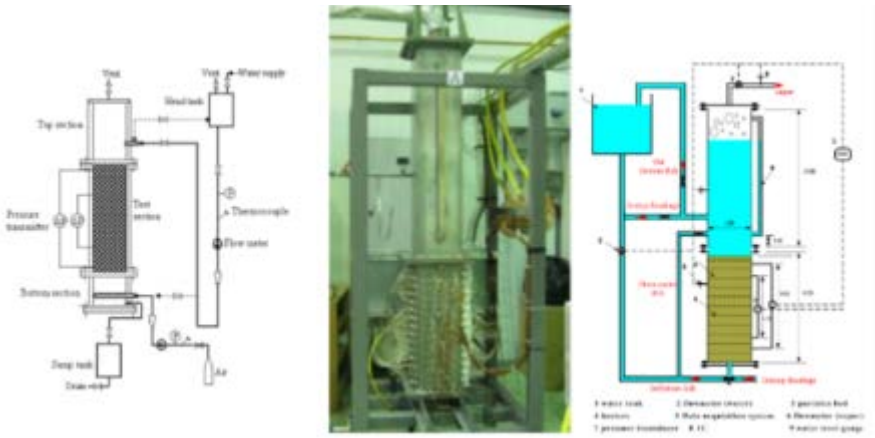

Figure 54: POMECO facility and of the test section

6.3.4 MISTEE

MISTEE (Figure 55) is a test facility to provide high-quality data for steam explosion study under well-controlled conditions equipped with a synchronized precise optical photography and X-ray visualization systems. The facility can also be applied to investigate the characteristics of boiling, bubble dynamics and multiphase flow.

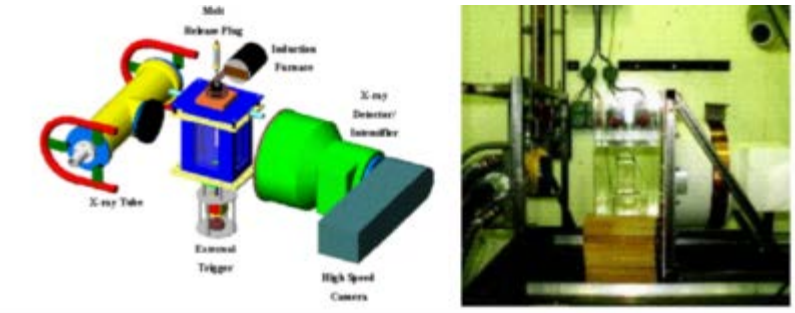

Figure 55: MISTEE facility

6.4 Experimental facilities at EK-MTA

6.4.1 CODEX

CODEX facility (Figure 56) studies the early phase of core degradation with electrically heated fuel bundles at high temperatures.
Several experiments have been carried out with VVER and PWR type fuel rods. High temperature experiments were carried out in steam and air atmospheres. The effect of final water quench on fuel integrity was investigated. The production of gases during the degradation of fuel bundle with B_4C control rod was simulated. Special tests have been carried out with the main conditions of the Paks-2 cleaning tank incident.
The VVER type bundle is constructed with seven fuel rods arranged on a hexagonal lattice. The PWR bundle includes nine rods in square arrangement. Two or three spacer grids are applied to fix the bundle. The heated length of the bundle is 600 mm. The cladding material was E110 (VVER) or Zircaloy-4 (PWR) in the previous tests.

Considering the flexibility of the CODEX facility several core degradation scenarios can be covered by the experiments.

- The fuel pressurization allows to simulate the ballooning and burst of fuel rod cladding. The further oxidation can lead to high degree of oxidation and to the formation of secondary hydrided structures. The deformed structure of the bundle can be used to investigate the coolability of degraded core.
- The water quench of high temperature bundles and the application of gas composition measurement devices can provide valuable information on the hydrogen generation. The use of different alloys can produce alloy specific data on oxidation and quench behavior.
- The facility is capable to simulate not only reactor accidents, but e.g. spent fuel pool accidents, too. The scenario starting with boil-off process and ending with air ingress can be accomplished in the CODEX facility.

Figure 56: CODEX test section

6.4.2 CERES

The CERES facility (Figure 57) was built for the experimental modelling of the cooling loop to be implemented in to remove heat from a VVER-440 reactor vessel in the late phase of a severe accident.
The scaling ratio of CERES is 1:1 for the external surface of reactor vessel and the elevations to provide driving forces for the natural circulation, while 1:40 slice of the vessel is modeled. CERES investigates the whole spectrum of phenomena of cooling of the flooded outer surface of reactor vessel in large scale for a wide range of thermal-hydraulic parameters. The cooling channel in the vessel model has different gap sizes between the vessel and cavity walls, having a “critical” narrow gap size. It is critical from the viewpoint of the heat extraction, because, to some extent, it can block the natural circulation flow. The length of coolant channel section is 900 mm from the elevation of 1300 to 2200 mm. The gap size of coolant channel is 20 mm if the vessel is cold and it is in symmetric position in the cavity. If the vessel is in asymmetric position, the vessel wall can contact the cavity wall causing the most narrowing gap size. To measure the effect of coolant channel contraction on the heat transfer, two different asymmetric channels were constructed. These are as follows: 9.7 mm, stepped-shape with 5 and 9.7 mm (half of channel with 5, the other half is 9.7 mm; stepped-shape with 9.7, 6.7, 5.4, 4.0, 3.0 mm).
Heaters provide heat load caused by the corium with values and distribution as specified in the test conditions according to numerical models.

Figure 57: CERES facility

6.5 Experimental facilities at JRC-Karlsruhe

6.5.1 FLF

FLF is a laser heating/melting and fast pyrometry facility (Figure 58 and Figure 59) to study the melting behaviour of pure compounds and binary systems under various atmospheres. Laser heating combined with fast pyrometry is the method used in the JRC Karlsruhe Material Research Unit for high temperature investigation of nuclear materials. The method can be perfectly applied to the analysis and laboratory-scale simulations of severe accidents in nuclear power plants. The heating agent is a Nd:YAG 4.5 kW continuous wave laser programmable with a complex power/time profile, permitting thermal cycles of variable duration from a few milliseconds up to some minutes, in order to test the material behavior as a function of the heating and cooling rates and the dwelling time at high temperature.
Experimental parameters can actually be optimized according to the sample features (volatility, chemical stability etc.) and the kinetics of the phase transformations under investigation. Temperature is measured on the heated sample surface by means of fast pyrometers. The typical temperature range for this type of experiments lies between 1800 K and 5000 K. The setup has been recently employed for the analysis of solid/liquid equilibria in fundamental corium sub-systems, such as the pseudo-binaries UO_2-ZrO_2, UO_2-PuO_2 and the ternary UO_2-PuO_2-ZrO_2. More components are being added to the studied materials, in particular constituents of the various reactor parts likely to melt into corium in case of a severe accident: cladding, moderators, concrete. The technique has also been successfully employed for the synthesis of corium simulants, by melting, for example, UO_2 directly in a Zircalloy cladding. The resulting samples can be investigated after the thermal cycles in order to study, by several methods, effects of possible segregation and non-congruent vaporization phenomena occurring at very high temperature. Experiments are carried out in an autoclave under medium-high pressure (from a few tens up to a few hundreds MPa) of an inert (helium or argon), reducing (argon + hydrogen) or oxidizing (air, steam) gas. This permits to suppress as much as possible evaporation phenomena in highly volatile samples, and to study the material synthesis and the behavior of phase transition points as a function of the gas nature and pressure. Moreover, an additional method has been applied to determine phase transitions, based on the detection, via a suited low-power (mW) probe laser, of changes in surface reflectivity that may accompany solid/liquid phase transitions. This method has been called the “Reflected Light Signal” (RLS). A particularly challenging parameter to measure is the high temperature emissivity of materials, for the high precision required even under extreme conditions. Yet, emissivity is a fundamental parameter that drives the thermal losses and the temperature detection. Thus, multichannel pyrometry for the study of the sample emissivity at high temperature is also being developed at JRC Karlsruhe.

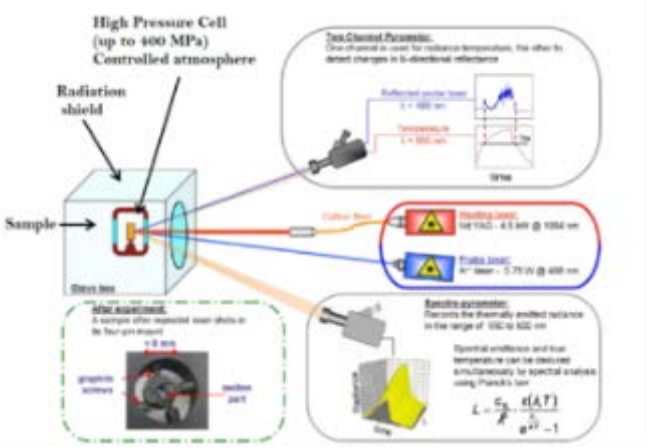

Figure 58: FLF functioning scheme

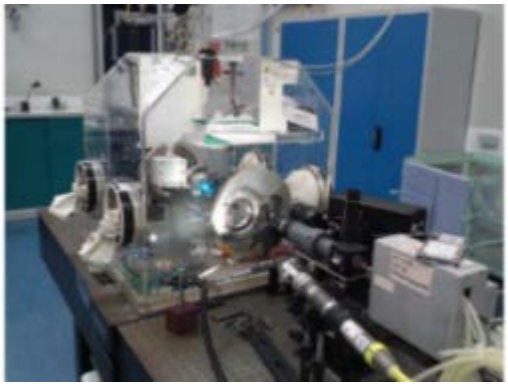

Figure 59: Photo of the FLF experimental facility

6.5.1.1 JRC-Karlsruhe Thermodynamic Property Measurement facilities

JRC Karlsruhe has a number of other facilities for the determination of thermodynamic properties. These include thermal conductivity, and diffusivity, Knudsen Cell effusion cell testing, as well as thermal capacity and electron-optical examination and analysis (TEM-EELS & SEM/EDX) in the materials science department. Other devices include X-ray diffraction (with Reitfeld analysis) in the Basic Actinide Research unit.

A shielded laser-flash device was designed and constructed at JRC for the measurement of highly γ-active samples (small disks). The samples are heated in a high-frequency furnace. A laser pulse of 2 ms is then applied to the front surface of the disk. The emerging temperature perturbation on the opposite surface is recorded by a photodiode-based pyrometer (0.05 K sensitivity) provided with a fast log-amplifier, and 24-bit A/D converter with a response time of the order of 10 s. The recorded thermograms, consisting of several thousands of points, are analyzed by a realistic and accurate mathematical expression of the pulse propagation in the sample.

The thermal diffusivity is then calculated together with the occurring heat losses by a numerical fitting procedure followed by a self-consistency check of the resulting heat losses. The precision of the thermal diffusivity measurements is better than 5%. From these values the thermal conductivity at the corresponding temperature can be calculated. The device can determine the values for temperatures ranging from 570 K to nearly 3000 K.

6.6 Experimental facility at ÚJV

6.6.1 COMETA

At ÚJV Řež, the cold crucible induction heating facility COMETA (Figure 60) has been constructed for powder oxide materials melting with melt temperatures up to 3000 °C. The facility is adapted for the operation with radioactive materials (in particular with UO_2) and intended for simulating real corium melts with prototypic materials. The cold crucible has an experimental capacity of about 1 kg of initial corium batch (250 cm^3 volume of melt) and can reach 3000 °C of melting temperature. The principle of cold crucible consists in concentrated heat inside the heated material. The power supply in this facility is a high-frequency generator, which provides a power of up to 60 kW in the melt at a frequency of 4.5 MHz. The movable frame enables the subsequent directed crystallization of the corium melt. The system is equipped by full computer control and measurement evaluation.
Although most of COMETA tests have been devoted to LWR issues, an experiment on UO_2-B_4C interaction for ASTRID has been carried out in COMETA [163] within SAFEST project.

Figure 60: Scheme of the COMETA facility

Figure 61: Photos of the two facilities of CVR Cold Crucible Laboratory

COMETA has been replaced in 2017 by new larger facilities forming the cold-crucible laboratory (Figure 61) at the Rez Research Centre (CVŘ).
The first furnace has a protective quartz glass tube (Figure 62 left) so that it is possible to operate in a chosen atmosphere, such as neutral argon gas. The cold crucible inner diameter is of 7.7 cm for a height of 7 cm. 1.5 to 2 kg of UO_2 can be melted. As COMETA, it is possible to move the crucible relative to the inductor to slowly vary the induced power.

The second furnace (Figure 62 right) operates only in air atmosphere. Its cold crucible is slightly smaller (∅5.2 x 5 cm) leading to melted UO_2 masses of 0.8-1 kg.

Figure 62: Photograph of the two cold crucible laboratory furnaces at CVR

6.7 Experimental facilities at Framatome GmbH

6.7.1 SICOPS

The SICOPS facility (Figure 63) is an experimental facility at Framatome Radiochemical Laboratory in Erlangen, Germany. It is used for studies of different phenomena of the interaction of molten corium with concrete or other sacrificial material and with protective material (SICOPS: Simultaneous Interaction of Molten Corium with Protective and Sacrificial Material) and to generate data on thermophysical and thermochemical processes during interaction of melt with concrete or other material.
Centerpiece of SICOPS is a high-frequency (1-4 MHz) furnace with a “cold crucible”. A prime feature of this technology, also called “skull-melting”, is that it ensures sustained heating of prototypical (UO_2-containing) oxidic/metallic corium melts in order to simulate the heat input from radioactive decay and establish realistic heat fluxes. Skull-melting circumvents the crucible material problem by formation of a "self-crucible", i.e. a 2- 3 mm thick crust of the same material as the melt at the cold crucible walls, which keeps the melt enclosed. This technology allows an almost crucible-free melting and, in principle, renders unlimited test durations possible. It has been used successfully for material studies with high temperature melts (up to ~3000 °C).
Tests with material masses of up to 20 kg molten material (simulant or prototypic, UO_2 containing melt) and with a generator power of maximum 100 kW can be performed. The facility was mainly used for tests on corium-concrete interaction (1-D, 2-D) with oxidic and mixed metallic/oxidic melts and for material studies. Recent tests were made with metallic/oxidic melts without concrete and relatively high metal load.
The cold crucibles have diameters of 5 to 20 cm. The melt temperature can be measured with thermocouples (internal and dip-in) and the melt surface temperature and surface motion pattern with a pyrometer. The thermocouples can also be used to determine heat fluxes or to measure the progression of melt into e.g. concrete providing data about transient processes of melt interaction with concrete or other material. Samples can be taken from the melt during an experiment.
The facility is equipped with several cooling circuits to determine power input into the crucible and heat losses (calorimetry). Furthermore, it can be run with different gases inside the test vessel and an off-gas measurement with an online gas mass spectrometer or oxygen sensors can be applied. This widens the spectrum of possible applications. For example, in a previous project the degree of oxidation of metallic melts by gas, released from concrete, could be measured under inert conditions.
Samples taken from the melt as well as the materials solidified inside the crucible after the end of a test can be analyzed by various methods, e.g. optical microscopy, SEM/EDX, chemical analyses.

Figure 63: SICOPS experimental facility

7 Conclusions

The work presented in this deliverable has identified the main phenomena occurring during core degradation, discharge and post-accident heat removal phase in the GEN IV fast reactors supported by ESNII. When needed, R&D issues and experimental needs were addressed in a general way or for the particular technology (SFR, LFR, GFR) or reactor design (ASTRID, MYRRHA, ALLEGRO).

An indicative assessment is given on the possibility of employing the SAFEST facilities in the investigation fields addressed in Table 4 and Table 5.

It is important to make a distinction between the exploitation of the facilities in the short-term- and in the long-term future. In the short-term, it is possible to represent with integral tests only phenomena not involving liquid metals. In the long-term, the reconversion of the installations for working with liquid metals is required, as the coolant plays an important role in the occurrence of specific phenomena.

7.1 Short-term view

In the short-term, the SAFEST facilities are not supposed to be upgraded to deal with liquid metals. However, the remaining R&D issues of the sodium technology and ASTRID design will already be investigated by both the PLINIUS-2 platform (CEA), for what concerns corium discharge, fuel-coolant interaction and interaction corium-sacrificial materials, and the CORRONA facility (CEA), for what concerns sacrificial material testing in sodium (investigation fields nº 19 in Table 5). Tests studying the binary interaction corium-core catcher can also be carried out in the SICOPS (Framatome GmbH), MOCKA and LIVE facilities (KIT). In particular, the LIVE facility (KIT) can be employed in support of the core catcher design of the ASTRID and ALLEGRO reactors. The DISCO facility can be also used in support of the ex-vessel core catcher design of ALLEGRO.

FLF (JRC), Cold Crucible Laboratory (CVŘ) and the VITI facility (in PLINIUS, CEA) can provide data on the material thermo-physical properties (investigation field nº 9) and chemical reactions (investigation field nº 6), for all kind of technologies.

As a general consideration, the SAFEST integral tests facilities are of limited use for the Lead/LBE cooled reactors in the short-term. In HLM systems, the liquid coolant is always present in every stage of the severe accidents and inevitably influences all the phenomena inside the core and the vessel. An exception is the issue related to gas bubbles effect on the debris coolability (investigation field n° 20), for which two facilities exist at KTH-NPS. The existing TALL infrastructure at Nuclear Power Safety (NPS) division, KTH, can be modified in order to provide capability of controllable gas bubble injection into HLM loop and/or 3-D test section. The influence of the injected bubbles on natural circulation and transient behavior can be studied. The other facility which is under construction is BUTRA (BUbble TRAnsport) built within MAXSIMA project. Controllable generation of very small single gas bubbles in liquid LBE by a novel technique based on vacuum cavities [164] has been demonstrated with this facility.

7.2 Long-term view

More issues can be investigated by the SAFEST facilities if refurbishment works are foreseen to deal with liquid metals. Some of the differences with water systems are:

- The coolant opaqueness
- The need of keeping the test section heated above the melting point of the liquid
- The corrosion on structural materials, for long-residence time of the coolant in the facility
- For HLMs (Lead/LBE), the additional mechanical loads on the facility due to the static pressure and the buoyancy force (structural materials are lighter than HLMs).
- The structural materials: no zirconium is employed but only stainless-steel

Qualification tests should be run, aiming to assess the compatibility of the facility internals and instrumentation with liquid metals. The experimental capabilities in presence of liquid metal must be re-assessed too.

The following sections of Par. 7.2 describe the possible long-term applications by groups of facilities. Each group of facility covers common investigation fields.

7.2.1 Fuel bundle degradation phase in pure LOF events

This group is formed by the QUENCH (KIT) and CODEX (EK-MTA) facilities.
The QUENCH and CODEX facilities can be refurbished to investigate phenomena related to integral tests on FA bundle degradation from loss of flow scenarios, hence the phenomena nº 2, 3, 4, 6, 7, 11, 16 listed in Table 4. The main changes regard the rod dimensions (fast reactor pins are thinner than LWR rods), and the structural materials (zirconium should be replaced by stainless steel).

7.2.2 Post-accident decay heat removal

The CERES facility (EK-MTA) is part of this group. It can be employed to qualify any decay heat removal system based on reactor pit flooding, like the MYRRHA RVACS.

A water loop for the simulation of the natural convection regime (investigation field nº 21 in Table 5) should be installed for this purpose, to demonstrate its long-term operation (Figure 40).

7.2.3 Molten material – coolant interactions and debris coolability

This group is formed by the PLINIUS-2 platform (CEA), the SWECOR platform (KTH) and the LIVE facility (KIT).

Like the PLINIUS-2 platform, the SWECOR platform is potentially able to investigate fuel coolant interaction, particle debris formation and coolability (investigation fields nº 17 and 20 in Table 5) in sodium fast reactors, if the refurbishment process of the facility to work with sodium is deemed feasible.

Concerning Lead/LBE technology the SES facility (SWECOR) can be used to study molten steel freezing in LBE (investigation field nº 11 in Table 4), as the molten steel can be spilled from the bottom of the test section and move upward by buoyancy.

The LIVE and the POMECO (SWECOR) facilities can investigate the field nº 20, related to the coolability of debris bed at the bottom of the vessel, in a HLM environment. The main change for the LIVE facility consists in pouring directly particles and not molten corium in a LBE pool. This facility may be also used for integral tests in support of the design of the ALLEGRO ex-vessel core catcher (see Par 5.3; investigation fields nº 18, 19, 20 in Table 5).

7.2.4 Material characterization

FLF (JRC), IS (ÚJV) and VITI (in the new PLINIUS-2 platform, CEA) facilities are part of this group.

The FLF and the other facilities at JRC-Karlsruhe can be employed in the investigation field nº 9 (Table 4), for the estimation of thermo-physical properties of fresh and irradiated components of the ESNII reactors (fuel, cladding, structural materials, etc…). The FLF facility might be used to validate the Lead/LBE saturation curve at higher pressures than the atmospheric one (local LBE boiling under static pressure).

The Cold Crucible Laboratory and the VITI facility can be used to study chemical reactions (investigation field nº 6), and thermophysical properties of molten fuel.

7.2.5 Sacrificial material testing

The PLINIUS-2 platform, MOCKA, LIVE and SICOPS facility can be used in support of the ASTRID and ALLEGRO core catcher design, to study interactions between molten corium and core catcher materials (investigation fields nº 18, 19). No particular facility upgrades are needed for this task. Corrosion tests of sacrificial materials in sodium will be carried out in the CORRONA facility.

7.3 High-priority phenomena to be investigated by the SAFEST facilities

Table 6 summarizes the high-priority phenomena to be investigated in the SAFEST facilities. The final list of phenomena is obtained from Table 4 and Table 5 considering the combination of the priority in investigating a phenomenon and the experimental capabilities of the SAFEST facilities. The final ranking is given on the base of the phenomena priority and availability of the SAFEST facilities (short/long term). Priority 2 is assigned to the R&D issues concerning ceramic materials for GFRs, because they will not be used in the first ALLEGRO core configuration [18].

Table 6: indicative assessment of the possibility of employing SAFEST facilities to investigate R&D issues of GEN IV technologies investigated in the SAFEST project

CORE DEGRADATION PHASE						
Nº	**Investigation field**	**Technology/project**	**Priority**	**SAFEST facility**		**Ranking**
				Short-term	Long-term	
1	Pin failure by loss of cooling	LFR	1		QUENCH, CODEX	2
		GFR	2	QUENCH, CODEX		2
2	Pin failure by cladding nitriding	GFR	2	QUENCH, CODEX		2
3	Pin failure due to axial thermal stresses	GFR	2	QUENCH, CODEX		2
4	Chemical reactions	ALL	1	IS, VITI, SWECOR		1
5	EOS functions and thermo-physical properties of materials in a degraded core	ALL	1	FLF, VITI, Cold Crucible Laboratory		1
6	Molten steel relocation and freezing in Lead/LBE	LFR	1		SWECOR	2

POST-ACCIDENT HEAT REMOVAL PHASE

Nº	Investigation field	Technology/project	Priority	SAFEST facility		Ranking
				Short-term	Long-term	
7	Corium discharge	ASTRID	1	PLINIUS-2, MOCKA	SWECOR	1
8	Wrapper failure	LFR	1		QUENCH, CODEX	2
9	Fuel coolant interaction	SFR	1	PLINIUS-2	SWECOR	1
10	Core catcher ablation by corium jets	SFR	1	PLINIUS-2, LIVE MOCKA, SICOPS		1
		GFR	1	LIVE, MOCKA, SICOPS		1
11	Sacrificial material testing	SFR	1	PLINIUS-2, LIVE, SICOPS, MOCKA, CORRONA,		1
		GFR	1	DISCO, LIVE, MOCKA, SICOPS,		1
12	Debris coolability	SFR	1	LIVE		1
		LFR	1	TALL, BUTRA	SWECOR	
13	Post accidental heat removal by natural convection	MYRRHA (RVACS)	1		CERES	2

8 References

[1] GIF, "Technology Systems," 2017. [Online]. Available: https://www.gen-4.org/gif/jcms/c_40486/technology-systems.

[2] GIF, "A Technology Roadmap for Generation IV Nuclear Energy Systems," U.S.DOE and GIF, 2002.

[3] GIF, "Technology Roadmap Upadate for Generation IV Nuclear Energy Systems," GIF, 2014.

[4] Joint Research Center, "Strategic Energy Technology (SET) Plan," JRC, 2014.

[5] European Commission, "The Sustainable Nuclear Energy Technology Platform," European Commission, 2007.

[6] SNETP, "ESNII The European Sustainable Nuclear Industrial Initiative," SNETP, 2010.

[7] SNETP, "ESNII: European Sustainable Nuclear Industrial Initiative: Implementation Plan 2013-15," 2013.

[8] SNETP, "European Sustainable Nuclear Industrial Initiative - Roadmap," SNETP, 2017. [Online]. Available: http://www.snetp.eu/esnii/.

[9] N. Devictor, "Status of the ASTRID project," in *ESNII+ Biannual Conference*, Brussels, Belgium, 2015.

[10] P. Agostini, et al., "Progress report on the Italian national program on fast reactors," in *Proceedings of the 49th Technical Working Group meeting on Fast Reactor*, 2016.

[11] FORATOM, "EURATOM to Continue Supporting R&D for Gen IV Nuclear Systems," 02 2016. [Online]. Available: https://www.foratom.org/newsfeed/euratom-to-continue-supporting-r-d-for-gen-iv-nuclear-systems/.

[12] IAEA, "Safety of Nuclear Power Plant: Design," IAEA, Vienna, 2016.

[13] IAEA, "Fundamental Safety Principles," IAEA, Vienna, 2006.

[14] A. Vasile, "SFR Core Design Performance and Safety," in *IAEA Education and Training Seminar/Workshop on Fast Reactor Science and Technology*, Bariloche, Argentina, 2012.

[15] R. Fernandez, et al., "The Evolution of the Primary System Design of the MYRRHA Facility," in *Proceedings of the International Conference on Fast Reactor and Related Fuel Cycles: Next Generation Nuclear Systems for Sustainable Development (FR17)*, Yekaterinburg, 2017.

[16] G. Grasso, et al., "The core design of ALFRED, a demonstrator for the Europeanlead-cooled reactors," *Nuclear Engineering and Design,* vol. 278, pp. 287-301, 2014.

[17] P. Dařílek, et al., "ALLEGRO Core Neutron Physics Studies," in *Proceedings of the International Conference on Fast Reactors and Related Fuel Cycles: Next Generation Nuclear Systems for Sustainable Development (FR17)*, Yekaterinburg, 2017.

[18] L. Bělovský, et al., "The ALLEGRO Experimental Gas Cooled Fast Reactor Project," in *Proceedings of the International Conference on Fast Reactors and Related Fuel Cycles: Next Generation Nuclear Systems for Sustainable Development (FR17)*, Yekaterinburg, 2017.

[19] Argonne National Laboratory, "Thermodynamic and Transport Properties of Sodium Liquid and Vapor," ANL, Argonne, 1995.

[20] OECD/NEA, Handbook on Lead-bismuth Eutectic Alloy and Lead Properties, Materials, Compatibility, Thermal-hydraulics and Technologies, 2015.

[21] "Thermophysical Properties of Fluid Systems," NIST, 2017. [Online]. Available: http://webbook.nist.gov/chemistry/fluid/.

[22] F. Serre, et al., "PLINIUS-2: a new corium facility and programs to support the safety demonstration of the ASTRID mitigation provisions under Severe Accident Conditions," in *Proceedings of ICAPP* , San Francisco - USA, 2016.

[23] I. Sato, et al., "Safety Strategy of JSFR Eliminating Severe Recriticality Events and Establishing In-Vessel Retention in the Core Disruptive Accident," *Journal of Nuclear Science and Technology,* vol. 48, no. 4, pp. 556-566, 2011.

[24] D. C. Crawford,et al., "RIA Testing Capability of the Reactor Test Facility," IAEA, 1999.

[25] INL, "Future Transient Testing of Advanced Fuels," INL, 2009.

[26] R. G. Palm, "TREAT F-series LMFBR loss-of-flow experiments," INIS, 1982.

[27] L. W. Deitrich,et al., "A Review of the Experiments and Results from the Transient Reactor Test (TREAT) Facility," ANL, 1999.

[28] E. W. Barts, et al., "Summary and Evaluation - Fuel Dynamics Loss of Flow Experiments (Test L2, L3, L4)," ANL, 1975.

[29] A. E. Wright, et al., ""Fast reactor safety testing in Transient Reactor Test (TREAT) in the 1980s"," IAEA, 1990.

[30] G. Heusener, et al., "The CABRI-programmes - motivations and achievements," in *Proceedings of the International Fast Reactor Safety Meeting*, Utah, 1990.

[31] M. Haessler, et al., "The CABRI 2 Programme - Overview on Results," in *Proceedings of the International Fast Reactor Safety Meeting*, Utah, 1990.

[32] I. Sato, et al., "Transient Fuel Behavior and Failure Condition in the CABRI-2 Experiment," *Nuclear Technology,* pp. 116-137, 2004.

[33] D. Struwe, et al., "Overview on Material Relocation Phenomena in Liquid Metal Fast Reactors as Consequence of Core Disruption - IWGFR-89," in *Proceedings of the IAEA-IWGFR technical committee meeting on material-coolant interactions and material movement and relocation in liquid metal fast reactors*, O-arai - Japan, 1994.

[34] T. Beck, V. Blanc, N. Chapoutier, J.M. Escleine, L. Gauthier, D. Haubensack, D. Occhipinti, M. Pelletier, M. Phelip, B. perrin, C. Venard, "Conceptual design of fuel and radial shielding sub-assemblies for ASTRID," in *Proceedings of the International Conference on Fast Reactors and Related Fuel Cycles: Next Generation Nuclear Systems for Sustainable Development (FR17)*, Yekaterinburg, Russia, 2017.

[35] F. Payot, F. Serre, A. Bassi, C. Suteau, E. Batyrbekov, A. Vurim A. Pakhnits, V. Vityuk, "The SAIGA experimental program to support ASTRID core assessment in severe accident conditions," in *Proceedings of the International Conference on Fast Reactors and Related Fuel Cycles: Next Generation Nuclear Systems for Sustainable Development (FR17)*, Yekaterinburg, Russia, 2017.

[36] F. Bertrand, et al., "Synthesis of the safety studies carried out on the GFR2400," *Nuclear Engineering and Design,* vol. 253, pp. 161-182, 2012.

[37] C. Contescu, "Initial Assessment of Environmental Effects on SiC/SiC composites in Helium-cooled Nuclear Systems," Oak Ridge National Laboratory, 2013.

[38] A.S. Epiney, "Improvement of the Decay Heat Removal Characteristics of the Generation IV Gas-cooled Fast Reactor", Lausanne: EPFL, 2010.

[39] K. Kamiyama, K. Konishi, I. Sato, J. Toyooka, K. Matsuba, V. A. Zuyev, A. V. Pakhnits, V. A. Vityuk, A. D. Vurim, V. A. Gaidaichuk, A. A. Kolodeshnikov, Y.S. Vassiliev, "Experimental studies on the upward fuel discharge for elimination of severe recriticality during core-disruptive accidents in sodium-cooled fast reactors," *J. Nucl. Sci. Technol.,* vol. 51, no. 9, pp. 1114-1124, 2014.

[40] G. Kayser, et al., "Summary of the SCARABEE-N Subassembly Melting and Propagation Tests with an Application to a Hypothetical Total Instantaneous Blockage in a Reactor," *Nuclear Science and Engineering,* vol. 128, pp. 144-185, 1998.

[41] K. Schleisiek, et al., "The Mol-7C In-Pile Local Blockage Experiments: Main Results, Conclusions, and Extrapolation to Reactor Conditions," *Nuclear Science and Engineering,* pp. 93-143, 1998.

[42] J-F Vigier, et al., "Analysis of LBE-fuel interaction: Homogeneous MOX, BN MOX and UO2/PuO2 - Deliverable D4.2," SEARCH, EU 7th FP project, 2015.

[43] T. Retegan, et al., "MOX/LBE interaction under different atmospheres - Deliverable 5.15," MAXSIMA, EU 7th FP project, 2015.

[44] E. Karlsson, et al., "MOX/LBE/Cladding interaction under different atmosphere - Deliverable D5.16," MAXSIMA EU 7th FP project, 2016.

[45] J.-F. Vigiers et al., "Interaction study between MOX fuel and eutectic lead-bismuth coolant," *Journal of Nuclear Materials,* vol. 467, pp. 840-847, 2015.

[46] OECD/NEA, "Handbook on Lead-bismuth Eutectic Alloy and Lead Properties, Materials Compatibility, Thermal-Hydraulics and Technologies," OECD/NEA, 2015.

[47] K. Plevacova, C. Journeau, P. Piluso, J. Poirrier, "An experimental study of the effect of boron carbide on SFR compositions," in *Proc. Int. Youth Nucl. Congress*, Capetown, South Africa, 2010.

[48] C. Journeau, M. Kiselova, I. Pozniak, P. Bezdicka, P. Svora, S. Bechta, "First Experiment on Interaction of Molten Uranium Oxide with Solid Boron Carbide," in *NUTHOS-12, 12th International Topical Meeting on Nuclear Reactor Thermal-Hydraulics, Operation and Safety*, Qingdao, P.R. China, 2018.

[49] JAEA, "SIMMER III: A Computer Program for LMFR Safety analysis," [Online]. Available: https://www.jaea.go.jp/jnc/zooarai/ejooarai/simmer/.

[50] T. Jeanne, "Mushy steel state for a new pins clad candling model," in *16th SIMMER III/IV Review Meeting*, Pisa, 2012.

[51] Japan Nuclear Cycle Development Institute, "“SIMMER-III: A Computer Program for LMFR Disruptive Accident Analysis- Version 3.A Model Summary and Program Description”," O-arai, 2003.

[52] J. Pacio, et al., "Fuel assembly blockage formation experiment," in *MYRTE WP3 Progress meeting*, Cadarache, 2015.

[53] J. Lim, A. Marino, A. Aerts, "Active oxygen control by a PbO mass exchanger in the liquid lead–bismuth eutectic loop: MEXICO," *Journal of Nuclear Science and Technology,* vol. 54, no. 1, pp. 131-137, 2016.

[54] J. Pacio, et al., "Final report on partially blocked wire wrapped LBE rod bundle experiment - Deliverable D3.4," MAXSIMA EU FP7 project, 2017.

[55] D.R. Armstrong, et al., "Explosive interaction of molten UO2 and liquid sodium," ANL-76-24, 1976.

[56] M.J.Bird et al., "Experimental studies of thermal interactions between thermite generated molten fuel and sodium," in *4th CSNI Specialist Meeting on fuel Coolant Interaction in Nuclear reactor safety*, Bournemouth, 1974.

[57] R.C. Asher, et al., "Experimental Work at Harwell on the Injection of Sodium into Liquid Steel," in *Specialist meeting on sodium/fuel interaction in fast reactors,*, Tokyo, 1976.

[58] T.Y. Chu,et al., "Medium scale melt-sodium fragmentation experiments," in *Proceedings of the international meeting on fast reactor safety technology*, Seattle - USA, 1979.

[59] G Berthoud, et al., "Analysis of large scale UO2-Na interactions performed in Europe," in *IAEA-IWGFR Technical Committee meeting on material coolant interactions and material movement*, 1994.

[60] M. Amblard, et al., "The EXCOBULLE experiments on the expansion of large two-phase bubbles," *Nucl. Eng. Des.,* vol. 61, pp. 459-468, 1980.

[61] C. Le Rigoleur, et al., "Review of European Out-of-Pile Tests and Analyses of Moltem Material Movement and Relocation and of Molten Material-Sodium Interaction," in *IAEA/IWGFR Technical Committee Meeting on Material-Coolant Interaction and Material Movement and Relocation in Liquid Metal Fast Reactors*, 1994.

[62] P. Soussan, et al., "Propagation and Freezing of Molten Material. Interpretation," in *International Fast Reactor Safety Meeting*, Snowbird, Utah, 1990.

[63] N. Rougnon-Glasson, Freezing of a hot fluid flowing on a cold substrate: modelling of the interfacial resistance, Grenoble: PhD Thesis, Institut National Polytechnique de Grenoble, 1993.

[64] M. Rahman, et al., "Experimental investigation of molten metal freezing on to a structure," *Experimental Thermal and Fluid Science,* pp. 198-213, 2007.

[65] B.W. Spencer,et al., "Results of Recent Reactor-Material Tests on Dispersion of Oxide Fuel from a Disruptive Core," in *Proceeding of International Topical Meeting on Fast Reactor Safety*, Knoxville - USA.

[66] G.P. DeVault, "SIMMER II analysis of the CAMEL II C6 andC7 experiments (Simulated fuel penetration into a primary control assembly," Los Alamos National Laboratory, 1985.

[67] K. Kamiyama, et al., "Experimental study on fuel-discharge behaviour through in-core coolant channels," *Journal of Nuclear Science and Technology ,* vol. 50, no. 6, p. 629–644, 2013.

[68] K. Konishi, et al., "The EAGLE project to eliminate the recriticality issue of fast reactors - Progress and Resulst of in-pile tests," in *NTHASS - 5th Korea-Japan Symposium on Nuclear Thermal-Hydraulics and Safety*, Jeju, South Korea, 2006.

[69] J. M. Seiler, G. Kayser and D. Wilhelm, "Synthesis of Research on Boiling Pool Thermalhydraulics at CEA and KfK," in *Technical Committee Meeting on Material-Coolant Interactions and Material Movement and Relocation on Liquid Metal Fast Reactor - Session D*, O-arai, Ibaraki, 1994.

[70] J.P. Breton, et al., "The SCARABEE Molten and Boiling Pool Test Series BF. Experimental Results, Modelling and Interpretation," in *International Fast Reactor Safety*, Snowbird, Utah, 1990.

[71] M. Bede, et al., "One component, volume heated, boiling pool thermohydraulics," in *International Topical Meeting on Nuclear Reactors Thermal Hydraulics*, 1993.

[72] L. Caldarola, "Current status of knowledge of molten fuel/sodium thermal interactions," 1974.

[73] G. Berthoud, "Vapor Explosions," *Annu. Rev. fluid Mech.,* vol. 32, pp. 573-611, 2000.

[74] S.J. Board, R.W. Hall, "Recent advances in the understanding of large scale steam explosions," in *Nucl. Install. Meet. Sodium-Fuel Interact.Nucl. Install. Meet. Sodium-Fuel Interact.Fast Reactors*, Tokyo, Japan,, 1976.

[75] D. Magallon, et al., "Pouring of 100-kg-scale molten UO2 into sodium," *Nucl. Technol.,* vol. 98, pp. 79-90, 1992.

[76] S. Kondo, K. Konishi, M. Isozaki, S. Imahori, A. Furutani, D.J. Brear, "Experimental study on simulated molten-jet coolant interaction," *Nuclear Engineering and Design,* vol. 155, pp. 73-84, 1995.

[77] H. Schins, F.S. Gunnerson, "Boiling and fragmentation behaviour during fuel-sodium interactions," *Nucl. Eng. Des.,* vol. 91, pp. 221-235, 1986.

[78] H. Schins, "A critical review of fuel coolant interactions with particular reference to UO2-Na," *Res Mechanica,* vol. 23, pp. 65-88, 1988.

[79] A. Le Belguet, "Etude de l'ébullition en film du sodiuim autour d'une sphere à haute temperature," Grenoble, France, 2013.

[80] M. Vanderhaegen, A. Le Belguet, "A review on sodium boiling phenomena in reactor systems," *Nucl. Sci. Eng.,* vol. 176, pp. 115-137, 2014.

[81] A. Le Belguet, et al., "Analysis of Film Boiling Heat Transfer on a High Temperature Sphere Immersed into Liquid Sodium," *J. Energ. Power Eng. ,* vol. 8, pp. 628-635, 2014.

[82] M. Farahat, et al, "Pool Boiling in Subcooled Sodium at Atmospheric Pressure," *Nucl. Sci. Eng.,* vol. 53, p. 240, 1974.

[83] M. Farahat, "Transient Boiling Heat Transfer from spheres to sodium," 1972.

[84] T. Chu, "Fragmentation of molten-core material by sodium," in *International topical meeting on LMFBR safety*, Lyon, France, 1982.

[85] J.D.Gabor, et al., "Breakup and quench of molten metal fuel in sodium," in *Safety of next generation power reactors*, Seattle, USA, 1988.

[86] T.P.Speis, H.K. Fauske , "UO2/Na interactions – Recent in- and out-of-pile experiments in the U.S. and their interpretation for fast reactor safety analysis," in *2nd specialist meeting on sodium fuel interaction in fast reactors*, Ispra, Italy, 1973.

[87] K. Matsuba, et al., "Distance for fragmentation of a simulated molten-core material discharged into a sodium pool," in *Proceedings of the 10th International Topical Meeting on Nuclear Thermal-Hydraulics, Operation and Safety (NUTHOS-10)*, 2014.

[88] H. Mizuta, et al., "Progress report on the molten UO2 drop experiment," in *2nd Specialist Meeting on sodium/fuel interaction in Fast Reactors*, Ispra, Italy, 1973.

[89] H. Mizuta et al., "Fragmentation of uranium dioxide after molten uranium dioxide-sodium interaction," *J. Nucl. Sci. Technol.,* vol. 11, no. 11, pp. 480-487, 1974.

[90] S. Nishimura, et al. , "Transformation and fragmentation behavior of molten metal drop in sodium pool," *Nucl. Eng. Des.,* vol. 237, pp. 2201-2209, 2007.

[91] Z.G. Zhang, K. Sugiyama , "Fragmentation of a single molten metal droplet penetrating into sodium pool: thermal and hydrodynamic effects on fragmentation in stainless steel," *Nucl. Technol.,* vol. 175, pp. 619-627, 2011.

[92] R. Meignein, et al., "Comparative review of FCI computer Models used in OECD-SERENA Program," in *ICAPP*, Seul, South Korea, 2005.

[93] C. F. M. Zabiego, "Corium-Sodium Interaction: The development of the SCONE software," in *NURETH-17 17th Conference on Nuclear Reactor Thermal Hydraulics*, Xi'an, China, 2017.

[94] M. Saito, et al., "Melting Attack of Solid plates by a high temperature liquid jet – Effect of crust formation," *Nucl. Eng. Des.,* vol. 121, pp. 11-23, 1990.

[95] H.S. Park, et al. , "Fine fragmentation of molten droplet in highly subcooled water due to vapor explosion observed by X-ray radiography," *Exp. Therm. Fluid Sci.,* vol. 29, pp. 261-361, 2005.

[96] C. Journeau, "Corium-Sodium and Corium-Water Fuel-Coolant-Interaction experimental programs for the PLINIUS2 Prototypic Corium Platform," in *Proc. NURETH-17*, Xi'an (China), 2017.

[97] M. Amblard, et al., "Recent JEF and CORECT I sodium/fuel interactions results," in *Specialist meeting on sodium fuel interaction in fast reactors*, Varese, Italy, 1973.

[98] M. Martini, et al., "Out of pile experiments related to sodium fuel interaction performed at CNEN (USTS/N)," in *2nd specialist meeting on sodium fuel interaction in fast reactors*, Ispra - Varese - Italy, 1973.

[99] J.D Gabor, et al., "Breakup and quench of molten metal fuel in sodium," in *Safety of next generation power reactors meeting*, Seattle - USA, 1988.

[100] R. E. Henry, et al., "Large scale vapor explosions," in *Fast Reactor Safety*, Beverly Hills - USA, 1974.

[101] H. Endo, et al., "Elimination of recriticality potential for the self-consistent nuclear energy system," *Progr. Nucl.Ener.,,* vol. 40, pp. 577-586, 2002.

[102] T. Nitheanandan, et al. , "Molten Fuel Moderator Interaction Program at Chalk River Laboratories," in *In Pacific Basin Nuclear Conference* , 2006.

[103] Y. C. Yen and A. Zehnder, "Melting Heat Transfer with Water Jet," *Int. J. Heat Mass Transfer,* vol. 16, pp. 219-223, 1973.

[104] M. J. Swedish, et al., "Surface Ablation in the Impigement Region of a Liquid Jet," *AIChE Journal,* vol. 25, no. 4, pp. 630-638, 1979.

[105] M. Epstein, et al., "Simultaneous Melting and Freezing in the Impigement Region of a Liquid Jet," *AIChE Journal,* vol. 26, no. 5, pp. 743-751, 1980.

[106] A. Benuzzi, et al., "Commission of the European Communities Joint Research Centre Contribution to LMBFR Safety Analysis," in *IAEA Conference on Nuclear power performance and Safety*, Vienna, 1987.

[107] D. Moxon, et al., "Ablation by a Liquid Jet," in *14th LMBWG meeting*, Brasimone, Italy, 1991.

[108] B.R. Sehgal, et al., "Experiments on Vessel Hole Ablation During Severe Accidents, Heat and Mass Transfer in Severe Nuclear Reactor Accidents.," in *International Symposium*, Kusadasi, Tukey, 1995.

[109] G. Albrecht, et al., "KAJET experiments on pressure-driven melt jets and their interaction with concrete," FZKA-7002, 2005.

[110] M. Saito, et al., "Melting attack of solid plates by a high temperature liquid jet – effect of crust formation," *Nucl. Eng. Des.,* vol. 121, pp. 11-23, 1990.

[111] K. Mikityuk, E. Girardi, J. Krepel, E. Bubelis, E. Fridman, A. Rineiski, N. Girault, F. Payot, L. Buligins, G. Gerbeth, N. chauvin, C. Latgé, J.C. Garnier, "ESFR-SMART: New HORIZON2020 project on SFR Safety," in *Proceedings of the International Conference on Fast Reactors and Related Fuel Cycles: Next Generation Nuclear Systems for Sustainable Development (FR17)*, Yekaterinburg, Russia, 2017.

[112] F. Payot, C. Journeau, C. Suteau, F. Serre, M. Gradeck, N. Rimbert, A. Lecoanet and A. Miassoedov, "A new experimental R&D program associated with the corium jet impingement on the ASTRID core catcher sacrificial materials," in *ICAPP*, Charlotte (US), 2018.

[113] B. Spindler, B. Tourniaire, J.M.Seiler,, "Simulation of MCCI with the TOLBIAC-ICB code based on the phase segregation model," *Nuclear Engineering and Design,* vol. 236, p. 2264–2270, 2006.

[114] K. Plevacova, et al., "Eutectic crystalization in the UO2-HfO2-Al2O3 ceramic phase diagram," *Ceram. Inter.,* vol. 40, pp. 2565-2573, 2014.

[115] C. Journeau, et al., "Experimental program and facilities for ASTRID development related to severe accidents," in *International conference Fast Reactors and related Fuel Cycles - FR13*, 2013.

[116] F. Balbaud-Célérier, et al., "Corrosion of structural materials in liquid metals used as fast reactors coolants," in *Int. Conf. Fast Reactor and related Fuel Cycles - FR13*, Paris, 2013.

[117] J. L. Courouau,et al., "Corrosion by oxidation and carburization in liquid sodium at 550°C of austenitic steels for sodium fast reactors," in *Int. Conf. Fast Reactor and related Fuel Cycles, FR13*, Paris, 2013.

[118] C. Journeau, et al., "Contributions of the VULCANO experimental programme to the understanding of MCCI phenomena," *Nuclear Engineering and Technology,* vol. 44, pp. 261-272, 2012.

[119] C. Journeau, et al., "Phase Macrosegregation during the slow solidification of prototypic corium," in *International Topical Meeting on Nuclear Reactor Thermal-Hydraulics - NURETH 10*, Seul - SK, 2003.

[120] L. Baker, et al., "Postaccident Heat Removal—Part I: Heat Transfer Within an Internally Heated, Nonboiling Liquid Layer," *Nucl. Sci. Eng.,* vol. 61, pp. 222-230, 1976.

[121] R. E. Faw and L. Baker, "Postaccident Heat Removal—Part II: Heat Transfer from an Internally Heated Liquid to a Melting Solid," *Nucl. Sci. Eng.,* vol. 61, pp. 231-238, 1976.

[122] F. A. Kulacki, et al., "High Rayleigh number convection in enclosed fluid layers with internal heat sources - report NUREG 75/065," Ohio State University, 1975..

[123] G. Fieg, "Heat Transfer measurements of internally heated liquids in cylindrical convection cells," in *4th PAHR Information Exchange Meeting*, Varese, Italy, 1978.

[124] J. M. Seiler, "Cooling of molten material liquid pool submitted to volumetric heating: new correlations for various cooling conditions," in *ENS/ANS Int. Conf. Thermal reactor Safety*, Avignon, France, 1988.

[125] J.M. Seiler, et al., "Transient refractory material dissolution by a volumetrically-heated melt," *Nucl. Eng. Des., 280, 420-4328, 2014.,* vol. 280, pp. 420-428, 2014.

[126] M. Bede, et al., "One component, volume heated, boiling pool thermalhydraulics," in *6th Int Topical Mtg Nucl. Reactor Thermal Hydraulics*, Grenoble, 1993.

[127] G. A. Greene, "Heat removal characteristics of volume heated boiling pools with inclined boundaries," Brookhaven Nat. Lab, 1980.

[128] D. Alvarez, et al., "Fuel levelling," in *5th post-accident heat removal information exchange meeting*, Karlsruhe, 1982.

[129] M. Shamsuzzaman, et al., "Numerical study on sedimentation behavior of solid particles used as simulant fuel debris," *Journal of Nuclear Science and Technology,* vol. 51, no. 5, p. 681–699, 2014.

[130] A. Karbodjian, et al., "A scoping study of debris bed formation in the DEFOR test facility," *Nucl. Eng. Des.,* vol. 239, no. 9, pp. 1653-1659, 2009.

[131] J. D. Gabor, et al., "Studies and experiments on heat removal from fuel debris in sodium," in *ANS Conference on fast reactor safety*, Beverly Hills, 1974.

[132] A. Konovalenko, et al., "Experimental and Analytical Study of the Particulate Debris Bed Self-leveling," in *9th International Topical Meeting on Nuclear Thermal-Hydraulics, Operation and Safety (NUTHOS-9),*, Kaohsiung, Taiwan, 2012.

[133] J.D. Gabor, et al., "Studies on Heat removal and Bed Levelling of Induction-heated Materials simulating Fuel Debris," in *2nd Post Accident Heat Removal information exchange meeting*, Albuquerque, 1975.

[134] Y. K. Dhir and I. Cation, "Study of Dryout Heat Fluxes in Bed of lnductively Heated Particles. NUREG-0262," University of California, Los Angeles, 1977.

[135] R.S. Keowen, et al., "Dryout of a fluidized particle bed with internal heat generation. UCLA-ENG-7919," UCLA, 1975.

[136] V.K. Dhir,et al., "Dryout heat fluxes in debris beds cooled at the bottom and having subcooled liquid at the top," *Nucl. Technol.,* vol. 46, pp. 356-361, 1979.

[137] D. Squarer, et al., "Dryout in Inductively Heated Bed With and Without Forced Flow," *Trans. Am. Nucl. Soc .,* vol. 34, p. 535, 1980.

[138] K. Hu, et al., "On the measurement and mechanism of dryout in volumetrically heated coarse particle beds," *Int. J Multiphase Flows,* vol. 17, no. 4, pp. 519-532, 1992.

[139] L. Barleon, et al., "Debris Bed Investigations with Adiabatic and Cooled Bottom," in *9th Mtg Liquid Metal Boiling Working Group (LMBWG)*, Rome, 1980.

[140] J. Rivard, "Debris Bed Studies and Experiments at Sandia Laboratories. NUREG/CR-0263," SNL, 1978.

[141] E. Takasuo, et al., "The COOLOCE experiments investigating the dryout power in debris beds of heap-like and cylindrical geometries," *Nucl. Eng. Des.,* vol. 250, pp. 687-700, 2012.

[142] S. Thakre, et al., "An experimental study on coolability of a particulate bed with radial stratification or triangular shape," *Nucl. Eng. Des.,* vol. 276, pp. 54-63, 2014.

[143] N. Chikhi,et al., "Evaluation of an effective diameter to study quenching and dry-out of complex debris bed," *Ann. Nucl. Ener.,* vol. 74, pp. 24-41, 2014..

[144] IWGFR, "Proceedings of the International Working Group on Fast reactors, Technical Committee Meeting on material Coolant Interaction and Material Movement and Relocation in Liquid metal Reactors, IWGFR-89, Japan," in *International Working Group on Fast reactors, Technical*

Committee Meeting on material Coolant Interaction and Material Movement and Relocation in Liquid metal Reactors, IWGFR-89, Japan.

[145] N. Sheriff and N. Davies, "Liquid Metal Natural Convection from Plane Surfaces: A review Including Recent Sodium Measurements," *Int. J. Heat Fluid Flow,* vol. 1, pp. 149-154, 1979.

[146] N. Davies and N. Sheriff, "Measurements of natural convection in sodium for fast reactor internal core catcher, Heat and Fluid Flow in Nuclear and Process Plant Safety," *I Mech E Conf. Pub.,* vol. 3, pp. 189-200, 1983.

[147] C. Le Rigoleur and D. Tenchine, "Sodium Natural Convection heat transfers around the internal core catcher of SUPERPHENIX 1: Experimental results and evaluation for reactor conditions," in *Int. Top. Mtg. Liquid Metal Fast Breeder reactor Safety and Related Design and Operation Aspects, ENS/ANS*, Lyon, 1982.

[148] A. K. Sharma, et al., "Experimental and Numerical Analysis of natural Convection in Geometrically Modelled Core Catcher of the Liquid-Metal-Cooled Fast Reactor," *Nucl. Technol.,* vol. 165, pp. 43-52, 2009.

[149] L. Gnanadhas, et al., "PATH – An experimental facility for natural circulation heat transfer studies related to Post Accident Thermal Hydraulics," *Nucl. Eng. Des.,* vol. 241, pp. 3839-3850, 2011.

[150] D. De Bruyn, "On-going activities in Belgium in the field of FR & ADS, 2016 status," in *IAEA TWG FR&ADS 49th annual meeting*, 2016.

[151] C. Journeau, et al., "European Corium Experimental Reasearch Roadmap," in *SAFEST 7FP EU Project*, 2017.

[152] X. Gaus-Liu, et al., "In-vessel melt pool coolability test –Description and results of LIVE experiments," *Nuclear Engineering and Design,* vol. 240, pp. 3898-3903, 2010.

[153] "PLINIUS-2: A versatile platform for severe accident mitigation device and simulation assessments,," in *ICAPP 14*, Charlotte, USA, 2014.

[154] S. A. Smirnov, "DNS of Molten corium pool inductively heated in cold crucible," in *OECD/NEA MASCA2*, Aix en Provence, France, 2007.

[155] S. Hellmann, M. Fischer, "SICOPS experiments on simultaneous interaction of molten corium with concrete and refractory material," in *OECD/NEA MCCI*, Cadarache, France, 2007.

[156] Y. Petrov et al., "Miscibility Gap Phenomena at Oxide Melting in Air at Ex-vessel Corium Simulation," in *International Congress Advanced Nuclear Power Plants*, Pittsburgh, USA, 2004.

[157] V. Natarajan, K.Ravichandran, "Experimental and Analytical Simulation of MFCI (Molten Fuel Coolant Interaction) during CDA (Core Disruptive Accident) in Sodium Cooled Fast Reactor," Chalmers University of Technology, 2011.

[158] J.H. Song, et al. , "An electromagnetic and thermal analysis of cold crucible melting," *Int. Comm. Heat Mass Transfer,* vol. 32, pp. 1325-1336, 2005.

[159] H.-Y. Kim, "Introduction of VESTA (Verification of Ex-vessel corium STAbilization) Facility and First Series Experiment," in *OECD NEA MCCI2*, Cadarache, France, 2010.

[160] M.T. Farmer , "A Summary of Findings from Melt Coolability and Concrete Interaction (MCCI) Program," in *ICAPP 07*, Nice, France, 2007.

[161] P. Piluso, et al. , "The urano-thermic reaction: an efficient SHS process to synthesize severe accident nuclear materials," *Int. J. Self-Propag. High-Temp.Synth,* vol. 18, pp. 241-251, 2009.

[162] C. Journeau, et al., "PLINIUS-2: A New Versatile Platform for Severe Accident Assessments,," in *NUTHOS-10*, Okinawa, Japan, 2014.

[163] C. Journeau, M. Kiselova, I. Pozniak, P. Bezdicka, P. Svora and S. Bechta, "First experiment on Interaction of Molten Uranium Oxide with Solid Boron Carbide," in *NUTHOS-2018*, Qindao, P.R.C., 2018.

[164] A. Konovalenko, P. Sköld, P. Kudinov, S. Bechta and D. Grishchenko, "Controllable Generation of a Submillimeter Single Bubble in Molten Metal Using a Low-Pressure Macrosized Cavity," *Metallurgical and Materials Transactions B,* vol. 48, no. 2, pp. 1064-1072, 1 Apr 2017.

[165] F. Payot, C. Journeau, C. Suteau, F. Serre, M. Gradeck, N. Rimbert, A. Lecoanet and A. Miassoedov, "A new experimental R&D program associated with the corium jet impingement on the ASTRID core catcher sacrificial materials," in *ICAPP* , Charlotte NC, 2018.